Facile protein and amino acid substitution reactions and their characterization using thermal, mechanical and optical techniques

Naresh K. Budhavaram

Dissertation submitted to the faculty of the Virginia Polytechnic Institute and State University in partial fulfillment of the requirements for the degree of Doctor of Philosophy in Biological Systems Engineering

Justin R. Barone (Committee Chair)
Chenming (Mike) Zhang
Zhiyou Wen
Louis A. Madsen

November 01, 2010

Blacksburg, Virginia

Keywords: Alanine, Cysteine, Lysine, Ovalbumin, Michael Addition Reactions, Glass Transition Temperature, Raman Spectroscopy, Hydrogels, Fibers, Microtubes.

Facile protein and amino acid substitution reactions and their characterization using thermal, mechanical and optical techniques

Naresh K Budhavaram

(Abstract)

The work focused on addressing four main objectives. The first objective was to quantify protein and amino acid substitution reactions. Michael addition reactions were used to modify the amino acids and protein. Amino acids alanine, cysteine, and lysine, and protein ovalbumin (OA) were substituted with different concentrations of ethyl vinyl sulfone (EVS). The substituted products were analyzed using Raman spectroscopy and UV-spectroscopy based ninhydrin assay. In case of alanine, Raman and UV results correlated with each other. With cysteine at lower EVS substitutions amine on the main chain was the preferred site while the substitution shifted to thiols at higher substitutions. This could only be discerned using Raman spectroscopy. Lysine has amines on the main chain and side chain while main chain amine was the most reactive site at lower concentrations of EVS while at higher concentrations side chain amines were also substituted. This information could be discerned using Raman spectroscopy only and not UV spectroscopy. In case of protein as observed by Raman and UV spectroscopy the reaction continued at higher concentrations of EVS indicating the participation of glutamine and asparagines at higher substitutions. However, the reaction considerably slowed down at higher EVS substitutions.

The second objective of the study was to decrease the glass transition temperature (T_g) of OA through internal plasticization and also study the effects of the substituents on the thermal

stability of OA. The hypothesis was by covalently attaching substituents to OA, number of hydrogen bonds can be reduced while increasing the free volume and this would reduce T_g. EVS, acrylic acid (AA), butadiene sulfone (BS) and maleimide (MA) were the four groups used. EVS was the most efficient plasticizer of all the four substituents. The T_g decreased with the increasing concentration of EVS until all of the reactive of groups on OA were used up. T_g decreased slightly with AA and BS while no change was observed with MA. However, the substituents showed exact opposite trend in thermal stability as measured using thermogravimetric analysis (TGA). The thermal stability of MA substituted OA was the highest and that of EVS substituted OA was least. FT-IR spectroscopy results indicated that all four substituents caused structural changes in OA. This implied that there were intermolecular interactions between substituted protein chains in case of AA, BS, and MA. This caused an increase in the thermal stability. EVS on the other hand is a linear chain monomer with a hydrophobic end group and hence could not participate in the intermolecular interactions and hence caused a decrease in T_g. As mentioned above the limitation to this technique is the number of available reactive groups on the protein. However, we successfully demonstrated the feasibility of this method in decreasing T_g of protein.

The third objective was to create hydrogels by crosslinking OA with divinyl sulfone (DVS). Protein hydrogels due to their biocompatible nature find applications in drug delivery and tissue engineering. For tissue engineering applications the hydrogels need to be mechanically stable. In this study the protein was substituted with EVS or AA and then crosslinked with DVS. The swelling ratio was measured as a function of pH. All the hydrogels showed the same trend and swelled the least at pH 4.5 which is the isoelectric point of the protein. At basic pH conditions EVS substituted hydrogels swelled the most while AA substituted hydrogels showed least

swelling. The static and dynamic moduli of the hydrogels were determined using tensile tester and rheometer respectively. The static modulus values were three times the dynamic modulus. The modulus of the control which is crosslinked OA was least and that of AA substituted OA was highest. The stress relaxation test also showed similar results in which AA substituted OA relaxed the most and the control relaxed the least. FT-IR of the dry hydrogels showed that the amount of hydrogen bonding increased with AA substitution. The hydrophilic AA end groups interacted with each other forming hydrogen bonds. These hydrogen bonds served as additional crosslinks there by increasing the modulus of the hydrogels. EVS on the other hand was incapable of interactions due to the lack of hydrophilic end groups. We were successfully able to create protein hydrogels and control the swelling and mechanical properties by varying the amount of substituted group.

The final objective of the study was to create and characterize microstructures from substituted alanine and lysine. Alanine and lysine were substituted with different concentrations of EVS. Bars and fibers were observed for alanine at moderate substitutions while at higher concentrations random structures were observed using scanning electron microscopy (SEM). Lysine formed tubes at moderate EVS substitutions and rosettes at high concentrations of EVS as evidenced by SEM. FT-IR results suggested that instead of carbonyl one of sulfonyl bonded to the available amine in modified amino acids. And only in this case fibers, tubes and rosettes were observed. X-ray diffraction (XRD) results supported this observation. Using these results we hypothesized that the self assembled structures very much depended on the amount of EVS present in the substituted product and sulfonyl forming β-sheet analogs with amine.

Dedication

Dedicated to my parents Brahmanandam (father) and Manohara (mother), Madhavi and Manju (sisters), Rakesh (brother), Akhila (niece), Vishwambhar (nephew), Ramesh and Narayana (brothers-in-law), Vijay Kumar (father-in-law), Krishnakantha (mother-in-law), Manasa and Unmisha (sisters-in-law), and my wife Prathyusha who always supported, loved and stood by me in good and bad times.

Attribution

Author Naresh K. Budhavaram is the major contributor and writer of the manuscript in chapter three of this dissertation. Co-author Dr. Justin R. Barone, Ph.D., Macromolecular Sciene and Engineering, Case Western Reserve University, Cleveland, OH (2000), Committee Chair provided advise, supervision, funding, and laboratory support.

Naresh and Dr. Barone are with Dept. of Biological Systems Engineering, 303 Seitz Hall, Virginia Tech, Blacksburg, VA 24061.

Acknowledgment

I would to like express my sincere gratitude to my advisor Dr. Justin Barone for his help, guidance and support throughout my graduate study. I am very thankful to him, as I learned and developed professionally and personally through his mentoring. I would like to thank my committee members, Dr. Mike Zhang, Dr. Zhiyou Wen, and Dr. Louis Madsen, for their support and for helping me meet my deadlines.

I would also like to thank Dr. Saied Mostaghimi, Dr. Jactone Arogo Ogejo, Denton Yoder, Barbara Taylor, Susan Rosebrough, and Amy Egan for their help and friendly discussions which made my stay at Virginia Tech happy and memorable.

My friends, Mohammed Rabius Sunny, Sachi Chander Nekkanti, Satyam Eleswarapu, Chaitanya Chopra, Pranitha Parimi, Vedavyas Duggirala, Abhranil Maiti, Navaneeta Dorbala, Neeta Jain Gupta, and Tila Khan made me look forward to weekends at Blacksburg with enthusiasm and excitement. Thanks to them and all my other friends and colleagues at Virginia Tech.

Finally, I would like to thank my lab-mates, friends at Ole Miss, and undergraduate friends who constantly supported me and wished for my success.

Contents

Chapter III

Chapter IV

Chapter V

Chapter VI

List of Figures

Chapter II

Chapter III

Chapter IV

Chapter V

Chapter VI

Chapter VII

List of Tables

Chapter II

Chapter III

Chapter V

Chapter I

Introduction

Proteins and peptides are polymers composed of various combinations of the 20 different naturally-occurring amino acids. Each amino acid is composed of a carboxylic acid group and a primary amine group that can condense to form a peptide bond and water. In addition, each amino acid has a different chemical "side group" making proteins and peptides versatile in terms of their natural chemistry. In nature, the different amino acids combine to form a protein polymer that can catalyze biochemical reactions, cause or heal disease, and give mechanical stability by supporting load. In terms of the first two, the industrial production of enzymes and biologics has become an important business and now accounts for billions of dollars in the biotech industry. However, it is the last function, to support load, that has traditionally utilized proteins in such non-food uses as biodegradable plastics, adhesives and textiles.[1, 2] Silk and wool are classic examples of proteins used in the textile industry. The purpose of the research described herein was to leverage the chemistry of existing amino acids, peptides, and proteins to create new materials for physical function, i.e., to support load. Specifically, we want to show how small chemical changes to proteins, peptides, and amino acids could produce large changes in structure and physical response. Some of the specific aspects we wanted to explore were morphology and physical properties such as thermal transitions, thermal stability, ability to hydrate, and modulus.

The diversity of chemical groups on amino acids allows for a plethora of chemistries to be performed. Our goal was to identify chemical reactions that could be performed in aqueous solution at near neutral pH without the use of complex catalysts. Therefore, it would be possible to maintain the integrity of the original protein if needed. The Michael addition is a nucleophilic

addition reaction that adds electron rich nucleophiles to electron poor electrophiles.[3] The Michael addition can be used to modify abundant nucleophilic amine and thiol groups on amino acids and proteins. The first part of the research was to characterize the nucleophilic addition of water soluble vinyl groups onto amino acids and proteins.

For plastics applications currently all the proteins are plasticized with an external plasticizing agent such as glycerol.[4, 5] This is because in their denatured state the proteins have high glass transition temperatures making them brittle at room temperature.[4-6] The externally plasticized proteins are susceptible to plasticizer migration issues over a period of time eventually rendering them useless. The second goal of the research was to attempt to change the glass transition and thermal degradation temperatures of proteins by chemically modifying the amino acid side groups.[1]

Hydrogels are another potential area where proteins can be used. Currently hydrogels are made from chemicals such as isopropylacrylamide, poly-(acrylic acid), and poly-(methacrylate).[7] The major requirements of hydrogels are ability to hydrate, rigidity, biocompatibility and biodegradability. To this end promising results have been achieved through the usage of chitosan and dextran based hydrogels.[8, 9] Elastin, collagen, and *de novo* synthesized proteins are the other biopolymers being investigated.[10-12] The third goal of the research was to synthesize and construct hydrogels from chemically modified proteins.

The other potential application of proteins and amino acids is in the burgeoning field of nano-materials.[13-17] Amino acids have been traditionally used as dietary supplements, food additives and nitrogen sources for micro-organisms in fermentation processes.[18, 19] However, amino acids are finding potential applications as nano-materials. Poly-alanine is frequently used for the synthesis of nano-fibers and poly-lysine as a coating agent for nano-structures.[20-23]

However, complicated synthetic and genetic engineering techniques have to be used for the synthesis of poly-amino acids since they do not occur naturally. There is still a lot of scope for the creation of new and useful nano-structures using naturally available amino acids like lysine and alanine. The fourth part of the research was to demonstrate the spontaneous formation of unusual structures such as tubes and spheres using chemically substituted amino acids.

An overarching goal of the research was to develop molecular spectroscopic techniques for biopolymers and biomaterials. Quantitative estimation of reactions is an important step for determining the kinetic parameters of the reaction, which is usually accomplished using analytical techniques like titration, chromatography and colorimetric assays.[24-26] These techniques require some sample preparation and it takes time to get the results. Fourier transform infrared (FTIR) and Raman spectroscopic techniques on the other hand are non destructive, require little to no sample preparation, and provide accurate results in less time. They have been used for assessment of reactions.[27] For proteins FTIR and Raman spectroscopy have been largely used for identifying changes in secondary structure.[28, 29] Though there are reports on the usage of FTIR and Raman spectroscopy for quantitative assessment of reaction, there is still a lot of unexplored territory.[30] For proteins, Raman spectroscopy has an advantage over FTIR because individual amino acids present can be resolved.[31]

Objectives

The main motivation of this study was to demonstrate that small chemical substitutions could produce large changes in proteins and amino acids. The specific goals were as follows:

- To quantify protein and amino acid substitution reactions using Raman spectroscopy
    - To identify the specificity of addition reactions on the amine and thiol sites present on amino acid and protein chains using Raman spectroscopy.

- To internally plasticize a model protein by synthetically varying the amino acid side group chemistry.
    - To identify the structural and thermal changes in the model protein as a function of substituted groups.
- To prepare hydrogels with varying crosslink density and amino acid side group chemistry by substituting a model protein rather than synthesizing a new one.
    - To determine the swelling and mechanical properties of the crosslinked protein as a function of crosslink density and substituted group chemistry.
- To create and characterize nanometer to micrometer sized structures using amino acids alanine and lysine substituted using the same chemistry developed in the aforementioned objectives.

Dissertation Organization

The work pertaining to the objectives of the current study that has been previously done has been summarized in the second chapter along with brief introduction to characterization techniques. Chapters 3 through 7 contain each individual objective written in the form of manuscript style with abstract, introduction, materials and methods, results and discussion, and conclusions. The findings of the current work have been summarized in chapter 8.

Chapter 3 is based on the Michael addition reaction of ethyl vinyl sulfone with amino acids and protein (Egg ovalbumin) that were quantified using Raman spectroscopy. Alanine, cysteine and lysine were the amino acids chosen for the study. Michael addition reaction takes place on amines and thiols and hence lysine with an amine and cysteine with a thiol on the side chain were selected. Alanine is a non-polar amino acid with no ionizable group on the side chain and hence was considered for comparison with lysine and cysteine. Ovalbumin is a semi-crystalline

protein with 385 amino acids, is 50% polar and all the natural amino acids are represented. Hence it was chosen as model protein. The Raman spectroscopy results were compared with UV-visible spectroscopy based ninhydrin assay.

The effects of substituent groups on the ovalbumin in terms of glass transition temperature and thermal stability were studied in chapter 4. Ethyl vinyl sulfone, acrylic acid, butadiene sulfone and maleimide were the substituent groups used in the study. The effects of side group size and end group chemistry on the protein were studied.

Chapter 5 discusses the usefulness of Michael addition reactions for creation of ovalbumin hydrogels. Hydrogels were prepared by crosslinking pure and substituted ovalbumin with divinyl sulfone. The mechanical and swelling properties as a function of substituted groups were studied.

Alanine and lysine substitutions with ethyl vinyl sulfone were studied in chapters 6 and 7 respectively. As mentioned in the above sections fibrous micro-structures were reported in the literature using poly-alanine and poly-lysine. Hence, we chose alanine and lysine for our work. The role of ethyl vinyl sulfone in the formation of various self assembled micro structures was studied.

References

1. Guérin-Dubiard, C.; Audic, J.-J., Egg-Protein-Based Films and Coatings. In 2007; pp 265-273.

2. Guilbert, S.; Morel, M.-H.; Gontard, N.; Cuq, B., Protein-Based Plastics and Composites as Smart Green Materials. In *Feedstocks for the Future*, American Chemical Society: Washington, DC, 2006; pp 334-350.

3. Mather, B. D.; Viswanathan, K.; Miller, K. M.; Long, T. E., Michael addition reactions in macromolecular design for emerging technologies. *Prog. Polym. Sci.* **2006,** 31, 487-531.

4. di Gioia, L.; Cuq, B.; Guilbert, S., Mechanical and water barrier properties of corn-protein-based biodegradable plastics. *J. Mater. Res.* **2000,** 15, (12), 2612-2619.

5. Athamneh, A. I.; Griffin, M.; Whaley, M.; Barone, J. R., Conformational Changes and Molecular Mobility in Plasticized Proteins. *Biomacromolecules* **2008,** 9, (11), 3181-3187.

6. Su, J. F.; Huang, Z.; Yang, C. M.; Yuan, X. Y., Properties of Soy Protein Isolate/Poly(vinyl alcohol) Blend "Green" Films: Compatibility, Mechanical Properties, and Thermal Stability. *J. Appl. Polym. Sci.* **2008,** 110, (6), 3706-3716.

7. Burkeev, M.; Tazhbaev, E.; Kazhmuratova, A.; Sugralina, L.; Zhaparova, L., Hydrogels of copolymers of β-vinyloxyethylamide of acrylic acid with unsaturated carboxylic acids. *Polymer Science Series B* **2007,** 49, (11), 257-260.

8. Lee, J. W.; Kim, S. Y.; Kim, S. S.; Lee, Y. M.; Lee, K. H.; Kim, S. J., Synthesis and characteristics of interpenetrating polymer network hydrogel composed of chitosan and poly(acrylic acid). *J. Appl. Polym. Sci.* **1999,** 73, (1), 113-120.

9. Hennink, W. E.; Talsma, H.; Borchert, J. C. H.; De Smedt, S. C.; Demeester, J., Controlled release of proteins from dextran hydrogels. *J. Controlled Release* **1996,** 39, (1), 47-55.

10. Leach, J. B.; Wolinsky, J. B.; Stone, P. J.; Wong, J. Y., Crosslinked [alpha]-elastin biomaterials: towards a processable elastin mimetic scaffold. *Acta Biomaterialia* **2005,** 1, (2), 155-164.

11. Lim, D. W.; Nettles, D. L.; Setton, L. A.; Chilkoti, A., Rapid Cross-Linking of Elastin-like Polypeptides with (Hydroxymethyl)phosphines in Aqueous Solution. *Biomacromolecules* **2007,** 8, (5), 1463-1470.

12. Mao, C.; Kisaalita, W. S., Characterization of 3-D collagen hydrogels for functional cell-based biosensing. *Biosens. Bioelectron.* **2004,** 19, (9), 1075-1088.

13. Channon, K.; MacPhee, C. E., Possibilities for 'smart' materials exploiting the self-assembly of polypeptides into fibrils. *Soft Matter* **2008,** 4, (4), 647-652.

14. Soest, J. J. G. v., The Development of Biopolymer-Based Nanostructured Materials: Plastics, Gels, IPNs, and Nanofoams. In *Feedstocks for the Future*, American Chemical Society: Washington, DC, 2006; pp 288-303.

15. Ji, Y.; Luo, Y.-F.; Jia, X.-R.; Chen, E.-Q.; Huang, Y.; Ye, C.; Wang, B.-B.; Zhou, Q.-F.; Wei, Y., A Dendron Based on Natural Amino Acids: Synthesis and Behavior as an Organogelator and Lyotropic Liquid Crystal13. *Angew. Chem. Int. Ed.* **2005,** 44, (37), 6025-6029.

16. Hermann, T., Industrial production of amino acids by coryneform bacteria. *J. Biotechnol.* **2003,** 104, (1-3), 155-172.

17. Leuchtenberger, W.; Huthmacher, K.; Drauz, K., Biotechnological production of amino acids and derivatives: current status and prospects. *Appl. Microbiol. Biotechnol.* **2005,** 69, (1), 1-8.

18. Williams, M., Dietary Supplements and Sports Performance: Amino Acids. *Journal of the International Society of Sports Nutrition* **2005,** 2, (2), 63 - 67.

19. Van De Merbel, N. C.; Zuur, P.; Frijlink, M.; Holthuis, J. J. M.; Lingeman, H.; Brinkman, U. A. T., Automated monitoring of amino acids during fermentation processes using on-line ultrafiltration and column liquid chromatography: application to fermentation medium improvement. *Anal. Chim. Acta* **1995,** 303, (2-3), 175-185.

20. Zhang, L.; Wan, M.; Wei, Y., Nanoscaled Polyaniline Fibers Prepared by Ferric Chloride as an Oxidant. *Macromol. Rapid Commun.* **2006,** 27, (5), 366-371.

21. Wang, X. C.; Ding, S. J.; Cao, J.; Wu, F. L.; Zhou, C.; Yang, Z. Z., Controlled synthesis of dendritic polyaniline fibers with diameters from nanosize to submicrometersize. *Chin. Chem. Lett.* **2005,** 16, (11), 1523-1526.

22. Kim, J.-B.; Premkumar, T.; Giani, O.; Robin, J.-J.; Schue, F.; Geckeler, K. E., Nanocomposites of poly(L-lysine) and single-walled carbon nanotubes. *Polym. Int.* **2008,** 57, (2), 311-315.

23. Ohtake, T.; Nakamatsu, K.; Matsui, S.; Tabata, H.; Kawai, T., Novel DNA nano-patterning design method utilizing poly-L-lysine patterning by nanoirnprint lithography. *Journal of Nanoscience and Nanotechnology* **2006,** 6, (7), 2187-2190.

24. Pitet, L. M.; Hait, S. B.; Lanyk, T. J.; Knauss, D. M., Linear and branched architectures from the polymerization of lactide with glycidol. *Macromolecules* **2007,** 40, (7), 2327-2334.

25. Rinde, E.; Troll, W., Colorimetric assay for aromatic amines. *Anal. Chem.* **1976,** 48, (3), 542-544.

26. Beckwith, A. C.; Paulis, J. W.; Wall, J. S., Direct estimation of lysine in corn meals by the ninhydrin color reaction. *J. Agric. Food. Chem.* **1975,** 23, (2), 194-196.

27. Jena, K. K.; Raju, K.; Prathab, B.; Aminabhavi, T. M., Hyperbranched polyesters: Synthesis, characterization, and molecular simulations. *J. Phys. Chem. B* **2007,** 111, (30), 8801-8811.

28. Gani, D.; Hendra, P. J.; Maddams, W. F.; Passingham, C.; Royaud, I. A. M.; Willis, H. A.; Zichy, V.; Cudby, M. E. A., Fourier transform Raman spectroscopy in the analysis of polypeptides. *Analyst* **1990,** 115, 1313-1318.

29. Ngarize, S.; Herman, H.; Adams, A.; Howell, N., Comparison of Changes in the Secondary Structure of Unheated, Heated, and High-Pressure-Treated β-Lactoglobulin and Ovalbumin Proteins Using Fourier Transform Raman Spectroscopy and Self-Deconvolution. *J. Agric. Food. Chem.* **2004,** 52, (21), 6470-6477.

30. Huang Yan, L. X.-y. a. Z. Y.-p., Quantitative Evaluation and Secondary Structure Analysis of Proteins Adsorbed on Biomaterial Surfaces Using FTIR. *Proceedings of the 2005 IEEE Engineering in Medicine and Biology 27th Annual Conference* **2005**, 4892-4895.

31. Tuma, R., Raman spectroscopy of proteins: from peptides to large assemblies. *Journal of Raman Spectroscopy* **2005,** 36, (4), 307-319.

Chapter II

Literature Review

Sustainability and green engineering have been the thrust of research areas in recent years. A lot of impetus has been given to renewable materials and green chemical reactions that use less toxic chemicals. Along with naturally available polysaccharides, chitosan and fermentation products like lactic acid, propanediol and biofuels, efforts are under way to utilize proteins for bio-based applications. In fact the use of silk and wool for textile applications can be dated centuries back. In the early 1930's, efforts were made to use agricultural proteins for industrial applications.[1] Since corn is one of the major agricultural products in the U.S., attempts were made to utilize corn zein, a protein extracted from corn, for film, coating and plastic applications.[2] However cost was one of the issues that led to the collapse of the zein market as petroleum-based polymers were available at a cheaper price. With petroleum prices peaking there is a renewed interest to utilize corn zein for industrial applications.[2-4] Other proteins being investigated are soy protein, wheat gluten, feather keratin, casein, and egg ovalbumin.[3, 5-18 19-22]

Proteins. The agricultural production of soy, mainly for food, has been increasing. The other common uses of soy protein are in adhesives, films, and bio-plastics. Similarly wheat gluten is a protein extracted from wheat, a traditional crop grown on a large scale in the U.S. and worldwide. A lot of people are allergic to gluten and as a result, gluten free products are available in the market leaving behind large amounts of gluten. There is huge potential market for bio-plastics made of gluten or reinforced gluten.[6, 9, 10, 15] Feather keratin and egg ovalbumin are from the poultry industry. Poultry is a huge market in the U.S. and as a result thousands of tons of waste are generated in the form of feather keratin. The high mechanical strength of

keratin has garnered a lot of attention and investigations are ongoing to use keratin for making bio-plastics.[19-22] The eggs produced on poultry farms have to undergo inspection and the ones that do not pass the inspection are discarded. The discarded eggs can be treated as a renewable source of feedstock.

Almost all of the films and plastics from proteins are prepared using thermal extrusion and/or injection molding. The proteins are mixed with an external agent known as a plasticizer and then extruded for obtaining a coherent film or pellet. The plasticizer function is to lower the glass transition temperature without which the protein films are dry and brittle. The theory is that plasticizer diffuses deep into the structure of proteins thereby breaking the hydrogen bonding and increasing the mobility of chains. This causes a decrease in the glass transition temperature and makes the proteins rubbery at room temperature.[23] The common plasticizers used are water, glycerol, and sorbitol, which are naturally available molecules and synthetically prepared amines such as diethanolamine and triethanolamine.[6, 24] Use of plasticizers has its problems: glycerol and water migrate out of the plastics making them brittle once again[6] and diethanolamine and triethanolamine usage has been avoided since they are potential carcinogens. As an alternate method proteins are blended with other materials to reinforce the properties and mitigate plasticizer migration and loss of modulus from plasticization.[6, 11, 17, 21]

The other potential method to lower the glass transition temperature is through internal plasticization, which is one of the objectives of the current work. The problem with external plasticizers is that the plasticizer and protein are held together by mere physical interactions. This makes the product susceptible to environmental conditions. Instead, if the plasticizer is attached to the protein through covalent interactions, there is a better chance of the product permanently retaining its properties. Proteins are very versatile in nature because of the amino

acids present on them. The amines and thiols present on the protein are perfect sites for protein modifications. It is possible to attach bulky monomers to the proteins at thiol and amine sites using simple nucleophilic reactions.[25] The crystallinity of polymers is mainly due to the hydrogen bonding between hydrophilic groups. The addition of bulky side groups would increase the distance between the protein chains and break the hydrogen bonding. In fact protein modification has been used in many instances mainly in the food industry.[26, 27] Acylation and succinylation of proteins is a common practice in the food industry.[26]

Hydrogels. The other potential market for protein-based products is in the medical industry. Biocompatibility and biodegradability are two desired properties of materials in medicine.[28] Until recently synthetic polymers played a major role in medical applications. However, advances in bio-based materials have shifted focus to using biomaterials. Silk protein is used for stitches in surgery because of its high mechanical properties.[29, 30] The other use of biopolymers is as gene therapy vectors.[31] Natural biopolymers have a natural edge over synthetic materials for medical applications since the body readily accepts them and does not cause any inflammation. Hydrogels are materials that have had some impact on the medical industry. Hydrogels are three dimensional (3D) structures that can retain many times more water than their weight without breaking up. The typical applications of hydrogels are in drug delivery, biosensors, and tissue engineering. For drug delivery and biosensor applications a stimuli-responsive hydrogel is desirable. The ability of the hydrogel to swell or contract with respect to changes in the environment such as pH and temperature is known as stimuli-responsive. Permanently crosslinked hydrogels, physically crosslinked reversible hydrogels and micellar-type hydrogels that are usually formed due to hydrophobic and/or hydrophilic interactions are a few types of commonly used materials.

Synthetic hydrogels are usually prepared using radical polymerization. The monomers and an initiator are added and UV-light or X-rays initiate the reaction.[32] Natural polymers like chitosan, dextran, and proteins in most cases have to be cross linked using small amounts of crosslinker.[32] A variety of crosslinkers are available which can be used for hydrogel synthesis. Annabi et al., synthesized hydrogels by crosslinking α-elastin with hexamethylene diisocyante in the presence and absence of CO_2.[33] Callaird et al., crosslinked soy protein using glyceraldehyde and glutarldehyde.[34] Chiu et al., prepared dextran hydrogels by radical copolymerization of methacrylated dextran with acrylic acid.[35] However in this case an initiation system was required for which ammonium peroxydisulfate and *N*,*N*,*N*′,*N*′-tetramethylethylenediamine were used. In some cases divalent ions have been used to crosslink the polymer chains.[36] Hence there is a lot of flexibility in choosing the crosslinkers. In the case of peptides, they can be designed to either have strong hydrophobic interactions or hydrogen bonding so that hydrogels are formed from self-assembly and not covalent bonding.

For tissue engineering applications biocompatible hydrogels are a must. A growing demand for organ transplants has been evidenced in the last decade. Many times there is a mismatch in the transplantation between the donor and patient. Instead 3D scaffolds can be used for most purposes as extracellular matrices (ECM) and the patient's own organ cells can be regenerated on it.[37] However for the cells to grow, a peptide cell receptor sequence such as arginine, glycine, and aspartic acid (RGD) is needed. This sequence is attached to the hydrogels chemically.[38] For instance Rowley et al., conjugated a pentapeptide GRGDY (Y = Tyrosine) to alginate which is an anionic polysaccharide and crosslinked it with Ca^{2+} ions. The hydrogels were used to grow myoblasts and as can be seen in Figure 1 the hydrogel with GRGDY sequence seeded after 4h

while nothing grew on the control which is just crosslinked alginate. The cell density of myoblasts increased over a period of 3 days.

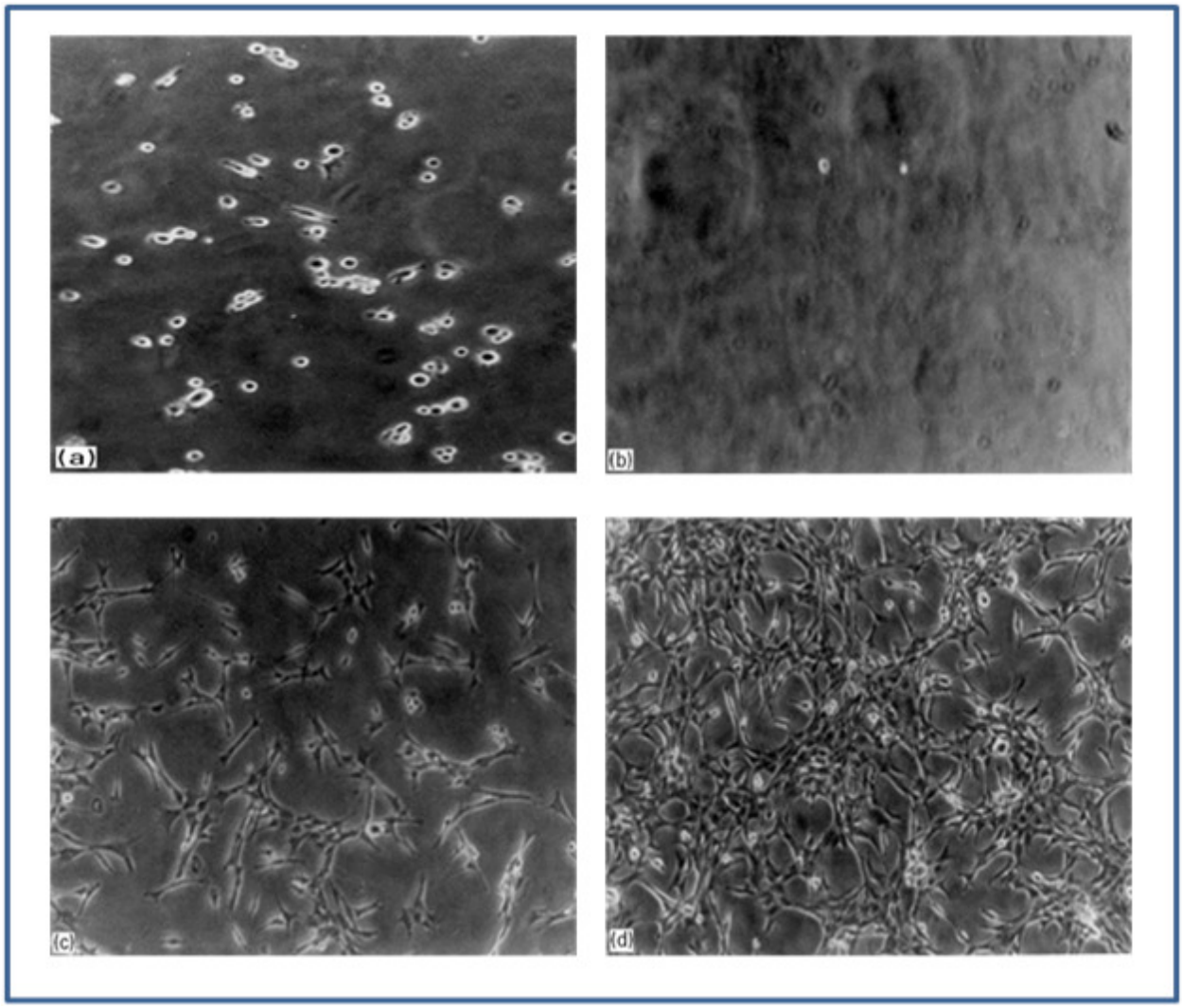

Figure 1. Photomicrographs of myoblasts adherent to alginate hydrogel surfaces after medium changing at 4 h post-seeding on GRGDY-modified surfaces (a), and control alginate surfaces (b).The myoblasts on GRGDY-modified alginate spread extensively after 24 h of culture (c), and proliferated greatly between days one and three (d). Reproduced from Rowley et al.,[36] with permission. Copyright 1999 Elsevier Science Ltd.

Even if synthetic hydrogels are biocompatible they usually can not be biodegraded which is required in most cases. Hence biodegradable natural polymers are preferred. Proteins are desired for scaffold applications because they are very similar in nature to natural extra cellular matrices. In fact collagen and elastin are natural extra cellular matrices (ECM) found in the body. Skin is made up of elastin while bone mainly consists of collagen with hydroxyapatite deposited in it. With synthetic polymers it is difficult for biomineralization to take place. Hence proteins are very much suited for tissue engineering applications. Silk was one of first proteins to be tried for biomedical applications.[29, 30, 38-40] Hydrogel synthesis from collagen and elastin proteins has also been attempted.[33, 41-43] Elastin is the protein of choice as it is rubbery and exhibits high toughness, a useful characteristic for hydrogels[44]. However elastin and collagen once they are removed from native conditions through extraction tend to lose physical and mechanical properties. In the case of extracted elastin it is insoluble in aqueous media making it a challenge to prepare hydrogels out of it. Moreover elastin is scarce in availability and expensive. Hence attempts were made to synthesize peptides with an elastin-like sequence using either genetic engineering methods or solid state peptide synthesis.[44-47] Solid state peptide synthesis is possible only for short peptide segments while *de novo* synthesis of proteins is usually an expensive task and the yields of proteins from fermentations are usually low limiting their availability on a large scale.[48]

As an alternative to this problem, naturally available proteins like soy, gluten and ovalbumin can be used to create 3D scaffolds with elastin-like properties. Our approach is to modify the amines and thiols present on the protein with both hydrophilic or hydrophobic groups and crosslink them with a crosslinking agent. The reactions are based on simple nucleophilic addition reactions known as Michael-type addition reactions. As will be shown in Chapter V, the

properties can be tuned by changing the chemistry of substituent, i.e., hydrophobic or hydrophilic.

Michael addition reactions. Also known as conjugate addition reactions these reactions are named after Arthur Michael.[49] A nucleophile known as a Michael donor reacts with an activated electrophilic alkene (olefin) also called a Michael acceptor and adds on to the carbon – carbon double bond. A mechanism of carbon Michael addition reaction is shown in Figure 2. The ethyl acetoacetate forms an enolate anion in the presence of a base catalyst. The anion which is a Michael donor then reacts with acrylate at the 1,4 ethyl acetoacetate site. The carbonyl present on the acrylate stabilizes the charge until proton transfer occurs and base is regenerated. The site specificity of 1,4 over 1,2 is owing to the enthalpic differences which is a driving force for this reaction.[49]

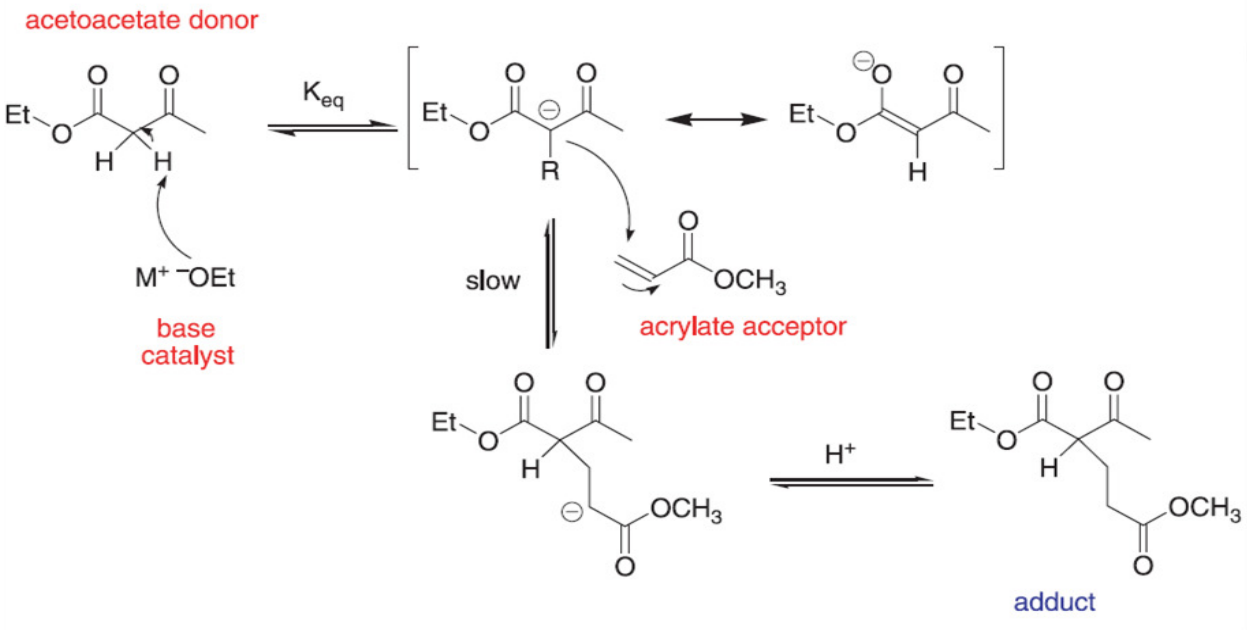

Figure 2. Carbon – Michael addition of Ethyl acetoacetate onto acrylate. Reproduced from Mather et al.,[49] with permission. Copyright 2006 Elsevier Sciences Ltd.

The reactions involving Michael donor groups other than carbon are regarded as Michael - type addition reactions. Amines and thiols fall into this category. Amines are strong nucleophiles and hence do not need any base while weak base is required to activate the thiols. It is also worth noting that secondary amines are more nucleophilic than primary amines.[49] However, the reaction also depends on the steric environment of the molecules and hence secondary amines might not react if there is steric hindrance. As for Michael acceptors, a variety of groups are available that have electron withdrawing capability. Vinyl sulfone, acrylates, and acrylamides can all be used for conjugate addition reactions.

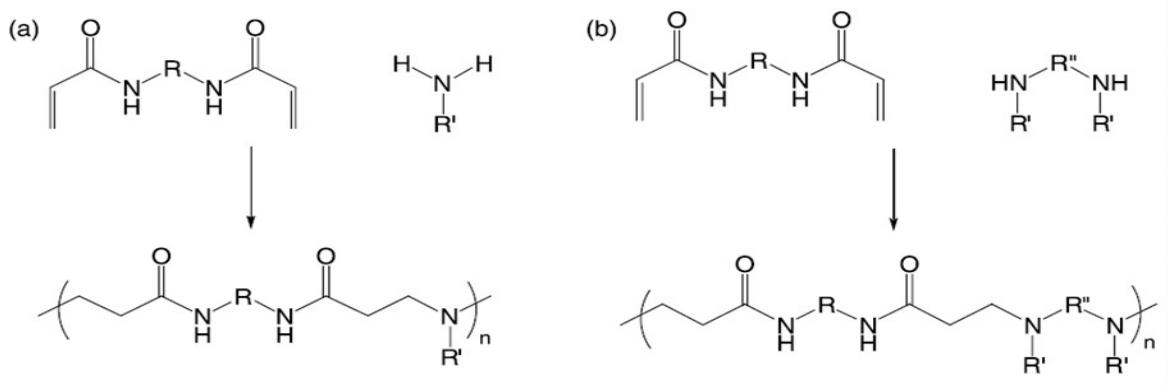

Figure 3. Poly (amido amine) synthesis via (a) primary and (b) secondary amines. Reproduced from Mather et al.,[49] with permission. Copyright 2006 Elsevier Sciences Ltd.

Michael – type addition reactions of amines are also referred to as aza - Michael addition reactions and can be seen in Figure 3. As mentioned above both primary and secondary amines participate in the reaction. Figure 3 (a) shows that the polymerization of bisacrylamide is accomplished using primary amines and polymerization of the same with secondary amines is shown in Figure 3 (b). These reactions take place in water at room temperature. The rate of reaction is faster in protic solvents like water and alcohol while it slows down when aprotic

solvents are used. Also, in aprotic solvents the final molecular weight of the polymer usually remains low.[49] Michael addition of primary and secondary amines to acetonitrile in the presence of lipase catalyst in toluene at room temperature was reported by de Souza et al.[50]

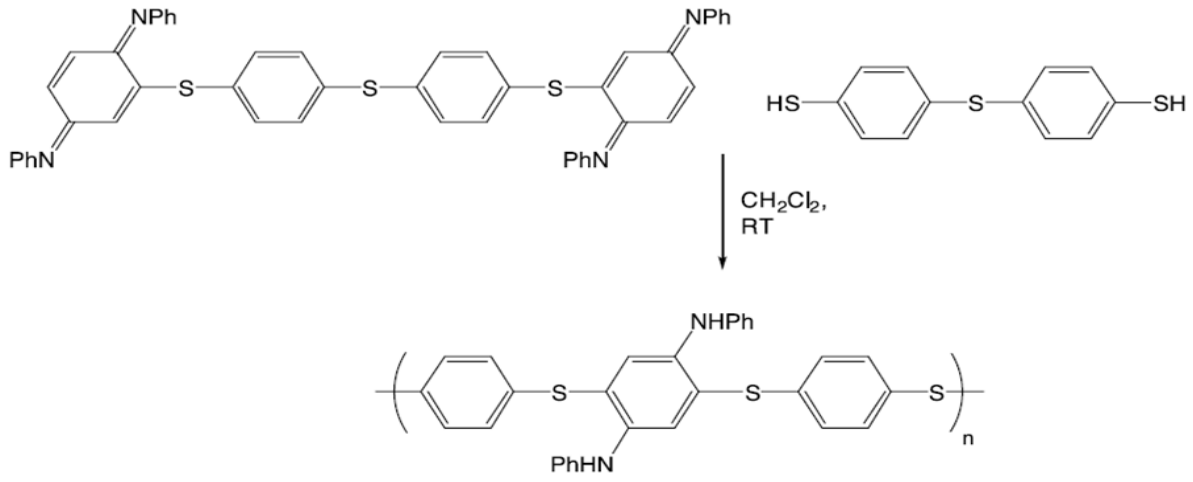

Figure 4. Polymerization of poly(thiophenylene) via Michael addition and oxidation. Reproduced from Mather et al.,[49] with permission. Copyright 2006 Elsevier Sciences Ltd.

Yamamoto et al.,[51] synthesized electro-responsive polymers by first reducing the *N*,*N*′-Diphenyl-1,4-phenylenediamine (PDA) to *N*,*N*'-diphenyl-1,4-phenylenediimine (PDI) and then crosslinking it with thiols at room temperature. These suggest the utility of Michael – type addition reactions in modifying the amine and thiol groups present on the protein (Figure 4). Michael – type additions on proteins have been reported in the literature. Ranucci et al.,[52] obtained modified bovine serum albumin (BSA) and human serum albumin (HSA) by grafting them with poly(aminoamine). Bovine erythrocyte superoxide dismutase was modified with polyethylene glycol derivatives for its applications in the medical industry.[53] Hydrogels were prepared by crosslinking polyethylene glycol with peptides containing thiols at the ends.[54]

Michael – type reactions with proteins can be run at physiological conditions in water. However, faster reaction kinetics can be achieved by running the reactions at higher pH. Sereikaite et al.,[55] crosslinked bovine serum albumin (BSA) with divinyl sulfone (DVS) and also prepared glycine dimers by crosslinking them with DVS. In this study, it was found that although the reaction ran well at physiological conditions, the reaction constant increased with an increase in pH. Also, high dimer yield was achieved at higher pH in less time. These simple yet

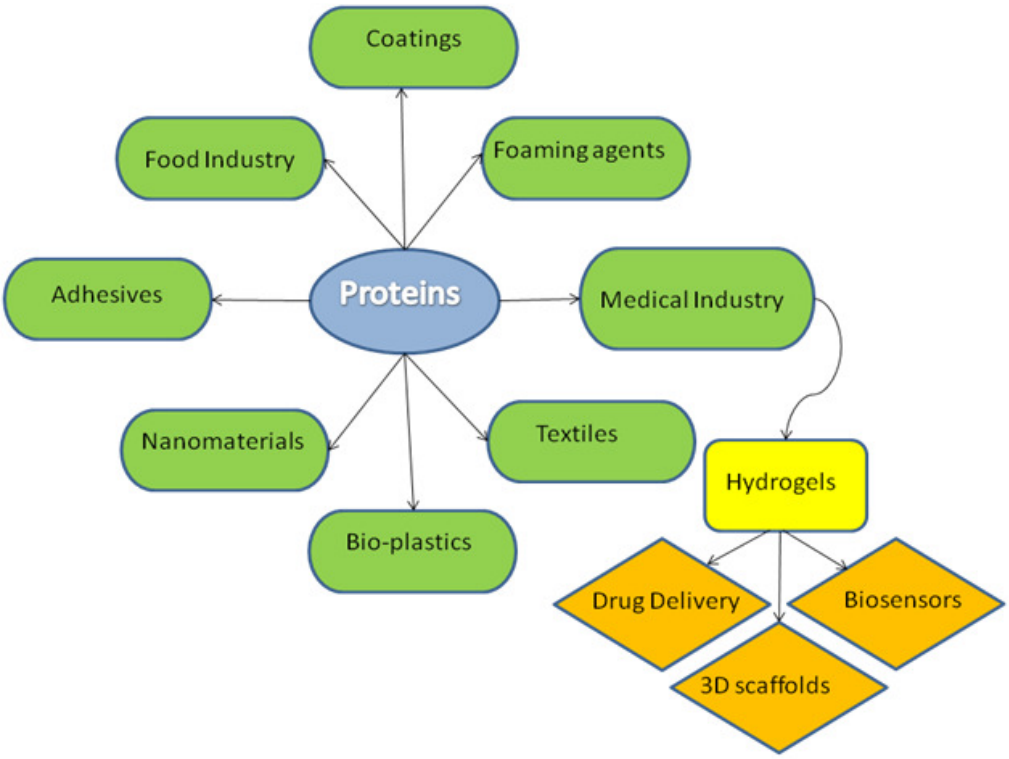

Figure 5. A schematic showing potential applications of modified proteins.

powerful reactions have been used in the current work to modify proteins and amino acids making them useful for a variety of applications. A summary of the uses of modified proteins is shown in Figure 5.

Model protein. Egg ovalbumin was used as the model protein in the current study. It has 385 amino acids with a molecular weight of 49670 g/mol.[56] It is semi crystalline, 50% polar and 50% non-polar and all the natural amino acids are represented. This makes ovalbumin a suitable candidate as a model protein. The sequence of amino acids present in ovalbumin is given in Figure 6 while the amino acid percentages can be found in Table 1. As shown in Table 1 it has 6 cysteine, 20 lysine, and 7 histidine residues. The cysteines are usually bonded to each other with disulfide linkages leaving only lysine and histidine as the possible sites for Michael – type addition reactions if the cystine bond is not reduced. However, we will show that there is a chance of other amine containing side chains present in the protein participating in the reaction along with secondary amines present on the backbone. As mentioned above efforts were made to create fibers from ovalbumin as early as the 1930's.[1] Bio-plastic preparation from egg white has been reported recently[8]. The focus of the current study is to prepare different biomaterials from ovalbumin using environmentally benign reactions and establish a protocol that can be used as a guide to modify other proteins.

GSIGAASMEFCFDVFKELKVHHANENIFYCPIAIMSALAMVYLGAKDSTRTQINKVVRF
DKLPGFGDSIEAQCGTSVNVHSSLRDILNQITKPNDVYSFSLASRLYAEERYPILPEYLQC
VKELYRGGLEPINFQTAADQARELINSWVESQTNGIIRNVLQPSSVDSQTAMVLVNAIVF
KGLWEKAFKDEDTQAMPFRVTEQESKPVQMMYQIGLFRVASMASEKMKILELPFASGT
MSMLVLLPDEVSGLEQLESIINFEKLTEWTSSNVMEERKIKVYLPRMKMEEKYNLTSVL
MAMGITDVFSSSANLSGISSAESLKISQAVHAAHAEINEAGREVVGSAEAGVDAASVSEE
FRADHPFLFCIKHIATNAVLFFGRCVSP

Figure 6. Egg ovalbumin sequence[57]. The letters in Green represent the Lysine (K) and Histidine (H) sites that have been shown to participate in addition reactions.

Table 1. Amino acids present on ovalbumin. Individual molecular weight, polarity, hydropathy and total molecular weight are shown.

Amino Acid	Molecular weight (Da)	Polarity	Hydropathy	Total # of each amino acid	Total M. Wt. of each amino acid (Da)
Alanine, Ala, A	89	nonpolar	1.8	34	3026
Arginine, Arg, R	174	polar	-4.5	15	2610
Asparagine, Asn,	132	polar	-3.5	17	2244
Aspartic Acid,	133	polar	-3.5	14	1862
Cysteine, Cys, C	121	polar	2.5	6	726
Glutamic Acid,	147	polar	-3.5	33	4851
Glutamine, Gln,	146	polar	-3.5	16	2336
Glycine, Gly, G	75	nonpolar	-0.4	19	1425
Histidine, His, H	155	polar	-3.2	7	1085
Isoleucine, Ile, I	131	nonpolar	4.5	25	3275
Leucine, Leu, L	131	nonpolar	3.8	32	4192
Lysine, Lys, K	146	polar	-3.9	20	2920
Methionine,	149	nonpolar	1.9	16	2384
Phenylalanine,	165	nonpolar	2.8	20	3300
Proline, Pro, P	115	nonpolar	-1.6	14	1610
Serine, Ser, S	105	polar	-0.8	38	3990
Threonine, Thr,	119	polar	-0.7	15	1785
Tryptophan,	204	nonpolar	-0.9	3	612
Tyrosine, Tyr, Y	181	polar	-1.3	10	1810
Valine, Val, V	117	nonpolar	4.2	31	3627
TOTAL				385	49670

Nanomaterials. One of the potential applications of proteins and amino acids is in the nanomaterials industry. As the name suggests nanomaterials are materials whose size is 10^{-9} meter and can be seen only through sophisticated equipment. If a material measures from 1-100 nm at least in one of the dimensions then it can be termed as a nanomaterial.[58] Higher functionality and better properties can be achieved by using nanomaterials. This is because as the size decreases the surface area increases thereby increasing the thermal, mechanical and/or optical properties of the material.[59]

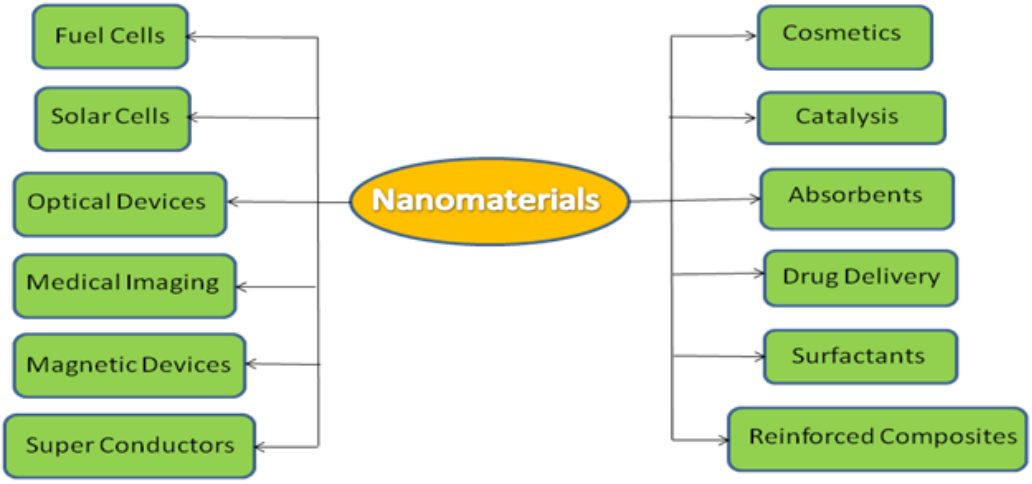

Figure 7. Current and potential applications of nanomaterials.

Nanomaterials are available in different shapes and new shapes are being reported every year.[58] The current applications of nanoparticles are enormous and are expected to increase as more and more new materials are being developed.[58, 59, 60] Figure 7 shows some of the current and potential applications of nanomaterials. The downside of nanotechnology is that the increase in new nano-sized particles is also increasing new types of contamination.[58] For instance, carbon nanotubes are increasingly being researched for their use in various applications. As a result the

production of nanotubes is growing and so is the human exposure to these nanotubes. In a study it was revealed that carbon nanotubes enter into the body mainly through inhalation and cause damage to DNA.[58] Bio-based materials that are also biodegradable could play an important role in minimizing the contamination risks.[61] This motivated us to synthesize nanoparticles using amino acids.

Amino acids. As mentioned above amino acids can be used for the synthesis of nanomaterials. There are twenty natural amino acids from which proteins are made. The list of amino acids is given in Table 1. The amino acids are categorized as either polar or nonpolar. They are natural products of metabolism in microorganisms and hence can be easily produced on a large scale using fermentation.[62, 63] The major utilities of amino acids are as diet supplements and nitrogen sources in fermentations.[64] With advances in technology amino acids are increasingly being used for more and more applications. Small to medium chain peptides are often used for drug delivery and stimuli-responsive hydrogel preparations.[44, 54, 65, 66] Drug templates conjugated with oligomeric peptides made from amino acids have been shown to enhance permeation into membranes thereby increasing drug activity.[65] For instance, the permeation of low molecular weight heparin was enhanced by conjugating it with 4 arginine oligomers.[65] Polymer thiolated with cysteine was shown to increase the absorption of insulin from the GI tract.[65] The use of peptides for hydrogel applications was previously mentioned in this chapter. The other important use of amino acids has been in the synthesis of nanomaterials. Nanofibers were successfully prepared from polyalanine peptide chains. [67, 68] Polylysine has been used in the preparation of nanocomposites along with carbon nanotubes.[69] Nanomaterials have been prepared not only from peptide segments but individual amino acids. Organogellators which can be used for gene therapy and drug delivery applications have been prepared from

glycine and aspartic acid based dendrons as shown in Figures 8 and 9.[70] Dendrimers from L-lysine were used to prepare self- assembled nanomaterials that could be disassembled using K^+ ions or base.[61] The nanostructures obtained using lysine dendrons can be seen in Figure 10.

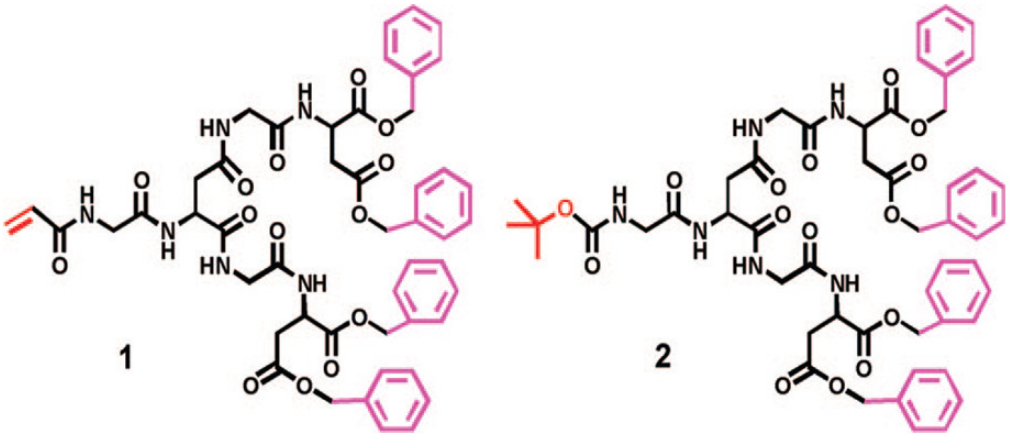

Figure 8. Dendrons prepared from Glycine and Aspartic acid. Reproduced from Kuang et al.,[70] with permission. Copyright 2008 American Chemical Society.

Alanine is the smallest natural amino acid that has chirality and can be used for making nonlinear optic materials which have applications in the fields of photonics and optoelectronics.[71, 72] For optical applications it is desired to grow a huge single crystal. Figure 11 shows the single crystal formed by doping alanine with Zinc Thiourea Chloride (ZTC). The key to success in the nanomaterial industry is to synthesize materials that are environmentally safe and also cheap, which is possible using amino acids and proteins.

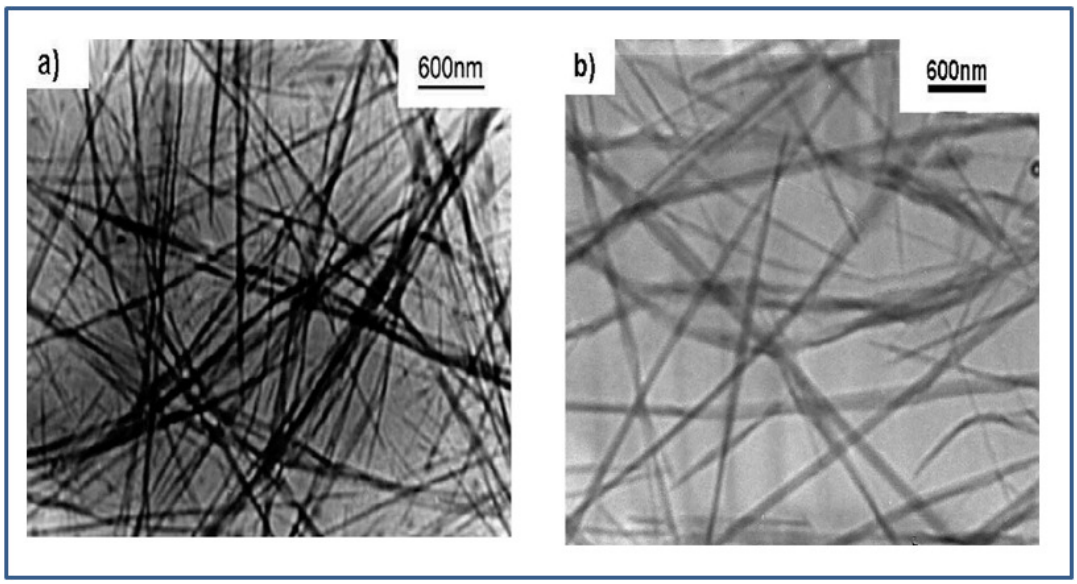

Figure 9. TEM images of xerogel made from 1 in chloroform (a) stained by uranyl acetate. (b) TEM image of a dried dilute gel of 2 in toluene. Reproduced from Kuang et al.,[70] with permission. Copyright 2008 American Chemical Society.

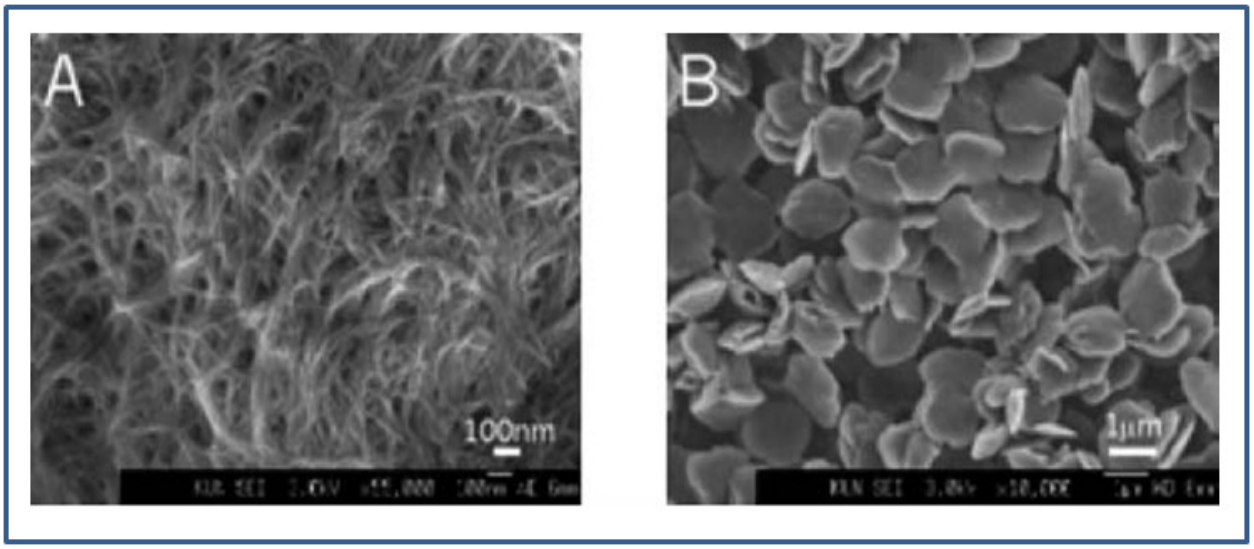

Figure 10. SEM images of materials formed from lysine dendrons using (A) 2 : 1 and (B) 1 : 4.5 dendron : diamine molar ratios. Reproduced from Smith, D.K.[61] with permission. Copyright 2006 Royal Society of Chemistry.

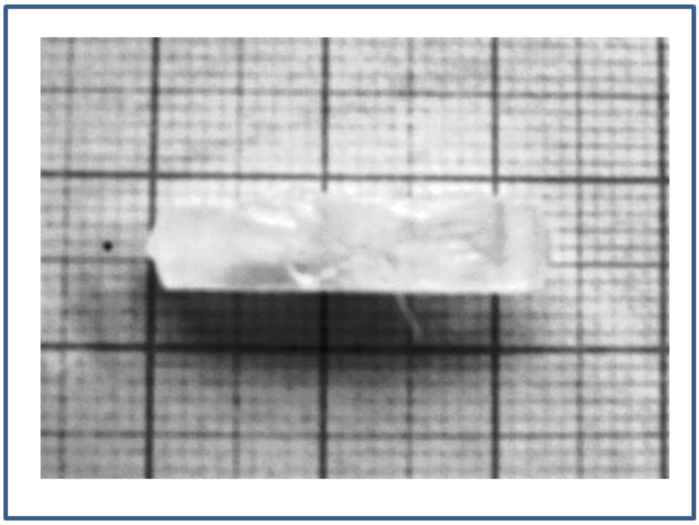

Figure 11. Crystal of Alanine doped with Zinc Thiourea Chloride (ZTC). Reproduced from Dhumane et al.,[71] with permission. Copyright 2008 Springer – Verlag.

Characterization methods. One of the most important aspects in the development of new materials is characterization. Qualitative and quantitative determination of a product or reaction would help minimize process costs by manufacturing the products at a cheaper price. Ever increasing new materials have created concerns about contamination after their disposal and the only way to monitor the products is through qualitative and quantitative estimations.[58] Hence well established techniques will help to trace the product throughout its journey from "cradle to grave". There are a lot of instruments available that can be used depending on the properties of the material. For instance, thermal properties of materials can be characterized using thermo gravimetric analysis (TGA) and differential scanning calorimetry (DSC), and mechanical properties can be measured using dynamic mechanical analysis and tensile testing. Experiment time and the accuracy of results vary from instrument to instrument and also depend on the product. However, fast and accurate characterization of materials is always desired.

Spectroscopic techniques such as Raman and Fourier transform infrared (FTIR) spectroscopy come under the category of methods that can be used for getting accurate results in less time. This is especially true in the case of small molecules, proteins, and amino acids. These complementary techniques are increasingly being used to determine the secondary structure of proteins and polypeptides.[73-78] These methods are mostly used for qualitative determination of products. However, they have the potential to be used for quantitative purposes. One of the aims of this study is to establish a protocol for quantitative estimation of addition reactions in proteins and amino acids using Raman spectroscopy. Below is a brief description of each of the instrument used in this study.

Fourier Transform – Infra Red spectroscopy (FTIR). The chemical groups such as –CH, -CO, -OH, -NH, and –SH present on the polymer absorb infra red radiation giving a unique spectra. Each molecule gives out a unique spectrum and this phenomenon can be taken advantage of to discern the chemical structure of the polymer.[79]

Raman Spectroscopy. Raman is similar to infra red and results from polarization of a molecule upon radiation. Raman spectrum is caused by inelastic collisions of the molecules. Raman is more sensitive to carbon chains (C-C and C=C) which often form the back bone of the polymer chain. Hence this technique reveals complimentary information to infra red spectroscopy. Raman is more commonly used to study the crystalline structure and orientation effects of the polymers.[79]

Differential Scanning Calorimetry (DSC). The glass transition temperature (T_g) and melting temperature (T_m) of polymers can be determined using DSC. It has two samples holders, one with an empty (reference) pan and the other filled with the sample. The differential power required to maintain both the pans at same temperature as a function of heating rate is measured.

A curve is obtained with heat flow on y-axis and temperature on x-axis. The mid point of inflection in the curve is the T_g and T_m is calculated from the slope of the peak that appears on the curve.[79]

Thermogravimetric analysis (TGA). TGA provides a quantitative measurement of mass change in materials as a function of time or heating rate. The sample with known mass is placed in a heating pan which then goes to a heating chamber. The dehydration and thermal degradation occur as the sample is heated at a certain rate and the degraded products escape through a vent. The degradation rate can be used to determine the over all thermal stability of the polymers.

X-ray diffraction (XRD). The structure of the polymer can be identified using XRD. It works on the principle of Bragg's law. When the x-ray's hit the atoms of polymer, they oscillate with the same frequency as the incoming beam. In a crystal with atoms arranged randomly these oscillations are out of phase resulting in the cancellation of energy. However, in a crystal where atoms are arranged in a regular patter, these oscillations are in phase and give rise to constructive interference. This phenomenon leads to a diffraction pattern which in turn can be used to determine the structure of the polymer.[80]

Tensile Tester. The Young's modulus of the materials can be determined using tensile tester. The specimen is subjected to either tension or compression under a certain strain rate and the resulting stress is measured. The slope of the stress – strain curve gives the Young's modulus.

Rheometer. The viscosity and shear modulus as a function of temperature, frequency, applied force or time can be determined using a rheometer. In this study rheometer was used for determining shear modulus as a function of stress. The specimen is placed in between two plates, one stationary and the other moving. The movable plate is oscillated at a fixed frequency while

the stress is varied. Both young's modulus and shear modulus can be correlated using the equation below.

$$E = 2(1 + \nu)G \quad (1)$$

where E is the young's modulus, G is the shear modulus and ν is poisson's ratio.

References

1. Lundgren, H. P.; O'Connell, R. A., Artificial Fibers from Corpuscular and Fibrous Proteins. *Industrial & Engineering Chemistry* **1944,** 36, (4), 370-374.

2. Lawton, J. W., Zein: A history of processing and use. *Cereal Chem.* **2002,** 79, (1), 1-18.

3. Kim, S., Processing and properties of gluten/zein composite. *Bioresour. Technol.* **2008,** 99, (6), 2032-2036.

4. Kim, S.; Sessa, D. J.; Lawton, J. W., Characterization of zein modified with a mild cross-linking agent. *Industrial Crops and Products* **2004,** 20, (3), 291-300.

5. Chiou, B. S.; Robertson, G. H.; Rooff, L. E.; Cao, T.; Jafri, H.; Gregorski, K. S.; Imam, S. H.; Glenn, G. M.; Orts, W. J., Water Absorbance and Thermal Properties of Sulfated Wheat Gluten Films. *J. Appl. Polym. Sci.* **2010,** 116, (5), 2638-2644.

6. Dicharry, R. M.; Ye, P.; Saha, G.; Waxman, E.; Asandei, A. D.; Parnas, R. S., Wheat gluten-thiolated poly(vinyl alcohol) blends with improved mechanical properties. *Biomacromolecules* **2006,** 7, (10), 2837-2844.

7. Gillgren, T.; Barker, S. A.; Belton, P. S.; Georget, D. M. R.; Stading, M., Plasticization of Zein: A Thermomechanical, FTIR, and Dielectric Study. *Biomacromolecules* **2009,** 10, (5), 1135-1139.

8. Jerez, A.; Partal, P.; Martinez, I.; Gallegos, C.; Guerrero, A., Egg white-based bioplastics developed by thermomechanical processing. *J. Food Eng.* **2007,** 82, (4), 608-617.

9. Lagrain, B.; Goderis, B.; Brijs, K.; Delcour, J. A., Molecular Basis of Processing Wheat Gluten toward Biobased Materials. *Biomacromolecules* **2010,** 11, (3), 533-541.

10. Lai, H. M.; Chiang, I. C., Properties of MTGase treated gluten film. *European Food Research and Technology* **2006,** 222, (3-4), 291-297.

11. Mariani, P.; Allganer, K.; Oliveira, F. B.; Cardoso, E.; Innocentini-Mei, L. H., Effect of soy protein isolate on the thermal, mechanical and morphological properties of poly (epsilon-caprolactone) and corn starch blends. *Polym. Test.* **2009,** 28, (8), 824-829.

12. Mooney, B. P., The second green revolution? Production of plant-based biodegradable plastics. *Biochem. J* **2009,** 418, 219-232.

13. Reddy, N.; Yang, Y., Novel Protein Fibers from Wheat Gluten. *Biomacromolecules* **2007,** 8, (2), 638-643.

14. Schilling, C. H.; Karpovich, D. S.; Tomasik, P., Biodegradable Plastics from Soy Protein and Polysaccharide Carboxylates. *Journal of Biobased Materials and Bioenergy* **2009,** 3, (4), 408-417.

15. Wretfors, C.; Cho, S. W.; Hedenqvist, M. S.; Marttila, S.; Nimmermark, S.; Johansson, E., Use of Industrial Hemp Fibers to Reinforce Wheat Gluten Plastics. *J. Polym. Environ.* **2009,** 17, (4), 259-266.

16. Endo, R.; Kamei, K.; Iida, I.; Yokoyama, M.; Kawahara, Y., Physical and mechanical properties of waterlogged wood treated with hydrolyzed feather keratin. *Journal of Archaeological Science* **2010,** 37, (6), 1311-1316.

17. Reddy, N.; Yang, Y. Q., Light-Weight Polypropylene Composites Reinforced with Whole Chicken Feathers. *J. Appl. Polym. Sci.* **2010,** 116, (6), 3668-3675.

18. Barone, J. R., Lignocellulosic Fiber-Reinforced Keratin Polymer Composites. *J. Polym. Environ.* **2009,** 17, (2), 143-151.

19. Barone, J. R.; Arikan, O., Composting and biodegradation of thermally processed feather keratin polymer. *Polym. Degrad. Stab.* **2007,** 92, (5), 859-867.

20. Barone, J. R.; Schmidt, W. F.; Gregoire, N. T., Extrusion of feather keratin. *J. Appl. Polym. Sci.* **2006,** 100, (2), 1432-1442.

21. Barone, J. R.; Schmidt, W. F.; Liebner, C. F. E., Compounding and molding of polyethylene composites reinforced with keratin feather fiber. *Compos. Sci. Technol.* **2005,** 65, (3-4), 683-692.

22. Barone, J. R.; Schmidt, W. F.; Liebner, C. F. E., Thermally processed keratin films. *J. Appl. Polym. Sci.* **2005,** 97, (4), 1644-1651.

23. Reddy, N.; Yang, Y., Biofibers from agricultural byproducts for industrial applications. *Trends Biotechnol.* **2005,** 23, (1), 22-27.

24. Sharma, S.; Hodges, J. N.; Luzinov, I., Biodegradable plastics from animal protein coproducts: Feathermeal. *J. Appl. Polym. Sci.* **2008,** 110, (1), 459-467.

25. Budhavaram, N. K.; Barone, J. R., Quantifying amino acid and protein substitution using Raman spectroscopy. *Journal of Raman Spectroscopy* **2010,** DOI: 10.1002/jrs.2738.

26. Kester, J. J.; Richardson, T., MODIFICATION OF WHEY PROTEINS TO IMPROVE FUNCTIONALITY. *J. Dairy Sci.* **1984,** 67, (11), 2757-2774.

27. Friedman, M.; Pang, J.; Smith, G. A., Ninhydrin-Reactive Lysine in Food Proteins. *J. Food Sci.* **1984,** 49, (1), 10-13.

28. Rzaev, Z. M. O.; Dinçer, S.; Piskin, E., Functional copolymers of N-isopropylacrylamide for bioengineering applications. *Prog. Polym. Sci.* **2007,** 32, (5), 534-595.

29. Scheibel, T., Silk - a biomaterial with several facets. *Applied Physics a-Materials Science & Processing* **2006,** 82, (2), 191-192.

30. Vepari, C.; Kaplan, D. L., Silk as a biomaterial. *Prog. Polym. Sci.* **2007,** 32, 991-1007.

31. Mitraki, A.; Raaij, M. J., Folding of β-Structured Fibrous Proteins and Self-Assembling Peptides. In *Protein Nanotechnology*, Vo-Dinh, T., Ed. Humana Press: Totowa, NewJersey, 2005; Vol. 300, pp 125-140.

32. Baroli, B., Hydrogels for tissue engineering and delivery of tissue-inducing substances. *J. Pharm. Sci.* **2007,** 96, (9), 2197-2223.

33. Annabi, N.; Mithieux, S. M.; Boughton, E. A.; Ruys, A. J.; Weiss, A. S.; Dehghani, F., Synthesis of highly porous crosslinked elastin hydrogels and their interaction with fibroblasts in vitro. *Biomaterials* **2009,** 30, (27), 4550-4557.

34. Caillard, R.; Remondetto, G. E.; Mateescu, M. A.; Subirade, M., Characterization of Amino Cross-Linked Soy Protein Hydrogels. *J. Food Sci.* **2008,** 73, (5), C283-C291.

35. Chiu, H.-C.; Lin, Y.-F.; Hsu, Y.-H., Effects of acrylic acid on preparation and swelling properties of pH-sensitive dextran hydrogels. *Biomaterials* **2002,** 23, (4), 1103-1112.

36. Rowley, J. A.; Madlambayan, G.; Mooney, D. J., Alginate hydrogels as synthetic extracellular matrix materials. *Biomaterials* **1999,** 20, (1), 45-53.

37. Drury, J. L.; Mooney, D. J., Hydrogels for tissue engineering: scaffold design variables and applications. *Biomaterials* **2003,** 24, (24), 4337-4351.

38. Bini, E.; Foo, C. W. P.; Huang, J.; Karageorgiou, V.; Kitchel, B.; Kaplan, D. L., RGD-functionalized bioengineered spider dragline silk biomaterial. *Biomacromolecules* **2006,** 7, (11), 3139-3145.

39. Wharram, S. E.; Zhang, X. H.; Kaplan, D. L.; McCarthy, S. P., Electrospun Silk Material Systems for Wound Healing. *Macromolecular Bioscience* **2010,** 10, (3), 246-257.

40. Fang, J.-Y.; Chen, J.-P.; Leu, Y.-L.; Wang, H.-Y., Characterization and Evaluation of Silk Protein Hydrogels for Drug Delivery. *Chemical & Pharmaceutical Bulletin* **2006,** 54, (2), 156-162.

41. Leach, J. B.; Wolinsky, J. B.; Stone, P. J.; Wong, J. Y., Crosslinked [alpha]-elastin biomaterials: towards a processable elastin mimetic scaffold. *Acta Biomaterialia* **2005,** 1, (2), 155-164.

42. Mao, C.; Kisaalita, W. S., Characterization of 3-D collagen hydrogels for functional cell-based biosensing. *Biosens. Bioelectron.* **2004,** 19, (9), 1075-1088.

43. Spencer, N. J.; Cotanche, D. A.; Klapperich, C. M., Peptide- and collagen-based hydrogel substrates for in vitro culture of chick cochleae. *Biomaterials* **2008,** 29, (8), 1028-1042.

44. Chow, D.; Nunalee, M. L.; Lim, D. W.; Simnick, A. J.; Chilkoti, A., Peptide-based biopolymers in biomedicine and biotechnology. *Materials Science & Engineering R-Reports* **2008,** 62, (4), 125-155.

45. Lim, D. W.; Nettles, D. L.; Setton, L. A.; Chilkoti, A., Rapid Cross-Linking of Elastin-like Polypeptides with (Hydroxymethyl)phosphines in Aqueous Solution. *Biomacromolecules* **2007,** 8, (5), 1463-1470.

46. Wu, Y.; MacKay, J. A.; R. McDaniel, J.; Chilkoti, A.; Clark, R. L., Fabrication of Elastin-Like Polypeptide Nanoparticles for Drug Delivery by Electrospraying. *Biomacromolecules* **2008,** 10, (1), 19-24.

47. Ghoorchian, A.; Cole, J. T.; Holland, N. B., Thermoreversible Micelle Formation Using a Three-Armed Star Elastin-like Polypeptide. *Macromolecules* **2010,** 43, (9), 4340-4345.

48. Goerke, A. R.; Swartz, J. R., High-level cell-free synthesis yields of proteins containing site-specific non-natural amino acids. *Biotechnol. Bioeng.* **2009,** 102, (2), 400-416.

49. Mather, B. D.; Viswanathan, K.; Miller, K. M.; Long, T. E., Michael addition reactions in macromolecular design for emerging technologies. *Prog. Polym. Sci.* **2006,** 31, 487-531.

50. de Souza, R.; Matos, L. M. C.; Goncalves, K. M.; Costa, I. C. R.; Babics, I.; Leite, S. G. F.; Oestreicher, E. G.; Antunes, O. A. C., Michael additions of primary and secondary amines to acrylonitrile catalyzed by lipases. *Tetrahedron Lett.* **2009,** 50, (17), 2017-2018.

51. Yamamoto, K.; Higuchi, M.; Takai, H.; Nishiumi, T., Novel Synthesis of Electroresponsive Poly(thiophenylene) through a Michael-Type Addition. *Org. Lett.* **2000,** 3, (1), 131-134.

52. Ranucci, E.; Bignotti, F.; Paderno, P. L.; Ferruti, P., MODIFICATION OF ALBUMINS BY GRAFTING POLY(AMIDO AMINE) CHAINS. *Polymer* **1995,** 36, 2989-2994.

53. Yamasaki, M.; Okabe, M.; Suzawa, T.; Yokoo, Y., New PEG2 type polyethylene glycol derivatives for protein modification. *Biotechnol. Tech.* **1998,** 12, (10), 751-754.

54. Lutolf, M. P.; Hubbell, J. A., Synthesis and physicochemical characterization of end-linked poly(ethylene glycol)-co-peptide hydrogels formed by Michael-type addition. *Biomacromolecules* **2003,** 4, (3), 713-722.

55. Sereikaite, J.; Bassus, D.; Bobnis, R.; Dienys, G.; Bumeliene, Z.; Bumelis, V. A., Divinyl sulfone as a crosslinking reagent for oligomeric proteins. *uss. J. Bioorg. Chem.* **2003,** 29, (3), 227-230.

56. Nisbet, A. D.; Saundry, R. H.; Moir, A. J. G.; Fothergill, L. A.; Fothergill, J. E., The complete sequence of Hen-Ovalbumin. *Eur. J. Biochem.* **1981,** 115, 335-345.

57. http://www.ncbi.nlm.nih.gov/protein/157879563?report=genpept&log$=seqview.

58. Englert, B. C., Nanomaterials and the environment: uses, methods and measurement. *J. Environ. Monit.* **2007,** 9, 1154-1161.

59. Aitken, R. J.; Chaudhry, M. Q.; Boxall, A. B. A.; Hull, M., Manufacture and use of nanomaterials: current status in the UK and global trends. *Occup Med (Lond)* **2006,** 56, (5), 300-306.

60. Lines, M. G., Nanomaterials for practical functional uses. *J. Alloys Compd.* **2008,** 449, (1-2), 242-245.

61. Smith, D. K., Dendritic supermolecules - towards controllable nanomaterials. *Chem. Commun.* **2006**, (1), 34-44. (http://dx.doi.org/10.1039/b507416a)

62. Hermann, T., Industrial production of amino acids by coryneform bacteria. *J. Biotechnol.* **2003,** 104, (1-3), 155-172.

63. Leuchtenberger, W.; Huthmacher, K.; Drauz, K., Biotechnological production of amino acids and derivatives: current status and prospects. *Appl. Microbiol. Biotechnol.* **2005,** 69, (1), 1-8.

64. Van De Merbel, N. C.; Zuur, P.; Frijlink, M.; Holthuis, J. J. M.; Lingeman, H.; Brinkman, U. A. T., Automated monitoring of amino acids during fermentation processes using on-line ultrafiltration and column liquid chromatography: application to fermentation medium improvement. *Anal. Chim. Acta* **1995,** 303, (2-3), 175-185.

65. Park, J. W.; Kim, S. K.; Al-Hilal, T. A.; Jeon, O. C.; Moon, H. T.; Byun, Y., Strategies for Oral Delivery of Macromolecule Drugs. *Biotechnology and Bioprocess Engineering* **2010,** 15, (1), 66-75.

66. Ozbas, B.; Kretsinger, J.; Rajagopal, K.; Schneider, J. P.; Pochan, D. J., Salt-triggered peptide folding and consequent self-assembly into hydrogels with tunable modulus. *Macromolecules* **2004,** 37, (19), 7331-7337.

67. Wang, X. C.; Ding, S. J.; Cao, J.; Wu, F. L.; Zhou, C.; Yang, Z. Z., Controlled synthesis of dendritic polyaniline fibers with diameters from nanosize to submicrometersize. *Chin. Chem. Lett.* **2005,** 16, (11), 1523-1526.

68. Zhang, L.; Wan, M.; Wei, Y., Nanoscaled Polyaniline Fibers Prepared by Ferric Chloride as an Oxidant. *Macromol. Rapid Commun.* **2006,** 27, (5), 366-371.

69. Kim, J.-B.; Premkumar, T.; Giani, O.; Robin, J.-J.; Schue, F.; Geckeler, K. E., Nanocomposites of poly(L-lysine) and single-walled carbon nanotubes. *Polym. Int.* **2008,** 57, (2), 311-315.

70. Kuang, G. C.; Ji, Y.; Jia, X. R.; Li, Y.; Chen, E. Q.; Wei, Y., Self-assembly of amino-acid-based dendrons: Organogels and lyotropic and thermotropic liquid crystals. *Chem. Mater.* **2008,** 20, (13), 4173-4175.

71. Dhumane, N. R.; Hussaini, S. S.; Dongre, V. G.; Ghugare, P.; Shirsat, M. D., Growth and characterization of L-Alanine-doped Zinc Thiourea Chloride single crystal (ZTC). *Applied Physics a-Materials Science & Processing* **2009,** 95, (3), 727-732.

72. Kumar, B. S.; Kumar, M. R. S.; Babu, K. R., Growth and characterization of pure and lithium doped L-alanine single crystals for NLO devices. *Cryst. Res. Technol.* **2008,** 43, (7), 745-750.

73. Bandekar, J., AMIDE MODES AND PROTEIN CONFORMATION. *Biochim. Biophys. Acta* **1992,** 1120, (2), 123-143.

74. Barth, A., Infrared spectroscopy of proteins. *Biochimica et Biophysica Acta (BBA) - Bioenergetics* **2007,** 1767, (9), 1073-1101.

75. Kong, J.; Yu, S., Fourier Transform Infrared Spectroscopic Analysis of Protein Secondary Structures. *Acta Biochimica et Biophysica Sinica* **2007,** 39, (8), 549-559.

76. Aliaga, A. E.; Osorio-Roman, I.; Garrido, C.; Leyton, P.; Cárcamo, J.; Clavijo, E.; Gómez-Jeria, J. S.; F, G. D.; Campos-Vallette, M. M., Surface enhanced Raman scattering study of l-lysine. *Vib. Spectrosc* **2009,** 50, (1), 131-135.

77. Edsall, J. T., Raman Spectra of Amino Acids and Related Substances III. Ionization and Methylation of the Amino Group. *The Journal of Chemical Physics* **1937,** 5, (4), 225-237.

78. Gani, D.; Hendra, P. J.; Maddams, W. F.; Passingham, C.; Royaud, I. A. M.; Willis, H. A.; Zichy, V.; Cudby, M. E. A., Fourier transform Raman spectroscopy in the analysis of polypeptides. *Analyst* **1990,** 115, 1313-1318.

79. Fried, J. R., *Polymer Science and Technology*. PTR Prentice Hall: New York, 1995; p 509.

80. Kakudo, M., *X-ray diffraction by polymers*. Kodansha LTD, Elsevier Publishing Company, and American Elsevier Publishing Company, INC.: Tokyo, Amsterdam and Newyork, 1972.

Chapter III

Quantifying amino acid and protein substitution using Raman spectroscopy*

Abstract

Raman spectroscopy can be a powerful tool for the characterization of modified amino acids and proteins. In addition to the potential for quantitative results, it offers the advantage of not requiring any sample preparation. Modification of amines and thiols on amino acids and proteins are common reactions used for medical, biological, food, and agricultural purposes. We hypothesized that the Raman spectrum could be used to quantify the reactions and would be more informative than typical characterization techniques such as the ninhydrin test. To prove the hypothesis, the amino acids alanine, cysteine, and lysine were modified with ethyl vinyl sulfone (EVS) using a nucleophilic addition reaction known as the Michael addition and the product was characterized using Raman spectroscopy. The Raman spectroscopy results were compared to UV-visible spectroscopy results based on ninhydrin analysis of the modified amino acids. The Raman spectroscopy analysis was able to discern site-specific reactions on the amino acids and suggested that more amino acid moieties were substituted than predicted using the ninhydrin test alone. Substitution of the full protein ovalbumin (OA) with EVS showed similar results. The ninhydrin test showed the substitution of primary amines and thiols but could not detect substitution of secondary amines remaining after loss of the primary amine.

Introduction

Protein modification is an important technology in the food and medical industries.[1] Determining whether the modification has taken place is a very critical step for all protein modifications. Qualitative identification is good but quantifying is better. Primary and secondary amines and thiols of individual amino acids and on amino acid side groups in full proteins are some of the easiest groups to chemically modify without damage to the native structure.[2] One of the most common tools used for quantitative analysis of amines and thiols is a ninhydrin based assay.[3-17] Ninhydrin reacts with amine and thiol groups, the absorbance of which can be detected using UV-visible spectroscopy.[3-5] The method developed by Moore and Stein for the determination of α-amine groups is considered a standard procedure.[13] However, unexplained subtleties exist in this process.[3] For instance, ninhydrin is not specific to α-amine groups, reacting with side chain amines and thiols as well, suggesting it is sensitive to, more generally, basic groups.[3-5] Despite these subtleties the ninhydrin reaction is very prominently used, often with variations in standard procedures.[4, 6-9, 14-18] Ninhydrin is often used to determine the lysine content in proteins.[4, 6-8, 17, 18] Friedman *et al*. found that the lysine content of several proteins can be accurately found using ninhydrin in lithium acetate-dimethyl sulfoxide.[7] Beckwith *et al*. determined the lysine content of corn meal using ninhydrin and stannous chloride with aqueous DMSO as solvent.[6] Hseih *et al.* used ninhydrin-ferric reagent to determine lysine content.[8] In this study it was shown that the reagent was specific only to lysine and hence the color reaction was from lysine and not other amino acids. These procedures work well and are well accepted. However, the procedure requires a lot of sample preparation and is in general tedious.

Raman spectroscopy can potentially be used as an alternative to ninhydrin analysis. Raman spectroscopy offers the advantage of being a rapid analysis tool with minimal to no sample

preparation. Raman spectroscopy also has the potential to produce accurate quantitative results. Raman spectroscopy has been traditionally used in the analyses of inorganic molecules and ions.[19, 20] Improvements in Raman spectroscopic techniques have increased its applicability in the areas of biology and pharmaceuticals. Raman spectroscopy is increasingly being used to characterize simple amino acids to complex structures like proteins, enzymes, bacteria, and viruses.[18, 21-33] Raman is insensitive to water and this provides an opportunity to characterize biological materials in solution thereby preserving their biological activity. Specific signature regions of amino acids exist in the Raman signal. For instance, the bulky aryl side group on tyrosine (Y) appears as a doublet at 820-860 cm^{-1} shift.[22] Likewise, the bulky phenylalanine (F) ring appears at 1000 cm^{-1} shift.[27] However, more subtle information on C-C, C-S, and N-H can also be acquired. Stewart and Fredericks studied all the amino acids using Raman spectroscopy and were able to find spectral signatures of each.[34] This study provides a basis for assigning Raman shifts for individual amino acids, data which is scarce in the literature.

For peptides and proteins, Raman spectroscopy has been used to study secondary structure.[24, 31, 35-39] Edwards was able to fully assign all Raman shifts in the keratin FT-Raman spectrum to chemical groups.[40, 41] However, Fourier transform-infrared (FT-IR) spectroscopy is more sensitive to protein secondary structure because it is determined by hydrogen bonding interactions between the polar C=O and H-N groups on neighboring molecules. FT-IR has been used extensively in the quantitative analysis of chemical reactions but there are few reports of Raman spectroscopy usage for the same.[42-47] Yu *et al.* estimated the extent of esterification in acetylated soy proteins based on the ratio of the 1737 cm^{-1} carboxylic Raman shift to the 1003 cm^{-1} Raman shift from phenylalanine.[45] Kuzuhara and Hori correlated the changes in disulfide Raman shifts in the FT-Raman spectrum of keratin with their reduction by thioglycolic acid.[48]

Amino acids, peptides, and proteins can be modified under mild reaction conditions without any damage to the native molecular structure or conformation using a nucleophilic addition reaction known as the Michael addition. First, a nucleophile is deprotonated. Once deprotonated, the nucleophile can donate an electron to an electrophile, in this case a vinyl group. As mentioned above the reaction takes place at room temperature and neutral pH and in an aqueous environment.[2, 49-51] In nucleophilic addition reactions, the rate of reaction can be increased with a pH increase.[52] Both amines and thiols on proteins participate in the reaction and it is possible to control where the reaction takes place based on the reaction pH relative to the pK_a of the amino acid functional group.[2, 49]

In this study, we go beyond the characterization of secondary structure using Raman spectroscopy to show that quantitative chemical results can be achieved. First using single amino acids and then full proteins, we compare the extent of reaction and specific reaction site of functionalized amine and thiol groups measured with Raman spectroscopy against standard protocols.

Materials and Methods

Materials. Technical grade egg ovalbumin (OA), dithiothreitol (DTT, mol. wt. 154.25 g/mol), L-lysine (K, mol. wt. 146.19 g/mol), and L-cysteine (C, mol. wt. 121.15 g/mol) were purchased from Sigma Aldrich (St. Louis, MO). Dialysis membranes with 3,500 g/mol molecular weight cut off and 95% ethyl vinyl sulfone (EVS, mol. wt. 120.17 g/mol) were obtained from VWR (Westchester, PA). L-alanine (A, mol. wt. 89.09 g/mol) was purchased from EMD Chemicals (Gibbstown, NJ). Ninhydrin (mol. wt. 178.18 g/mol) was obtained from MP Biomedicals (Solon, OH). All of the materials were used as obtained without any further modifications.

Substitution. For amino acid substitution, 0.5 g of amino acid was added to 30 ml of pure deionized (DI) water and the pH was adjusted to 9 using 4M NaOH or 3.3M HCl. After the amino acid was completely soluble, the desired amount of EVS was added to the solution and reacted for 24 hr at 30°C. Following reaction, the solution was dried on Teflon-coated aluminum foil for 2 days at ambient conditions.

For ovalbumin substitution, 5 g of OA was added to 50 ml of pure DI water. The pH was adjusted to 9 using borate buffer. To this solution, 0.0017 g (equivalent to moles of cysteine present on OA) DTT was added to solubilize the protein. The solution was stirred for 30 min producing soluble OA. At this point, EVS was added to the OA solution and further stirred at 30ºC for 24 hrs. The solution gelled during reaction. Therefore, water was added to the gelled solution and stirred for 1 hr to produce a solution suitable for dialysis. The reacted solution was dialyzed against pure DI water for 24 hours and the water was changed twice. The dialyzed solution was dried on Teflon-coated aluminum foil at ambient conditions.

Calculation of molar amounts. For the amino acids, the molar amount of EVS was matched to the number of potential reactive groups on the amino acid. For example, alanine had one primary amine, NH_2, on the α-carbon with a dissociation constant of pK_2=9.7. At pH 9, the ratio of deprotonated to protonated primary amine $[NH_2]/[NH_3^+]$ was 0.20. Therefore, 16.7% of the primary amine groups were deprotonated and available for nucleophilic addition reactions with vinyl groups. For primary amines, this value was doubled to represent the fact that secondary amines could also react. However, this assumed the dissociation constant of the secondary amine of the substituted alanine α-carbon was the same as the primary amine and this was potentially a wrong assumption. Similarly, cysteine (pK_2=10.8, side group dissociation constant pK_R=8.3) had $[NH_2]/[NH_3^+]$=0.02 and $[S^-]/[SH]$=4.70 and lysine (pK_2=9.2, pK_R=10.8) had

$[NH_2]/[NH_3^+]$=0.67 for the amine on the α-carbon and $[NH_2]/[NH_3^+]$=0.02 for the side group amine (ε-amine). A similar calculation was performed for the lysine primary and secondary amines, cysteine thiols, and histidine (H, pK_R=6.0) secondary amines of OA yielding 12.6 potential reactive groups (PRG) per OA molecule. The amines of asparagine (N) and glutamine (Q) were not counted because of the poor acid/base properties of the amide side groups. However, it has been shown that these amino acids may have limited reactivity with ninhydrin, showing color at low wavelengths.[3] In addition, the side group of arginine (R) was not counted because the side group dissociation constant, pK_R, was 12.5 yielding very little potential deprotonated groups for nucleophilic addition. The N-terminus of the OA molecule was omitted because of potential post-synthetic modification yielding unreactive groups.[53]

Ninhydrin analysis. Ninhydrin analysis was performed to determine the number of unreacted amine groups in the sample. A protocol described by Hwang and Ederer [14] was followed but ethanol was used instead of 1:1 acetone:butanol solution. Meyer [54] studied the ninhydrin reaction in various solvents and showed that the reaction sensitivity increased with ethanol as the solvent. A 15 mg sample was weighed into tubes and 5 mL of phosphate buffer solution at pH 7.4 added. The tubes were vortexed to solubilize the samples. Finally, 1 mL ninhydrin solution (0.35 g ninhydrin in 10 ml ethanol) was added. A blank was prepared by adding 1 mL of ninhydrin solution to 5 mL of the buffer solution. The tubes were then placed in boiling water and heated for 10 min. After 10 min of reaction the hot tubes were immediately transferred into an ice bath and cooled for 15 min. When ninhydrin reacted with alanine and lysine, a purple color developed whereas a reddish-brown color was observed in ninhydrin-reacted cysteine.

UV-visible spectroscopy. An Evolution 300 UV-visible Spectrophotometer (Thermo Scientific, MA, USA) equipped with VISION Pro software was used for ninhydrin analysis of substituted amino acids and proteins. The samples after reaction were diluted to 29 parts of buffer to 1 part of sample and a wavelength scan was done from 300-700 nm. Peaks in the UV-visible spectrum were compared after normalizing at 300 nm and the ninhydrin control showed no absorbance.

Nitrogen (N) analysis. To determine reaction yields of substituted OA, N analysis was performed using an Elementar Vario MAX CNS Analyzer (Hanau, Germany). The reaction yield was determined by comparing the experimentally determined amount of nitrogen to the expected amount of nitrogen on the substituted protein.

Raman spectroscopy. Characterization of all samples was performed on a Bruker Senterra dispersive Raman spectrometer (Bruker Optics, MA, USA). Protein and amino acid samples were analyzed as dried films without further sample preparation. Each spectrum was collected at 785 nm excitation with a laser power of 100 mW and a spectral resolution of 9-15 cm^{-1}. A 20 x microscope objective was used and sample integration time was 20 s with 10 co-additions. Raman spectra were collected over nine different regions on the sample surface, baseline corrected, and averaged. OPUS software was used for data collection and manipulation.

Results and Discussion

Amino acids. Table I lists relevant shifts in the Raman spectra of the substituted amino acids. Based on the Michael addition reaction mechanism, Raman spectroscopy made it possible to follow the loss of the C=C on EVS, the loss of deprotonated NH on alanine, cysteine, and lysine, and the change in S^- (deprotonated thiol) on cysteine. In the region 3300-2800 cm^{-1} shift there were Raman shifts of large area attributed to amine stretches, ν(NH), and carbon-hydrogen

Table I. Substituted amino acid and protein Raman shifts (cm^{-1}).

Assignment	Alanine	Cysteine	Lysine	Ovalbumin
ν(SH)	-	2573	-	2570
ν(C=C)[a]	1611	1611	1611	1611
δ(CH)	1354	1340	1343	1340
δ(NH_3^+), δ(NH^+)	1141	1127	1150	1167, 1151
δ(NH_2), δ(NH)	1107	1085	1097, 1050	1076
ν(SO_2)[a]	1118	1118	1118	1119
ν(CN)	1012	1035	998	997
NH rock	844	866	855	848
CH on C=C[a]	698	698	698	698
ν(CS)[a]	665	665	665	665
νSS+ν(S^-)	-	491	-	500

[a]on EVS

stretches, ν(CH), but there was a lot of overlap between the amino acids and EVS in this region. Typically, the "fingerprint" region of 1800-0 cm^{-1} shift is utilized because of the many different chemical features that appear. For each amino acid-EVS sample, the spectra were normalized at the CH deformation, δ(CH) at around 1350 cm^{-1}shift, which was a region exclusive to the amino acids. The normalization was to cancel experimental artifacts that may have influenced the intensity. Although the δ(NH) and ν(CN) Raman shifts were discernible in the amino acid spectra, the ν(SO_2) Raman shift interfered with them at moderate EVS concentration, which made it difficult to quantify reactions with them. So it was difficult in principle to monitor the formation of C-N bonds as amines were substituted with EVS. As such, the ν(C=C), CH on C=C, and ν(CS) on EVS and NH rock and thiol/thiolate Raman shifts were used to quantify reactions because the other reactant did not interfere with resolution of these Raman shifts. Ninhydrin reacted with amines to produce Ruhemann's Purple that absorbed in the UV-visible spectrum at 570 nm. UV-vis absorbance at 570 nm showed a rapid decrease in the substitution range [EVS]/[NH]~0-1 with no further change afterwards as shown in Figure 1(a). The

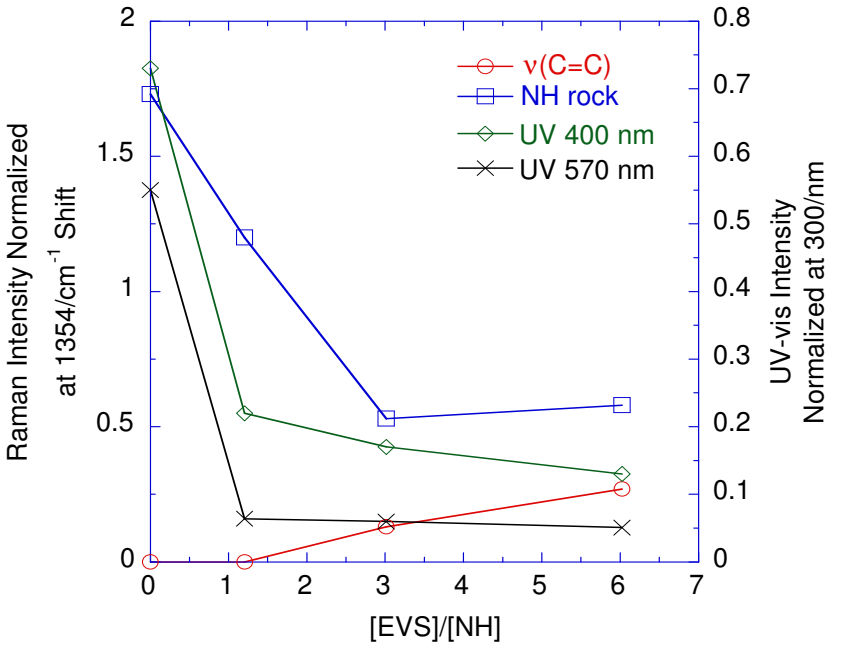

Figure 1(a). The ν(C=C) and NH rock normalized Raman shifts compared to normalized ninhydrin-based UV-vis absorbances. The abscissa is the ratio of EVS added to deprotonated NH on alanine.

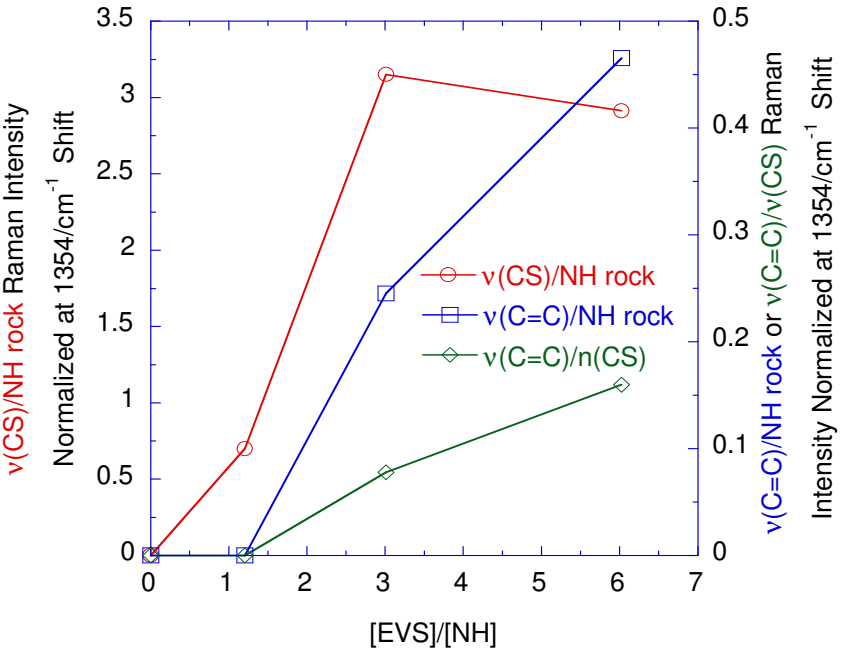

Figure 1(b). Raman shift normalizations of substituted alanine. The abscissa is the ratio of EVS added to deprotonated NH on alanine.

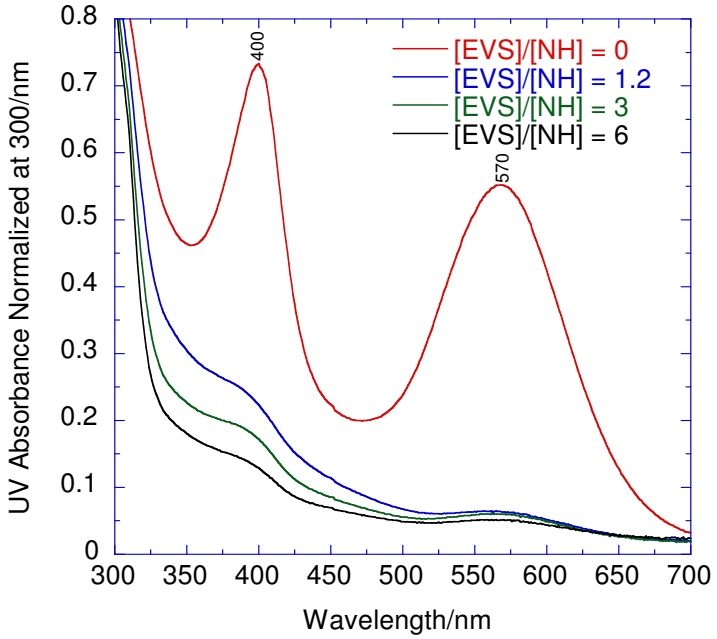

Figure 1(c). Normalized ninhydrin-based UV-vis absorbance of Alanine reacted with EVS in various concentrations.

ninhydrin reaction was also a nucleophilic addition reaction and was dependent on the amount of deprotonated nucleophile available.[55]

In the Raman spectra, ν(C=C) on EVS did not appear until [EVS]/[NH]~1. Therefore, all the EVS reacted with deprotonated amines on alanine up to this point. The amount of NH decreased with reaction but did not stop decreasing at [EVS]/[NH]~1 as evidenced by the NH rock in Figure 1(a). This suggested that NH was reacting further. The ratio ν(CS)/NH rock in Figure 1(b) compares the total amount of EVS to reactive groups on alanine. The ratio ν(C=C)/NH rock compares the reactive groups on EVS to the reactive groups on alanine. The difference between these two ratios quantified the amount of unreacted EVS and it was observed that most of the EVS after [EVS]/[NH]~1 was unreactive, but not all of it. The ratio ν(C=C)/ν(CS) was the

result showing that about 10-20% of the EVS molecules reacted after [EVS]/[NH]~1. In Figures 1(a) and 1(c), the UV-vis absorbance at 400 nm decreased rapidly at [EVS]/[NH]~0-1 then decreased slowly at higher [EVS]/[NH]. It has been suggested that the 400 nm and 570 nm absorbances quantify the same phenomenon.[55] However, the two UV-vis absorbances changed differently with substitution. The Raman spectroscopy results suggested that all EVS reacted up to [EVS]/[NH]~1 but at higher concentrations some EVS reacted and some remained unreacted. Therefore, the 570 nm UV-vis absorbance was not adequate in describing the reaction at all substitutions. Based on the Raman spectroscopy results, the 400 nm absorbance more accurately described the entire substitution. This may have meant that the 400 nm absorbance included contributions from secondary amines after all the primary amines were reacted and that the 570 nm absorbance only considered primary amines. It could also have meant that substitution shifted the pK_2 of alanine to further deprotonate amines for reaction and this was only described by the 400 nm absorbance. Alanine contained only one potential reactive group and the agreement between the 400 nm UV-vis absorbance and the Raman spectral analysis was reasonable.

For EVS-substituted cysteine, similar behavior to EVS-substituted alanine was observed in the UV-vis results and ν(C=C) Raman shift as shown in Figure 2(a) except the UV-vis absorbance values were much lower. For cysteine, the NH rock decreased up to a substitution of [EVS]/[S^-]~1, then increased, suggesting it was finished reacting or at least reaction at the α-carbon NH had slowed considerably at higher substitution. At pH 9, the thiolate ion, S^-, was more prevalent than thiol, which is shown in Figure 2(b) and expected from the pK_R=8.3. As can be seen in Figure 2(d), pure cysteine at pH 7 had a large Raman shift intensity at 2573 cm^{-1} indicative of free SH groups. The ν(SH) Raman shift intensity decreased significantly at pH 9

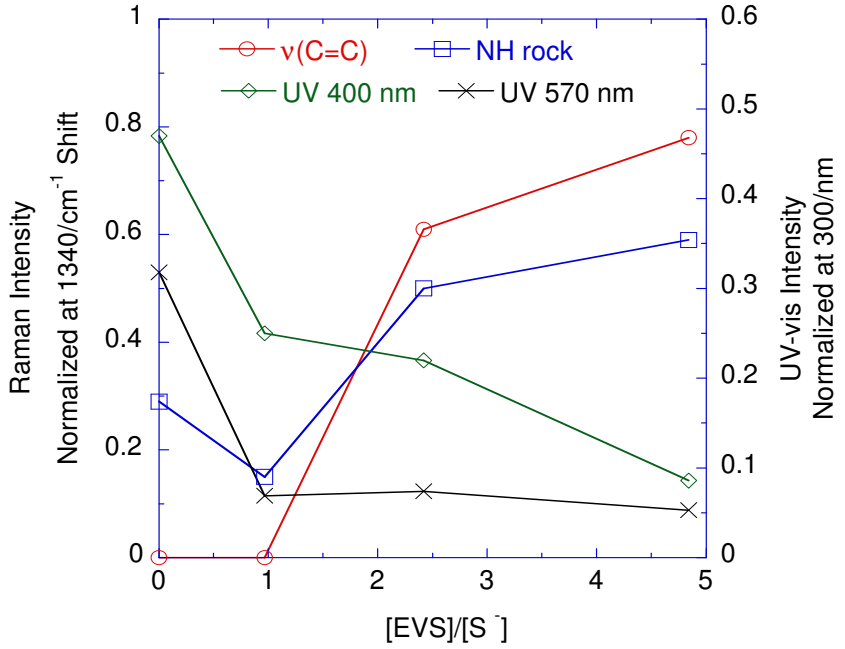

Figure 2(a). The ν(C=C) and NH rock normalized Raman shifts compared to normalized ninhydrin-based UV-vis absorbances. The abscissa is the ratio of EVS added to thiolate (deprotonated thiol, S^-) available on cysteine.

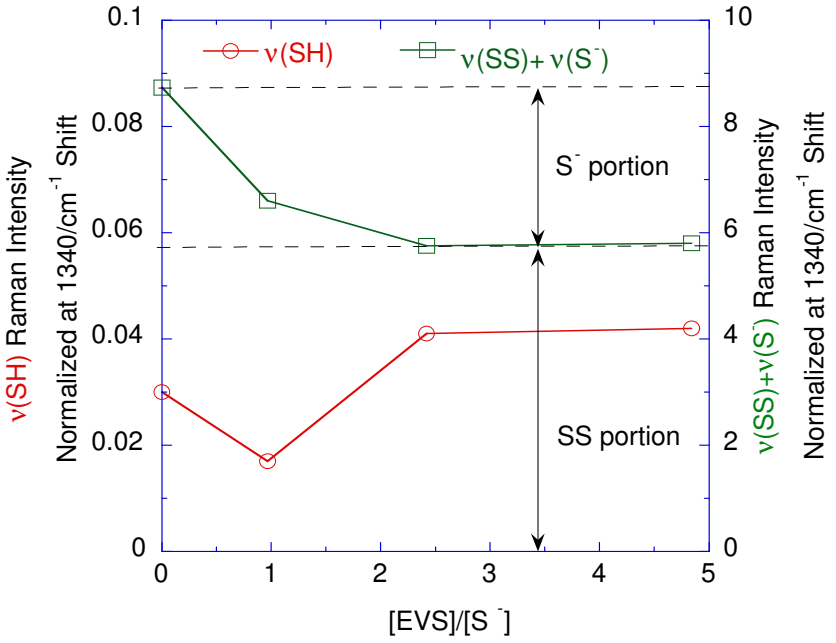

Figure 2(b). Raman shift normalizations of substituted cysteine. The abscissa is the ratio of EVS added to thiolate (deprotonated thiol, S^-) available on cysteine.

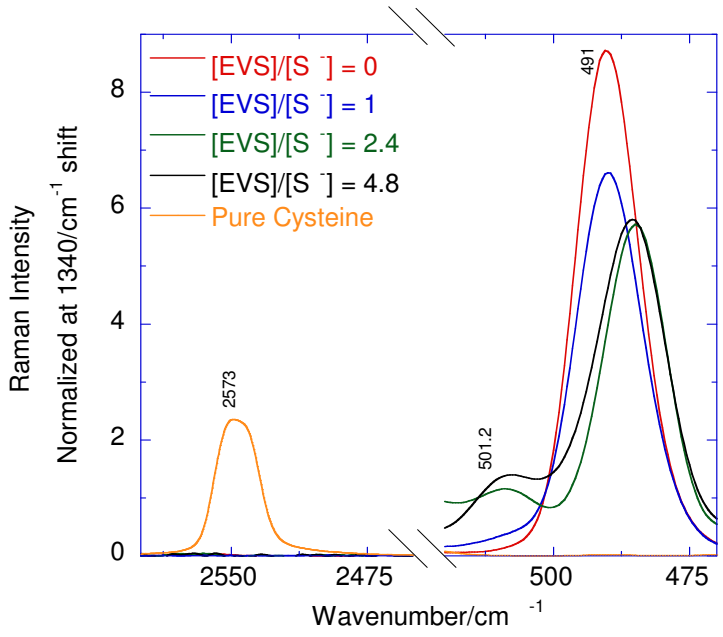

Figure 2(c). Comparison of normalized Raman intensity spectra of pure and substituted Cysteine in the regions 2600 – 2475 cm^{-1} shift (SH bond) and 520 – 470 cm^{-1} (S-S bonds).

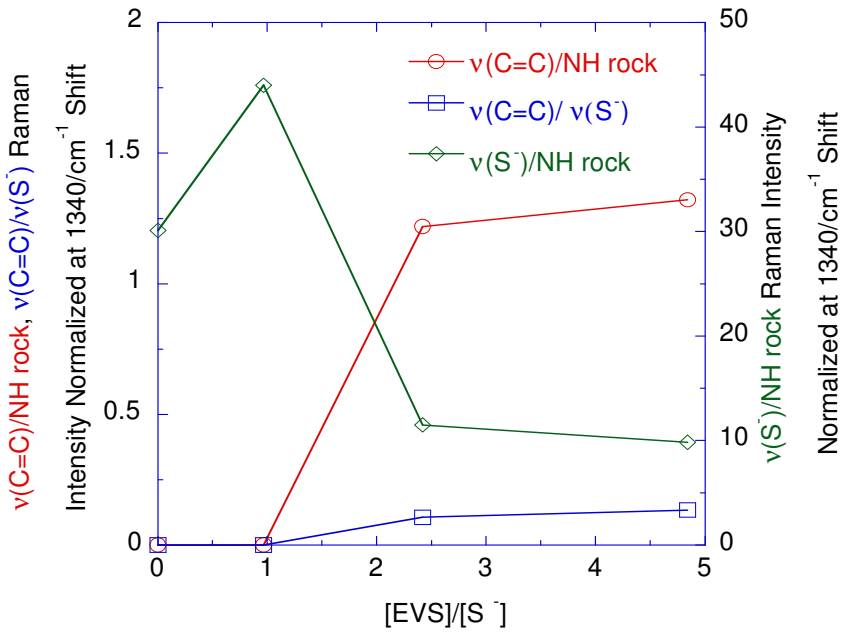

Figure 2(d) Raman shift normalizations of substituted cysteine. The abscissa is the ratio of EVS added to thiolate (deprotonated thiol, S^{-}) available on cysteine.

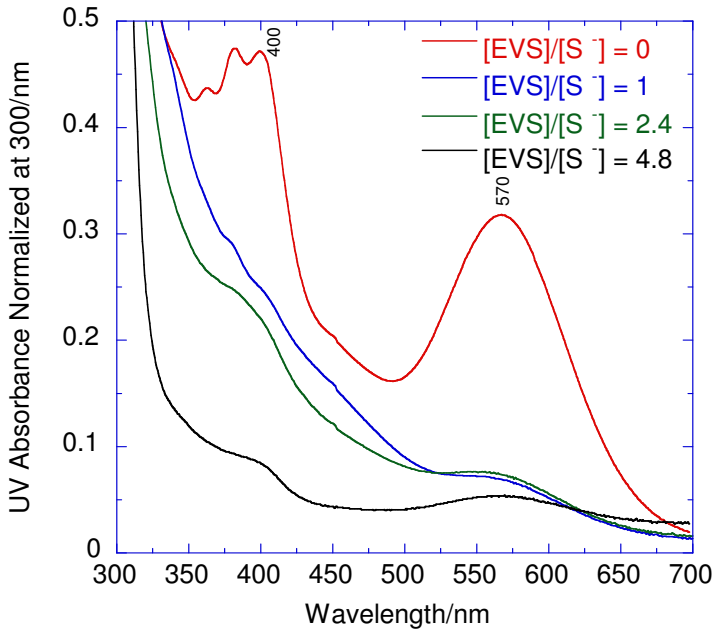

Figure 2(e). Normalized ninhydrin-based UV-vis absorbance of substituted cysteine.

suggesting there was a contribution from thiolate so a portion of the peak was also assigned to even for pure cysteine, i.e., [EVS]/[S^-]=0. There may be some reaction of thiol from [EVS]/[S^-]~0-1 based on the decrease in the Raman shift intensity of ν(SH) that would be dependent on deprotonation with substitution, i.e., a shifting pK_R. However, the very limited reaction stopped at a substitution of about 1. The Raman shift intensity of the thiol was a fraction of a percent of the thiolate so the effect of the thiol relative to existing thiolate was small.

The strong Raman shift at 491 cm^{-1} was assigned to ν(SS), which was a typical assignment. However, this Raman shift changed with substitution in the absence of a reducing agent, (S^-). The contributions of the individual components to the ν(SS)+ν(S^-) Raman shift intensity are shown in Figure 2(b) with SS remaining unchanged and S^- changing because the disulfide was stable and the thiolate was reactive. This also suggested that at pH 9, some cysteines formed

cystine bonds. The amount of thiolate was about 1/3 of the total groups contributing to the 491 cm^{-1} Raman shift intensity. Indeed, the probability of S-S bonding was just as high as S-C-C bonding at these conditions.[2]

The concentration of thiolate ions decreased rapidly up to [EVS]/[S^-]~1 then decreased at a slower rate at higher concentrations. EVS was able to react with deprotonated S^- and NH at low substitution but not equally. For every S^- there was 0.034 NH capable of reacting. The rate of decrease of the ν(NH) and ν(S^-) Raman shifts at [EVS]/[S^-]~0-1 were directly proportional to the reaction rate and describe the rate of consumption of each group with EVS substitution. The slopes were -0.14 for ν(NH) and -2.19 for ν(S^-) indicating that the thiolate was the preferred reaction site.[56]

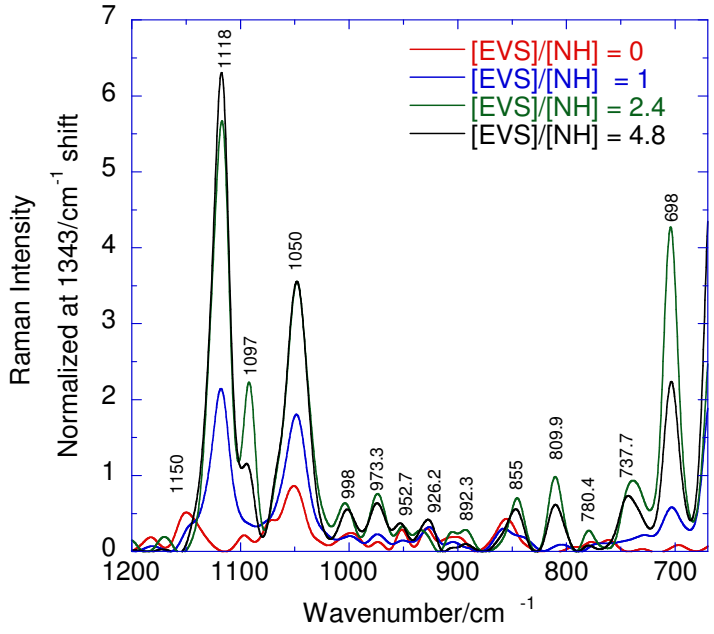

Figure 3(a). Normalized Raman spectra of substituted lysine in the region 1200 – 700 cm^{-1} shift.

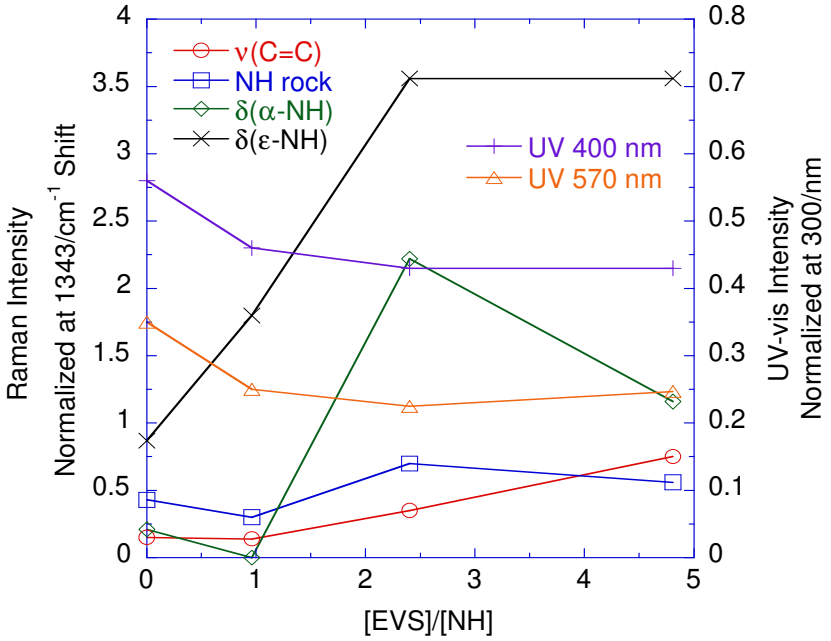

Figure 3(b). The ν(C=C), NH rock, and deformations of α-NH and ε-NH normalized Raman shifts compared to normalized ninhydrin-based UV-vis absorbances. The abscissa is the ratio of EVS added to deprotonated NH available on lysine.

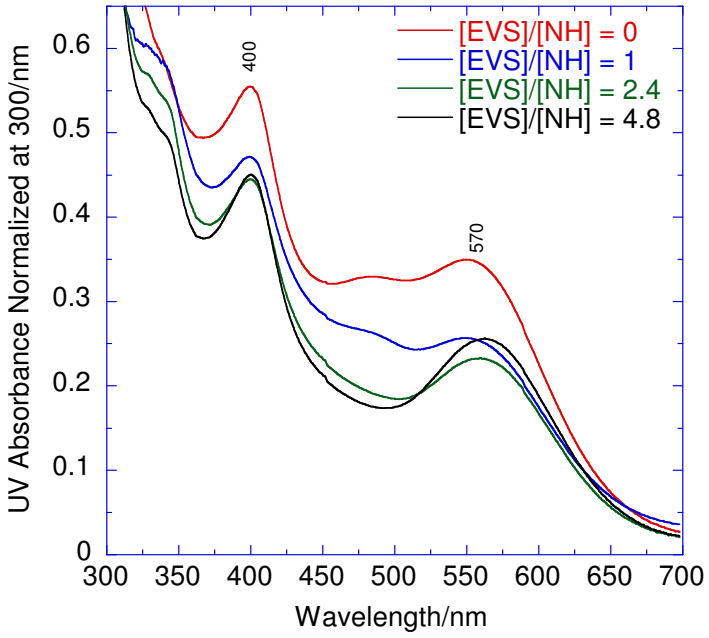

Figure 3(c). Normalized ninhydrin-based UV-vis absorbance of substituted Lysine.

The ratio of ν(C=C)/NH rock increased more than ν(C=C)/ν(S^-) so reaction was favored at S^- as shown in Figure 2(d). In other words, C=C on EVS was not reacting but remaining free relative to NH. Relative to S^-, it was being consumed. The ratio of thiolate to NH increased at low concentration showing that some NH reacted then steadily declined because further reaction at higher EVS concentrations was predominantly at S^-. Re-examining the UV-vis data in Figures 2(a) and 2(e) showed that the 400 nm absorbance was again more definitive in describing reaction and that the initial portion could be assigned to amine reaction and the later portion to thiolate reaction although this was only after considering the Raman spectroscopy data. Raman spectroscopy had a clear advantage over the ninhydrin test with the ability to discern SH, S^-, SS, and NH from the same experiment.[57] Lysine contained two primary amines, one on the α-carbon and one on the side group at the ε-carbon. $pK_2<pK_R$ on lysine making the α-NH_2 25 times more reactive than the ε-NH_2 at pH 9.

For each amino acid, concurrent amine Raman shifts appeared in the ranges of 1150-1127 cm^{-1}, 1107-1085 cm^{-1}, and 1035-998 cm^{-1} shift, all originating from various modes of the NH and CN on the α-carbon. In the lysine Raman spectrum, the ε-NH_2 was discernible as a separate, very large Raman shift at 1050 cm^{-1} as shown in Figure 3(a). For lysine, δ(α-NH) was assigned at 1097 cm^{-1} shift and δ(ε-NH) was assigned at 1050 cm^{-1} shift making it possible to monitor reaction at both amines.

Referring to Figuress 3(b) and 3(c), there was not nearly as much change in the UV-vis absorption as there was with alanine and cysteine and a strong finite absorption existed at high [EVS]/[NH] concentration because there were many amine sites not reacted with EVS that were capable of reacting with ninhydrin. At first glance, Raman shift intensity changes in ν(C=C) and NH rock on lysine as EVS was substituted were similar to alanine and cysteine. Unlike alanine

and cysteine, Figure 3(d) shows that ν(C=C)/NH rock increased slowly at low substitution instead of remaining constant. This meant that there was unreacted EVS relative to total NH.

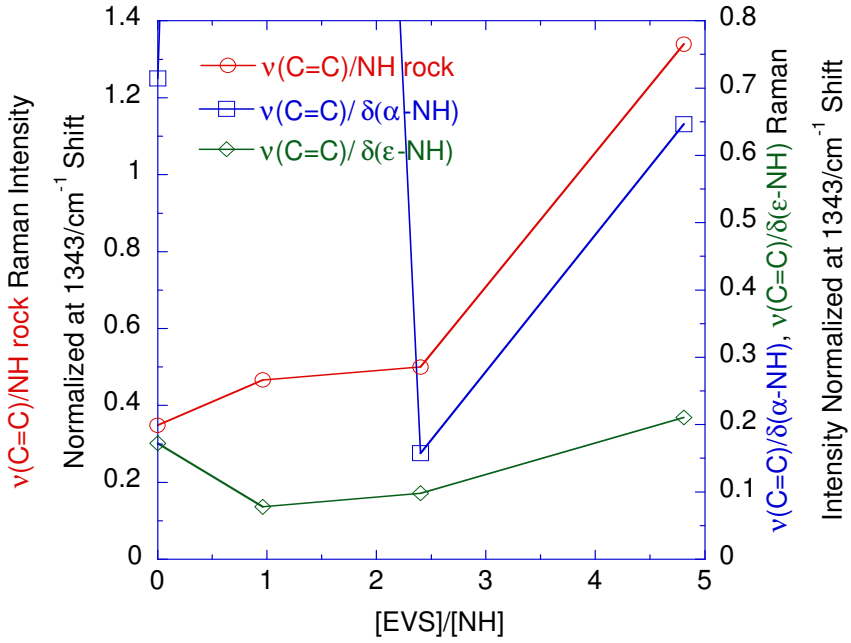

Figure 3(d). Raman shift normalizations of substituted lysine. The abscissa is the ratio of EVS added to deprotonated NH available on lysine.

The abscissa contained the "expected" substitution based on pK_a relative to pH. A substitution of 1 meant all of the expected α- and ε-NH was substituted. Clearly, one was favored over the other.

The δ(NH) Raman shifts could be used to discern where the reaction was happening as a function of EVS substitution. In alanine, EVS reacted with NH_2 thoroughly up to an expected substitution of 1. Further reaction was slower as more NH had to become accessible and there was larger than expected substitution. In cysteine, the thiolate and the α-NH_2 were reacting up

to expected substitutions of 1 with the thiolate the more reactive site. At higher substitutions the thiolate completely dominated the reaction and again substitutions were larger than expected. So the preferred site can be predicted from the pK_a relative to pH but reaction occurred at all available sites when there was opportunity. As the opportunities to react decreased, either the reaction slowed (alanine) or the preferred site dominated (cysteine). For lysine, this was no different as shown in Figures 3(b) and 3(d) where the α-NH was the only reactive site at low substitution and was completely consumed by [EVS]/[NH]~1. Since the ν(C=C)/δ(ε-NH) decreased at [EVS]/[NH]~0-1 it suggested that C=C was decreasing in concentration relative to the ε-NH so EVS was reacting at the α-NH. Fig. 3(a) contains the normalized Raman spectra for substituted lysine. The δ(α-NH) at 1097 cm^{-1} for [EVS]/[NH]=1 was considered to be 0 even though it was difficult to discern the actual peak. This was for several reasons: 1) the ratio ν(C=C)/NH rock increased but ν(C=C)/δ(ε-NH) decreased from [EVS]/[NH]~0-1 so one of the amines had to be consumed faster and it was not the ε-NH, which was strong and easily discernible at any substitution; 2) relative to the adjacent EVS peaks δ(α-NH) was getting smaller even though its absolute value was showing more prominently with EVS substitution; 3) based on the trend of taking the ratio of the adjacent EVS peaks to δ(α-NH), the Raman shift intensity at 1097 cm^{-1} and [EVS]/[NH]=1 should show prominently and it did not. Further reaction at higher substitutions shifted to the ε-NH. The amount of ε-NH relative to EVS was decreasing at higher substitutions thus increasing ν(C=C)/δ(ε-NH). The UV-vis absorbances at 400 nm and 570 nm showed the limited reaction but could not discern whether it was on the α- or ε-amine like the Raman spectroscopy analysis could.

Ovalbumin. The full protein possessed a richer Raman spectrum than the single amino acids and analysis was obscured by too many Raman shifts concurrent with EVS as can be seen in

Figures 4(a) and 4(b). For example, the ν(C=C) Raman shift of EVS was obscured by the Amide I shift of the protein originating in secondary structure not present in single amino acids. Therefore, quantitative analysis of the full protein was more difficult. There was no change in ν(SS), ν(S^-) at 500 cm^{-1} outside of being influenced by the EVS Raman shift at 471 cm^{-1} as shown in Figure 4(c), indicating that the reduced disulfide was re-oxidized to SS and not reactive with EVS. Note that DTT was dialyzed out and did not contribute to the SH or SS/S^- Raman shifts. The biggest difference in the full protein was the lack of an amine on the α-carbon, which was the most reactive site in alanine and lysine. Therefore, the most reactive groups of the amino acids, thiolate and α-amine, were not present in the full protein. Figure 4(d) shows that in absence of a direct measure of C=C from ν(C=C) on EVS, the adjacent ν(CS) or CH on C=C could be used. This was based on the observation of an inflection in the curves at [EVS]/[PRG]~1. Although not exactly the reactive site, the Raman shift from CH on C=C was directly attached to the reactive site and was a reliable peak to quantify the reaction because there was a larger change in ν(CS) indicating simply more CS from unreacted EVS so the CH on C=C and ν(CS) peaks did not behave equally. The NH rock showed a rapid decrease up to an inflection at substitution of [EVS]/[PRG]~1 then a slower decrease. The rapid rise of ν(CS) suggested simply more EVS relative to protein. The CH on C=C and NH rock Raman shifts, with more gradual changes after [EVS]/[PRG]~1 and CH on C=C increasing and NH rock decreasing, indicated that some further reaction occurred but not at the rate that reaction occurred at [EVS]/[PRG]<1, which was also observed in the individual amino acids. The three NH deformations shown in Figure 4(e) show a similar trend. The Raman shift data indicated that the protein was fully reacted at [EVS]/[PRG]~1 to 4, which meant that some side groups may become reactive because they had a changing pK_R as the protein was substituted or arginine,

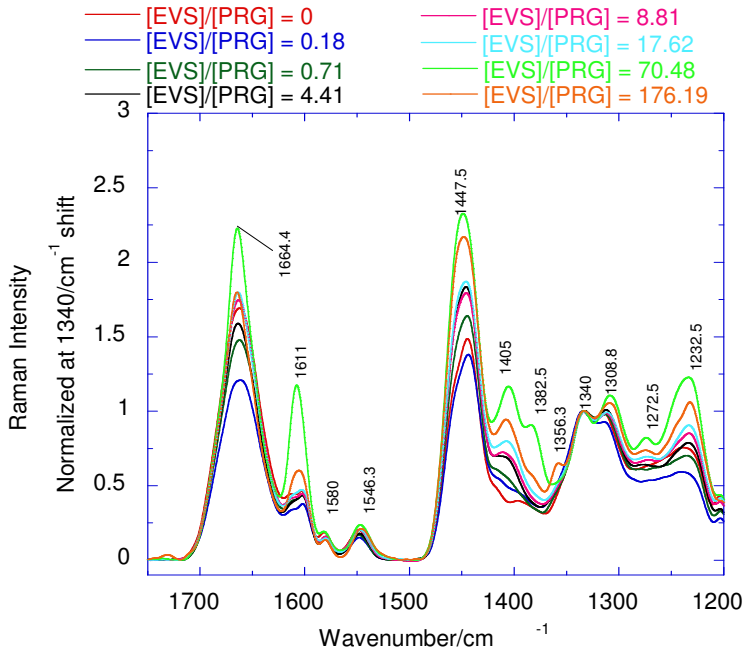

Figure 4(a). Normalized Raman spectra of substituted Ovalbumin in the region 1700 – 1200 cm^{-1} shift.

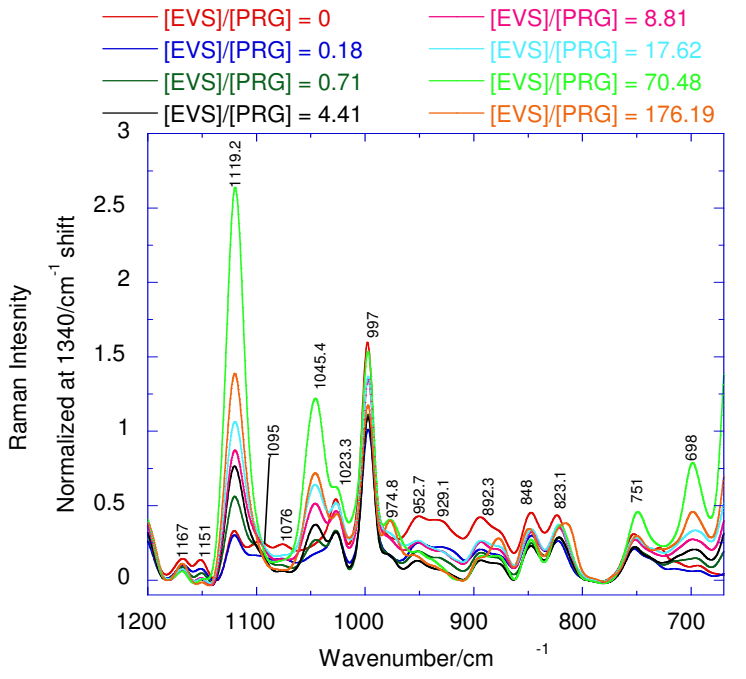

Figure 4(b). Normalized Raman spectra of substituted Ovalbumin in the region 1200 – 700 cm^{-1} shift.

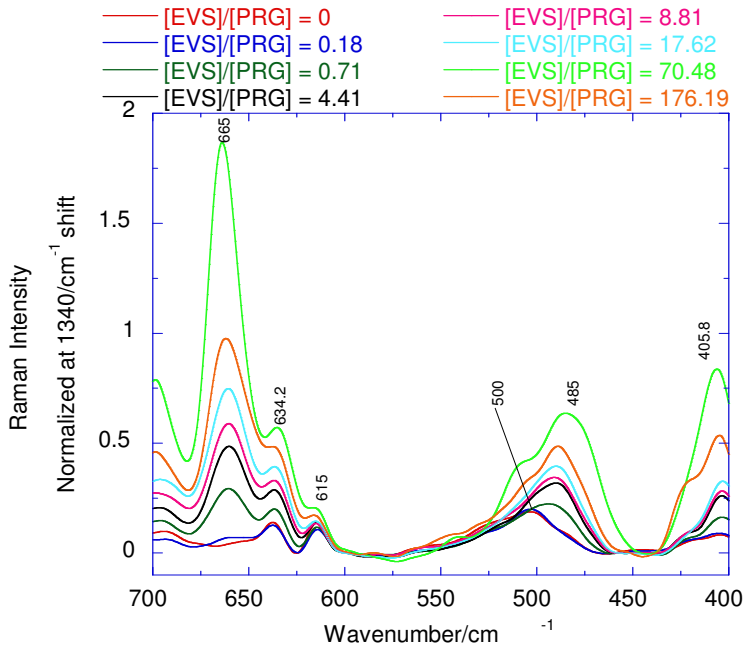

Figure 4(c). Normalized Raman spectra of substituted Ovalbumin in the region 700 – 400 cm^{-1} shift.

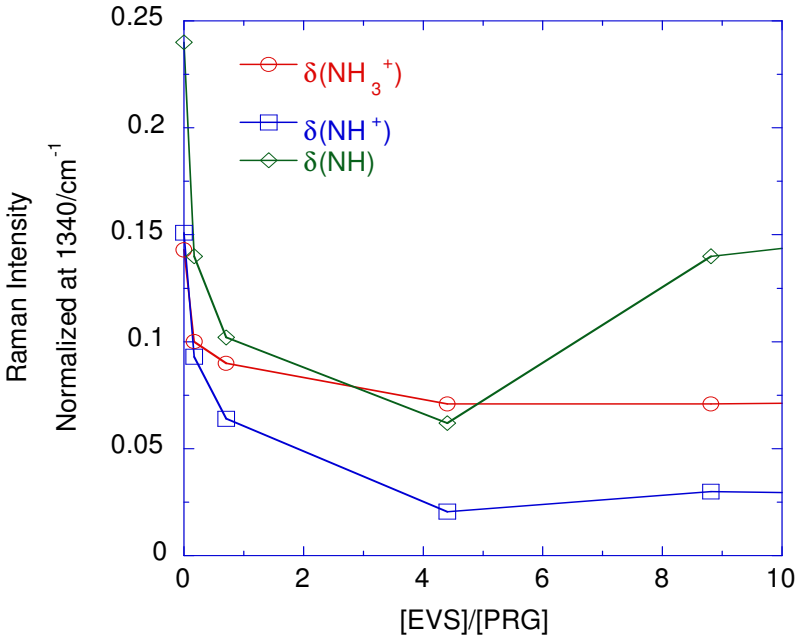

Figure 4(d). The CH on C=C, ν(CS), and NH rock normalized Raman shifts. The abscissa is the ratio of EVS added to deprotonated potential reactive groups (PRG) on ovalbumin.

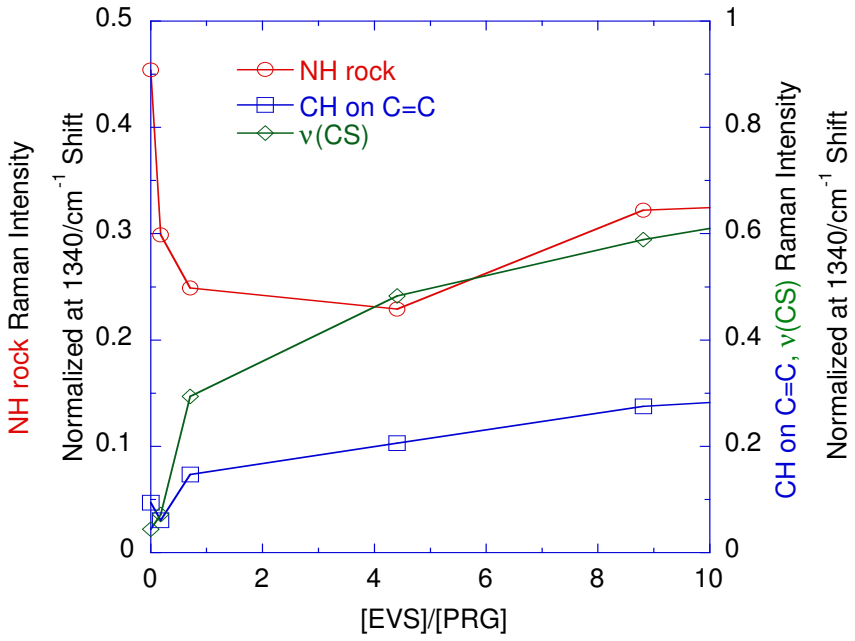

Figure 4(e). The δ_1(NH), δ_2(NH) and δ_3(NH) normalized Raman shifts. The abscissa is the ratio of EVS added to deprotonated potential reactive groups (PRG) on ovalbumin.

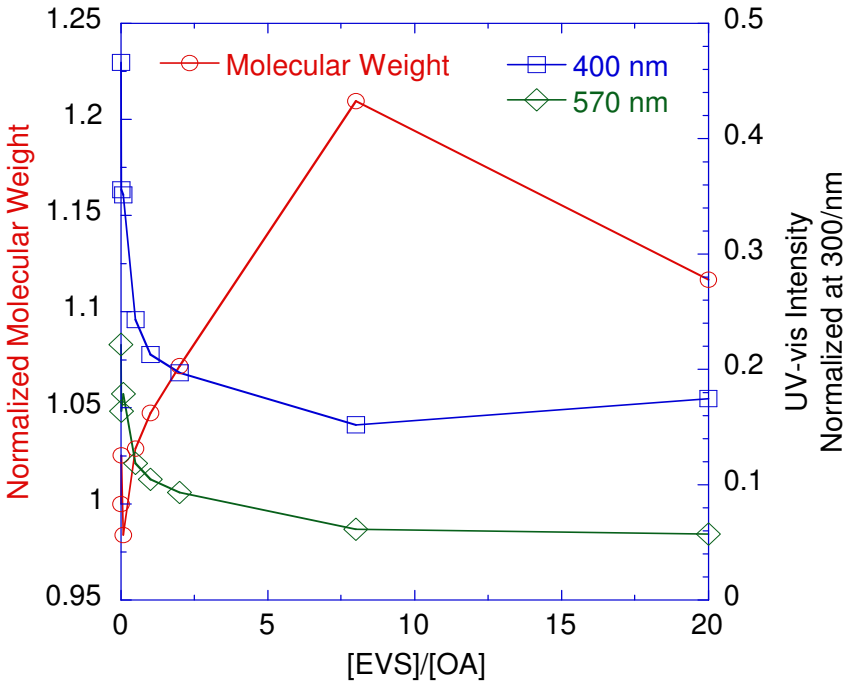

Figure 4(f). Normalized ninhydrin-based UV-vis absorbances and nitrogen content molecular weight analysis of substituted ovalbumin. The abscissa is the ratio of EVS added to deprotonated potential reactive groups (PRG) on ovalbumin.

asparagine, and glutamine could be substituted to an extent. The UV-vis results (both at 400 nm and 570 nm) and molecular weight analysis (based on nitrogen) of the modified protein samples shown in Figure 4(f) correlated with CH on C=C in Figure 4(e). Similar to the Raman spectroscopy data, gradual changes can be observed for [EVS]/[PRG]>1 for both the molecular weight analysis data and UV-vis results.

Conclusions

The amino acids alanine, cysteine, and lysine and the full protein ovalbumin were substituted at deprotonated amine and thiol groups using a facile nucleophilic addition reaction. The degree of substitution and substitution sites could be accurately quantified using Raman spectroscopy without any additional sample preparation. This was accomplished by observing the changes in the reactive sites of the substituent, in this case EVS, and the reactive amine or thiol groups of the amino acid or protein. The reactive sites that most accurately described the substitution were ν(C=C), CH on C=C, and ν(CS) Raman shifts on EVS and the NH rock and disulfide/thiolate Raman shifts on amino acids and protein. The Raman spectroscopy results were in good agreement with a standard ninhydrin-based UV-vis assay. Raman spectroscopy offered distinct advantages over the UV-vis assay by exactly showing the reaction sites. In the case of cysteine, which was traditionally found to be difficult to quantify with the ninhydrin test, the thiols, disulfides, thiolates, and deprotonated amines could be monitored. For amino acids with α-amines and side group amines, Raman spectroscopy was able to discern if the reaction was taking place on primary or secondary amines at the α or side group sites. The techniques developed for the single amino acids were applied successfully to the characterization of the substitution of the full protein ovalbumin.

References

1. Tolstoguzov, V. B., Physico-chemical modification of food proteins: Food emulsions. *Nahrung / Food* **1998,** 42, (03-04), 205-209.

2. Mather, B. D.; Viswanathan, K.; Miller, K. M.; Long, T. E., Michael addition reactions in macromolecular design for emerging technologies. *Progress in Polymer Science* **2006,** 31, 487-531.

3. Friedman, M., Applications of the Ninhydrin Reaction for Analysis of Amino Acids, Peptides, and Proteins to Agricultural and Biomedical Sciences. *J. Agric. Food. Chem.* **2004,** 52, (3), 385-406.

4. Whitaker, J. R., Ninhydrin Assay in the Presence of Thiol Compounds. *Nature* **1961,** 189, (4765), 662-663.

5. Chaplin, F. M., The Use of Ninhydrin as a Reagent for the Reversible Modification of Arginine Residues in Proteins. *Biochem. J* **1976,** 155, 457-459.

6. Beckwith, A. C.; Paulis, J. W.; Wall, J. S., Direct estimation of lysine in corn meals by the ninhydrin color reaction. *J. Agric. Food. Chem.* **1975,** 23, (2), 194-196.

7. Friedman, M.; Pang, J.; Smith, G. A., Ninhydrin-Reactive Lysine in Food Proteins. *J. Food Sci.* **1984,** 49, (1), 10-13.

8. Hsieh, C. L.; Hsiung, K. P.; Su, J. C., Determination of Lysine with Ninhydrin-Ferric Reagent. *Anal. Biochem.* **1995,** 224, (1), 187-189.

9. Abernathy, D. G.; Spedding, G.; Starcher, B., Analysis of Protein and Total Usable Nitrogen in Beer and Wine Using a Microwell Ninhydrin Assay. *Journal of the Institute of Brewing* **2009,** 115, (2), 122-127.

10. Friedman, M., Solvent effects in reactions of amino groups in amino acids, peptides, and proteins with .alpha.,.beta.-unsaturated compounds. *J. Am. Chem. Soc.* **1967,** 89, (18), 4709-4713.

11. Friedman, M., Solvent effects in the absorption spectra of the Ninhydrin chromophore. *Microchem. J.* **1971,** 16, (2), 204-209.

12. Pearce, K. N.; Karahalios, D.; Friedman, M., Ninhydrin Assay For Proteolysis in Ripening Cheese. *J. Food Sci.* **1988,** 53, (2), 432-435.

13. Moore, S.; Stein, W. H., A MODIFIED NINHYDRIN REAGENT FOR THE PHOTOMETRIC DETERMINATION OF AMINO ACIDS AND RELATED COMPOUNDS. *The Journal of Biological Chemistry* **1954,** 211, (2), 907-913.

14. Hwang, M.-N.; Ederer, G. M., Rapid Hippurate Hydrolysis Method for Presumptive Identification of Group B Streptococci. *J. Clin. Microbiol.* **1975,** 1, (1), 114-115.

15. Yanari, S., THE REACTION OF NINHYDRIN WITH DIPEPTIDES: DIFFERENCES IN REACTION RATES AND THEORETICAL YIELDS. *The Journal of Biological Chemistry* **1955,** 220, (2), 683-685.

16. Yu, P. H.; Davis, B. A., Deuterium isotope effects in the ninhydrin reaction of primary amines. *Cellular and Molecular Life Sciences* **1982,** 38, (3), 299-300.

17. Slobodian, E.; Mechanic, G.; Levy, M., Contribution of E-Amino Groups to Ninhydrin Color Production in Proteins. *Science* **1962,** 135, (3502), 441-442.

18. Quong, D., Stability of chitosan and poly-L-lysine membranes coating DNA-alginate beads when exposed to hydrolytic enzymes. *J. Microencapsulation* **1999,** 16, (1), 73-82.

19. Chowdhury, J.; Ghosh, M., Concentration-dependent surface-enhanced Raman scattering of 2-benzoylpyridine adsorbed on colloidal silver particles. *J. Colloid Interface Sci.* **2004,** 277, (1), 121-127.

20. Vogel, E.; Meuer, P.; Kiefer, W.; Urlaub, R.; Thull, R., Investigation of organically modified titanium substrates with SERS. *J. Mol. Struct.* **1999,** 482-483, 241-244.

21. Aliaga, A. E.; Osorio-Roman, I.; Garrido, C.; Leyton, P.; Cárcamo, J.; Clavijo, E.; Gómez-Jeria, J. S.; F, G. D.; Campos-Vallette, M. M., Surface enhanced Raman scattering study of l-lysine. *Vib. Spectrosc* **2009,** 50, (1), 131-135.

22. Arp, Z.; Autrey, D.; Laane, J.; Overman, S. A.; Thomas, G. J., Tyrosine Raman Signatures of the Filamentous Virus Ff Are Diagnostic of Non-Hydrogen-Bonded Phenoxyls: Demonstration by Raman and Infrared Spectroscopy of p-Cresol Vapor†,‡. *Biochemistry* **2001,** 40, (8), 2522-2529.

23. Benevides, J. M.; Bondre, P.; Duda, R. L.; Hendrix, R. W.; Thomas, G. J., Domain Structures and Roles in Bacteriophage HK97 Capsid Assembly and Maturation. *Biochemistry* **2004,** 43, (18), 5428-5436.

24. Carrier, D.; Pézolet, M., Raman spectroscopic study of the interaction of poly-L-lysine with dipalmitoylphosphatidylglycerol bilayers. *Biophys. J.* **1984,** 46, (4), 497-506.

25. Edsall, J. T., Raman Spectra of Amino Acids and Related Substances III. Ionization and Methylation of the Amino Group. *The Journal of Chemical Physics* **1937,** 5, (4), 225-237.

26. Façanha Filho, P. F.; Freire, P. T. C.; Lima, K. C. V.; Mendes Filho, J.; Melo, F. E. A.; Pizani, P. S., High temperature Raman spectra of L-leucine crystals. *Brazilian Journal of Physics* **2008,** 38, 131-137.

27. Gani, D.; Hendra, P. J.; Maddams, W. F.; Passingham, C.; Royaud, I. A. M.; Willis, H. A.; Zichy, V.; Cudby, M. E. A., Fourier transform Raman spectroscopy in the analysis of polypeptides. *Analyst* **1990,** 115, 1313-1318.

28. Lee, H. I.; Kim, M. S.; Suh, S. W., Raman Spectroscopy of L-Phenyl alanine, L-Tyrosine, and their Peptides Adsorbed on Silver Surface. *Bulletin Korean Chemical Society* **1988,** 9, (4), 218-223.

29. Mendham, A. P.; Dines, T. J.; Withnall, R.; Mitchell, J. C.; Chowdhry, B. Z., Vibrational spectroscopic studies of the structure of di-amino acid peptides. Part II: cyclo(L-Asp-L-Asp) in the solid state and in aqueous solution. *Journal of Raman Spectroscopy* **2009,** 40, (11), 1498-1507.

30. Ngarize, S.; Herman, H.; Adams, A.; Howell, N., Comparison of Changes in the Secondary Structure of Unheated, Heated, and High-Pressure-Treated β-Lactoglobulin and Ovalbumin Proteins Using Fourier Transform Raman Spectroscopy and Self-Deconvolution. *J. Agric. Food. Chem.* **2004,** 52, (21), 6470-6477.

31. Painter, P. C.; Koenig, J. L., The solution conformation of poly(L-lysine). A Raman and infrared spectroscopic study. *Biopolymers* **1976,** 15, (2), 229-240.

32. Rohleder, D.; Kocherscheidt, G.; Gerber, K.; Kiefer, W.; Kohler, W.; Mocks, J.; Petrich, W., Comparison of mid-infrared and Raman spectroscopy in the quantitative analysis of serum. *Journal of Biomedical Optics* **2005,** 10, (3), 031108.

33. Tuma, R., Raman spectroscopy of proteins: from peptides to large assemblies. *Journal of Raman Spectroscopy* **2005,** 36, (4), 307-319.

34. Stewart, S.; Fredericks, P. M., Sufrace-enhanced Raman spectroscopy of amino acids adsorbed on a electrochemically prepared silver surface. *Spectrochemica Acta Part A* **1999,** 55, 1641 - 1660.

35. Pelton, J. T.; McLean, L. R., Spectroscopic methods for analysis of protein secondary structure. *Analytical Biochemistry* **2000,** 277, 167-176.

36. Niskikawa, N.; Tanizawa, Y.; Tanaka, S.; Horiguchi, Y.; Asakura, T., Structural change of keratin protein in human hair by permanent waving treatment. *Polymer* **1998,** 39, (16), 3835-3840.

37. Rintoul, L.; Carter, E. A.; Stewart, S. D.; Fredericks, P. M., Keratin orientation in wool and feathers by polarized Raman spectroscopy. *Biopolymers* **2000,** 57, 19-28.

38. Kuzuhara, A., Analysis of structural change in keratin fibers resulting from chemical treatments using Raman spectroscopy. *Biopolymers* **2005,** 77, 335-344.

39. Pielesz, A.; Freeman, H. S.; Weselucha-Birczynska, A.; Wysocki, M.; Wlochowicz, A., Assessing secondary structure of dyed wool fibre by means of FTIR and FTR spectroscopies. *Journal of Molecular Structure* **2003,** 651-653, 405-418.

40. Akhtar, W.; Edwards, H. G. M., Fourier-transform Raman spectroscopy of mammalian and avian keratotic biopolymers. *Spectrochimica Acta Part A* **1997,** 53, 81-90.

41. Edwards, H. G. M.; Hunt, D. E.; Sibley, M. G., FT-Raman spectroscopic study of keratotic materials: horn, hoof, and tortoiseshell. *Spectrochimica Acta Part A* **1998,** 54f, 745-757.

42. Etzion, Y.; Linker, R.; Cogan, U.; Shmulevich, I., Determination of Protein Concentration in Raw Milk by Mid-Infrared Fourier Transform Infrared/Attenuated Total Reflectance Spectroscopy. *J. Dairy Sci.* **2004,** 87, (9), 2779-2788.

43. Sheng, G.-P.; Yu, H.-Q.; Wang, C.-M., FTIR-spectral analysis of two photosynthetic H2-producing strains and their extracellular polymeric substances. *Appl. Microbiol. Biotechnol.* **2006,** 73, (1), 204-210.

44. Rodrigues, J.; Faix, O.; Pereira, H., Determination of Lignin Content of Eucalyptus globulus Wood Using FTIR Spectroscopy. *Holzforschung* **2009,** 52, (1), 46-50.

45. Yu, Z.; Ma, C.-Y.; Yuen, S.-N.; Phillips, D. L., Raman spectroscopic determination of extent of O-esterification in acetylated soy protein isolates. *Food Chem.* **2004,** 87, (3), 477-481.

46. Bosch Reig, F.; Gimeno Adelantado, J. V.; MartnezMartínez, V. P.; Moya Moreno, M. C. M.; Doménech Carbó, M. T., FT-IR quantitative analysis of solvent mixtures by the constant ratio method. *J. Mol. Struct.* **1999,** 480-481, 529-534.

47. Bunaciu, A. A.; Aboul-Enein, H. Y.; Fleschin, S., Quantitative analysis of bucillamine and its pharmaceutical formulation using FT-IR spectroscopy. *Il Farmaco* **2005,** 60, (8), 685-688.

48. Kuzuhara, A.; Hori, T., Reduction mechanism of thioglycolic acid on keratin fibers using microspectrophotometry and FT-Raman spectroscopy. *Polymer* **2003,** 44, 7963-7970.

49. Tortora, M.; Cavalieri, F.; Chiessi, E.; Paradossi, G., Michael-Type Addition Reactions for the In Situ Formation of Poly(vinyl alcohol)-Based Hydrogels. *Biomacromolecules* **2006,** 8, (1), 209-214.

50. Ranucci, E.; Bignotti, F.; Paderno, P. L.; Ferruti, P., MODIFICATION OF ALBUMINS BY GRAFTING POLY(AMIDO AMINE) CHAINS. *Polymer* **1995,** 36, 2989-2994.

51. Elbert, D. L.; Hubbell, J. A., Conjugate Addition Reactions Combined with Free-Radical Cross-Linking for the Design of Materials for Tissue Engineering. *Biomacromolecules* **2001,** 2, (2), 430-441.

52. Sereikaite, J.; Bassus, D.; Bobnis, R.; Dienys, G.; Bumeliene, Z.; Bumelis, V. A., Divinyl sulfone as a crosslinking reagent for oligomeric proteins. *uss. J. Bioorg. Chem.* **2003,** 29, (3), 227-230.

53. Nisbet, A. D.; Saundry, R. H.; Moir, A. J. G.; Fothergill, L. A.; Fothergill, J. E., The complete sequence of Hen-Ovalbumin. *Eur. J. Biochem.* **1981,** 115, 335-345.

54. Meyer, H., The Ninhydrin Reaction and its Analytical Applications. *Biochem. J* **1957,** 67, 333-340.

55. Friedman, M.; Sigel, C. W., A Kinetic Study of the Ninhydrin Reaction*. *Biochemistry* **1966,** 5, (2), 478-485.

56. Friedman, M.; Cavins, J. F.; Wall, J. S., Relative Nucleophilic Reactivities of Amino Groups and Mercaptide Ions in Addition Reactions with α,β-Unsaturated Compounds1,2. *J. Am. Chem. Soc.* **1965,** 87, (16), 3672-3682.

57. Whitaker, J. R., Ninhydrin assay in the presence of thiol compounds. *Nature* **1961,** 189, 662-663.

Chapter IV

Protein substitution affects glass transition temperature and thermal stability

Abstract

When proteins are removed from their native state they suffer from two deficiencies: (1) glassy behavior with glass transition temperatures (T_g) well above room temperature and (2) thermal instability. The glassy behavior originates in multiple hydrogen bonds between amino acids on adjacent protein molecules. Proteins, like most biopolymers, are thermally unstable. Substituting ovalbumin with linear and cyclic substituents using a facile nucleophilic addition reaction can affect T_g and thermal stability. More hydrophobic linear substituents lowered T_g by interrupting intermolecular interactions and increasing free volume. More hydrophilic and cyclic substituents increased thermal stability by increasing intermolecular interactions. In some cases, substituents instituted cross-linking between protein chains that enhanced thermal stability. Internal plasticization using covalent substitution and external plasticization using low molecular weight polar liquids show the same protein structural changes and a signature of plasticization is identified.

Introduction

Currently, there is a large effort to develop polymers from renewable sources in direct response to the price of petroleum. For example, polylactic acid (PLA) is currently the largest volume renewable polymer sold commercially and is made from the fermentation of cornstarch. PLA has the potential to be cost and property competitive with some petroleum-based polymers if a suitable fermentation substrate is used. Agriculture is diverting more corn supply into ethanol and less into food and PLA prices have increased and supplies decreased because it is the tertiary priority. It would be advantageous to find a source for renewable polymers that does not compete with food or fuel. Proteins that are the by-product of agriculture and food processing are not derived from petroleum and are not a primary food product so they do not compete with food or fuel and will not be compromised when demand for those products rises. Proteins contain nitrogen and sulfur and cannot be directly converted to fuel very easily. So making polymers from by-products could be very cost effective if suitable processing methods can be found.

Nature builds high performance structures by rational assembly of proteins. For example, feather has a density of ρ~0.8 g/cm^3, modulus of E~1.5-10.0 GPa, stress to break of σ_b=100-200 MPa, and strain to break of ε_b~5-26% in its native state depending on hydration and type of feather.[1-7] Isolated and re-processed keratin formed into, for instance, films maintains this modulus but ε_b decreases to ~1% and increases to ρ~1.4 g/cm^3.[8] It is the interaction of the proteins at the different length scales that come together to form a macroscopic material of high properties. When the individual proteins are separated from the native structure they no longer possess the properties of the original assemblage. The proteins are typically very brittle when isolated and this limits their usefulness. Experimental observations and theoretical treatments of

biopolymeric structures show that it is indeed the rational assembly that is responsible for the high toughness and low density.[9-13] Unique to proteins are the richness of interactions available between two molecules. Proteins typically rely on covalent, ionic, hydrogen bonding, and hydrophobic interactions. Proteins have high modulus because each amino acid can interact multiple times with another amino acid on another molecule. When removed from the natural assemblage, these interactions are also responsible for the very high glass transition temperatures (T_g) of proteins that make them glassy and brittle.

To compensate for the brittle behavior of isolated proteins they are typically plasticized with low molecular weight polar compounds that can include water, glycerol, ethylene glycol and its polymers, propylene glycol and its polymers, sorbitol, diethylene glycol-monomethyl ether, diethanolamine, and acylated monoglycerides.[14-23] Plasticization comes at a large cost to strength and stiffness.[23] Plasticizers decrease inter-molecular interactions and increase free volume. Native protein structures do not require plasticization to the high levels necessary with isolated protein structures, although they do require a small amount of hydration for proper function. The largest problem with plasticizers may be migration, which occurs naturally but is hastened by increased temperature or exposure to water because of their hydrophilic nature. Therefore, it would be advantageous to increase the flexibility of proteins without large costs to strength and stiffness and without having a diffusible component in the product.

The Michael addition is a nucleophilic addition reaction between electron-rich nucleophiles and electron-poor electrophiles.[24-26] Specifically, the protein contains nucleophilic primary (-NH_2) and secondary (-NH) amines and thiols (-SH) that add to electron-poor carbon-carbon double bonds in substituted olefins (CH_2=CH-R). The reaction proceeds at room temperature and near neutral pH in water making it a very facile and green reaction. The high nucleophilicity

of amines and thiols means that no catalyst is required although a slightly basic solution can increase kinetics.[25] Depending on the chemistry of R, the functionality of the protein can be altered. Depending on the size of R, the ability of two protein molecules to hydrogen bond to one another could be affected. Protein functionalization using the Michael addition reaction has been reported previously but with different intents. Ranucci *et al*[24] modified bovine serum albumin (BSA) and human serum albumin (HSA) by grafting poly (amido amine) chains onto the proteins without denaturing the protein for drug delivery applications. Sereikaite *et al*[25] and references therein modified BSA by crosslinking it with divinylsulfone (DVS) also for potential biomedical applications.

In this study, modification of egg albumin (EA) protein through the Michael addition reaction has been investigated. Technical egg albumin is a non-edible refuse protein from the food industry. Egg albumin (EA) or ovalbumin contains 385 amino acids, 185 of which are polar, 6 are cysteine, and all amino acids are present.[27] It has a molecular weight of 49,670 g/mol. EA is soluble in its native form but after processing becomes insoluble presumably because the intra-molecular cystine bonds are converted to inter-molecular.[28] Many eggs do not pass USDA inspection so there is lots of egg albumin available. Egg albumin is 41% α-helix, 34% β-sheet, 13% random coil, and 12% β-turn so it has potential for high physical properties.[29] Efforts for utilizing egg albumin as polymers started as long ago as the 1940's.[30-32] EA has been covalently modified using ethyl vinyl sulfone (EVS) a chemical with a hydrophobic end on the other side of the carbon-carbon double bond and acrylic acid (AA) a compound with a hydrophilic end on the other side of the carbon-carbon double bond. The effect of EVS and AA substitution on EA was investigated using Fourier transform-infrared (FT-IR) spectroscopy,

differential scanning calorimetry (DSC), thermo gravimetric analysis (TGA), and x-ray powder diffraction (XRD).

Materials and Methods

Materials. Technical grade egg ovalbumin, dithiothreitol (DTT), reagent grade BS (mol. wt. 118.15 g/mol), AA (mol. wt. 72.01 g/mol), and MA (mol. wt. 97.07 g/mol) were purchased from Sigma Aldrich (USA). Dialysis membranes with 3500 g/mol molecular weight cut off and 95% EVS (mol. wt. 120.17 g/mol) were obtained from VWR (USA). All of the materials were used as obtained without any further modifications.

Substitution. 5 g of OA was added to 50 ml of deionized water. The pH was adjusted to 9 using borate buffer solution. To this solution, 0.0017 g (equivalent to moles of cysteine present on OA) DTT was added and the solution stirred for 30 min producing soluble OA. [33] At this point, various concentrations of substituents were added to the OA solution and further stirred at 30ºC for 24 hrs. The substituent level was determined by the amount of deprotonated to protonated nucleophile on the amino acid side group, i.e., $[NH_2]/[NH_3^+]$ or $[S^-]/[SH]$. For OA, the lysine primary amines (K, pK_R=10.8), cysteine thiols (C, pK_R=8.3), and histidine secondary amines (H, pK_R=6.0) yielded 12.6 potential reactive groups (PRG) per OA molecule at pH 9. The amines of asparagine (N) and glutamine (Q) were not counted because of the poor acid/base properties of the amide side groups, although this may not be entirely true.[34] The side group of arginine (R) was not counted because the side group dissociation constant, pK_R, was 12.5 yielding very little potential deprotonated groups for nucleophilic addition. Finally, the secondary amine of the α-carbon was assumed highly inaccessible because of its position on the protein main chain and potential to hydrogen bond to another main chain. The N-terminus of the

OA molecule was omitted because of potential post-synthetic modification yielding unreactive groups.

Addition of EVS, BS, and MA did not affect pH. Addition of AA reduced the solution pH to 4 and 4N NaOH was added to adjust pH back to 9. The solutions were then dialyzed against deionized water for 24 hours and the water was changed every 12 hours. The dialyzed solution was poured onto Teflon-coated aluminum foil and dried at ambient conditions. During reaction, the EVS and BS solutions gelled. Water was added to the gelled solution and stirred for 1 hr before dialysis. The dried samples were ground into fine powders using a mortar and pestle.

Nitrogen analysis. To determine reaction yields of substituted OA, nitrogen analysis was performed using an Elementar Vario MAX CNS Analyzer (Hanau, Germany). The reaction yield was determined by comparing the experimentally determined amount of nitrogen to the expected amount of nitrogen as the protein was substituted.

Thermal analysis. Thermal analysis was performed on 8-10 mg samples in a nitrogen atmosphere. Given the difficulties associated with thermal analysis of biopolymers, at least three samples were analyzed using three different instruments so the glass transition (T_g) and thermal degradation (T_d) temperatures could be well defined.[35-37] The samples were analyzed on TA Instruments' SDT Q600 simultaneous DSC/TGA (differential scanning calorimeter/thermogravimetric analyzer), DSC Q100, and TGA Q500. For DSC, a two-cycle analysis was used. In the first cycle, the sample was equilibrated at 30ºC then heated to 150ºC at a rate of 10ºC/min, equilibrated at 150ºC for two minutes, then air-cooled to 30ºC. In the second cycle, the sample was heated to 300ºC at a rate of 10ºC/min. The glass transition temperatures were clearly defined and good agreement was found between samples and instruments. For thermal stability analysis using TGA, the samples were heated to 600ºC at a rate of 10ºC/min.

Fourier transform-infrared (FT-IR) spectroscopy. A Thermo-Nicolet 6700 FT-IR spectrometer with a Smart Orbit diamond ATR cell was used. The spectrum was collected with a total of 64 scans and a resolution of 4 cm^{-1} and then baseline corrected and smoothed. Deconvolution of the Amide I band into individual components was accomplished with OMNIC v 7.3 software. The spectral region 1750-1590 cm^{-1} of the original spectrum was fitted with Gaussian/Lorentzian peaks. The number of peaks and their position were determined by the automatic peak finding feature of the program at low sensitivity and full width at half height of 3.857.

X-ray powder diffraction (XRD). XRD patterns were recorded on a PANalytical X'Pert PRO X-ray diffractometer (Westborough, MA) using Co radiation generated at 40 kV and 40 mA. Scanning was done with a Theta/Theta goniometer from 2-70 °2θ with a step size of 0.0668545 °2θ at a time of 600 s. The incident wavelength was λ=0.179 nm.

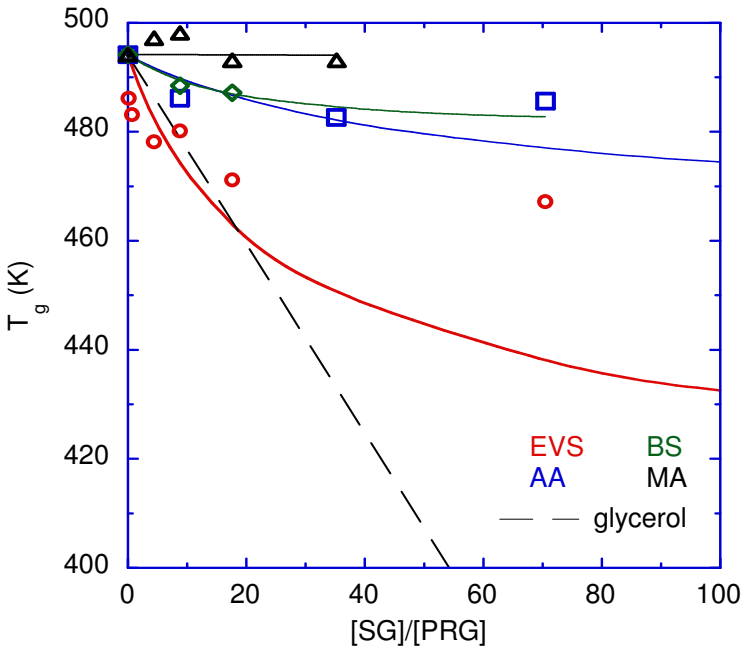

Figure 1. Change in glass transition temperature, T_g, with OA substitution.

Results and Discussion

Glass transition temperature. The experimentally determined T_g of OA reduced with DTT was 221°C, which was close to the value of 208°C found by Katayama et al., for native OA using high ramp rate DSC.[38] Discrepancies originated in our use of reduced OA, which would make more amino acids available for hydrogen bonding thus increasing T_g, and a more typical, slower DSC heating rate for polymers. Figure 1 shows the reduction of OA T_g with substitution. Lines are fits of the T_g data to the Couchman-Karasz equation, which has been shown to fit biopolymer T_g data reasonably well

$$\ln\left(\frac{T_g}{T_{g,sg}}\right) = \frac{w_p \ln\left(\frac{T_{g,p}}{T_{g,sg}}\right)}{w_{sg}\left(\frac{T_{g,p}}{T_{g,sg}}\right) + w_p} \qquad (1)$$

where w_p was the weight fraction of OA protein, w_{sg} was the weight fraction of substituted group (EVS, AA, BS, and MA), and $T_{g,p}$ was the glass transition temperature of OA which was 494 K (221°C).[37, 39] The glass transition temperature of the substituted group, $T_{g,sg}$, was treated as a fitting parameter with $T_{g,sg}$ = 420, 465, 480, and 494 K providing the best fits for EVS, AA, BS, and MA data, respectively. For comparison, the plasticization of OA with glycerol is included. Figure 1 shows that EVS covalently attached to OA was a very efficient plasticizer, even more so than glycerol, up to a mild degree of substitution. However, EVS could not reach the ultimate level of plasticization of glycerol, which was T_g reducing to room temperature. Figure 1 has the ratio of substituent groups to potential reactive groups, [SG]/[PRG], plotted on the abscissa. Asymptotic behavior was observed after [SG]/[PRG]~5-10, which could have indicated that the maximum amount of EVS had been added to OA and would not change T_g anymore. It also suggested that the original PRG calculation did not account for all reactive

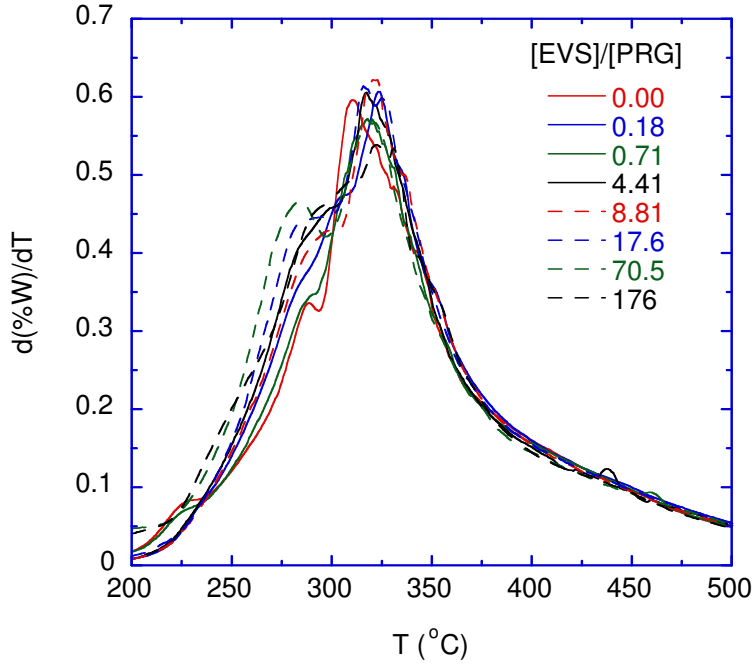

Figure 2 (a). dTGA analysis of OA substituted with EVS.

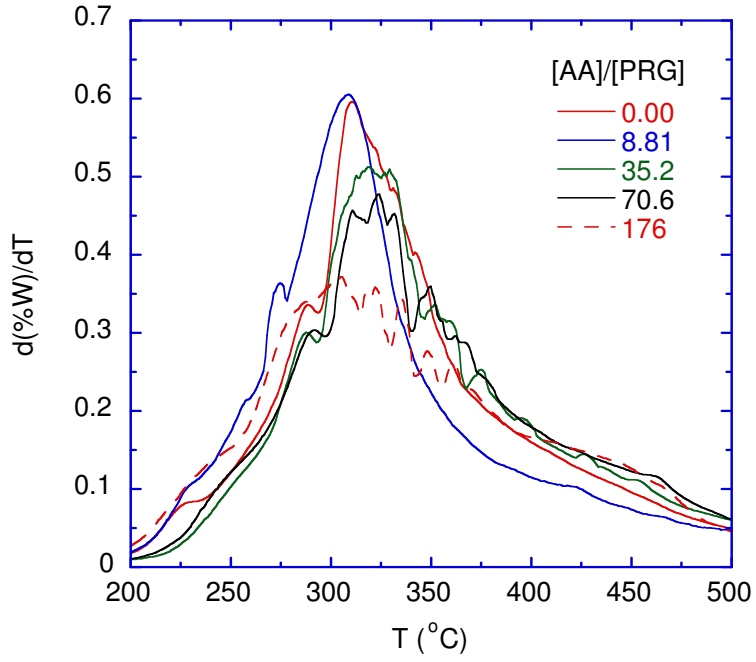

Figure 2(b). dTGA analysis of OA substituted with AA.

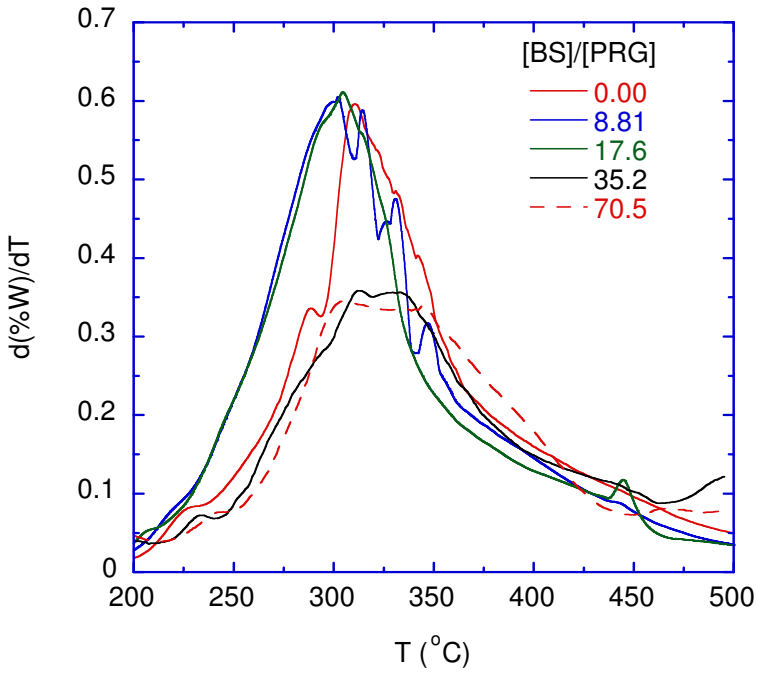

Figure 2(c). dTGA analysis of OA substituted with BS.

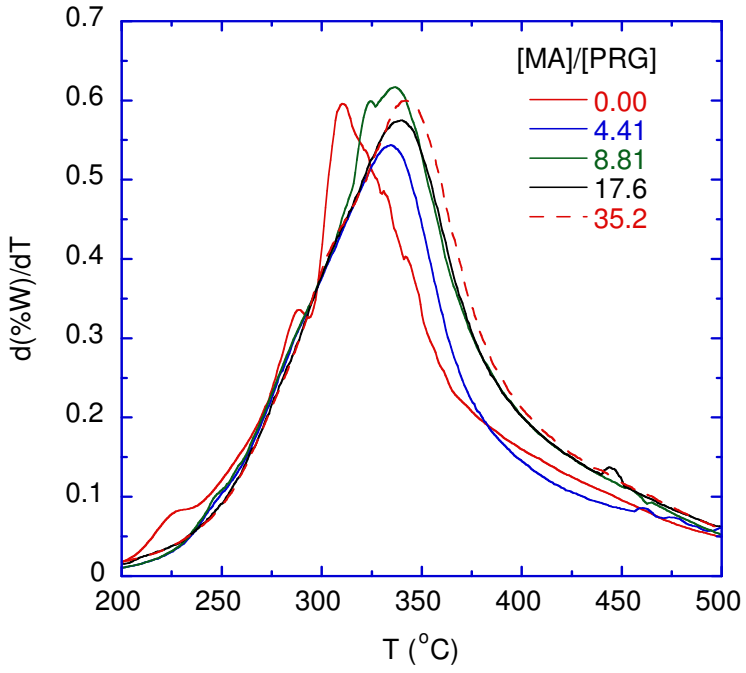

Figure 2(d). dTGA analysis of OA substituted with MA.

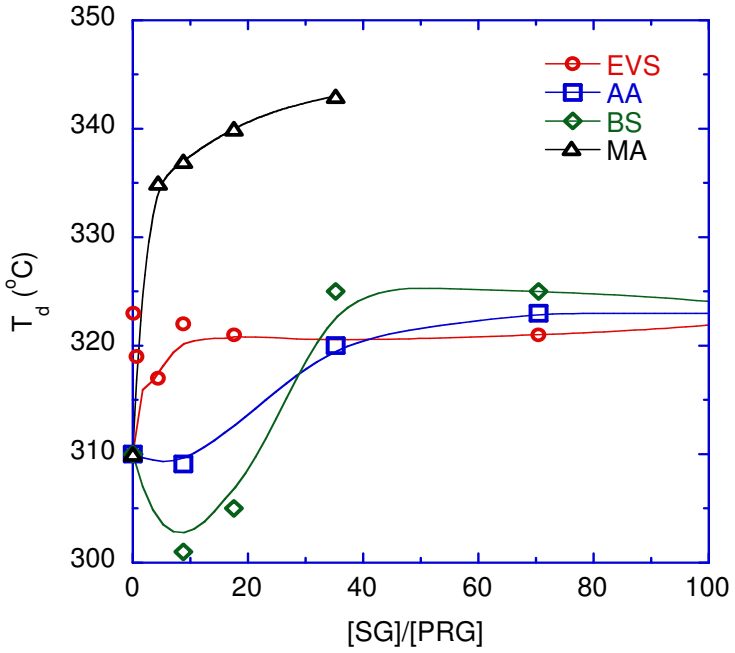

Figure 3. Change in thermal degradation temperature, T_d, with OA substitution.

groups. The fitting parameter T_g=420 K fit the data well in the [SG]/[PRG]~0-10 range but not at higher ratios. AA and BS provided very little internal plasticization and MA none at all.

Thermal stability. The first derivative of sample weight loss with temperature, dTGA, quantified the thermal stability of polymers by depicting two phenomena: the peak maximum was a measure of the overall degradation temperature, T_d, and the peak area was the rate of degradation. Figure 2(a-d) shows the dTGA behavior for all of the substituted OA materials. The effect of substitution on T_d is shown in Figure 3. For EVS substituted OA, a new dTGA peak emerged around 285°C with increasing EVS addition. The increase of the new dTGA peak was concurrent with the decrease of the primary dTGA peak around 320°C and the conservation of the two peaks meant no overall change in the degradation rate of OA-EVS. OA-BS showed peak broadening in this area (~285°C). OA-EVS and OA-MA displayed a steady increase in T_d until saturating at [SG]/[PRG]~6 with no significant change in degradation rate. OA-AA and

OA-BS showed a decrease in T_d until [SG]/[PRG]~8 then an increase in T_d until saturating at [SG]/[PRG]~30 and it was upon the increase in T_d that the degradation rate decreased.

Structural changes with substitution. In the FT-IR spectra, the 1300-1200 cm^{-1} and 1150-1025 cm^{-1} regions were signature regions of the protein and substituent making quantitative assessment of structure difficult (data not shown). The presence of substituent was easily discernible as sharper, more discrete peaks superimposed on top of broader protein peaks.

Protein structural changes during plasticization manifested as changes in the Amide I peak.[37] Amide I described the state of protein carbonyls, mostly from the main chain, and were highly correlated with protein secondary structure.[40] It was also sufficiently far from substituent peaks, with the AA carbonyl appearing at 1694 cm^{-1}, the MA carbonyl appearing at 1687 cm^{-1}, and ν(C=C) on EVS and BS appearing at 1611 cm^{-1}. As OA was substituted, the Amide I or ν(C=O) peak around 1630 cm^{-1} broadened. The peak broadening originated in changing states of ν(C=O) on main chain amides, i.e., their participation in β-sheet, random coil, or α-helix conformations. The results of Amide I peak deconvolution are shown in Figure 4. Included in each data set is the change in OA secondary structure between the native OA and reduced, solubilized, and solution cast OA. The native OA deconvolution results show the same β-sheet and random coil content as Ngarize et al., but less α-helix.[41] In our deconvolution we assigned peaks to β-turns at 1668 cm^{-1} and antiparallel β-sheets at 1683 cm^{-1}. As these structures and α-helix all appeared at the highest wavenumbers in the peak, our deconvolution added a contribution from antiparallel β-sheets while reducing the α-helix contribution. Predominantly, we were interested in the change in β-sheet relative to random coil, which described the maximum and minimum hydrogen bonding states, respectively, and therefore could potentially correlate with the glass transition. Upon reduction of OA, there was a loss of β-sheet structure with a concurrent and nearly equal

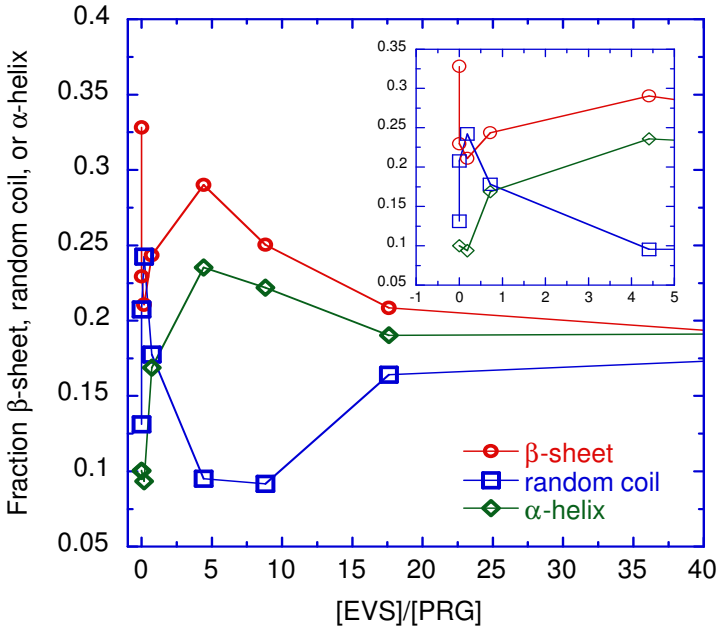

Figure 4(a). Results of Amide I peak deconvolution for OA substituted with EVS.

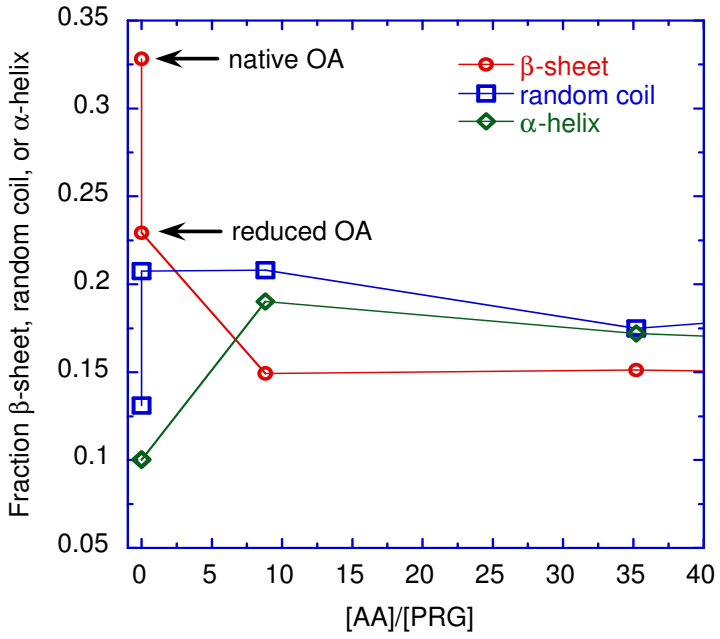

Figure 4(b). Results of Amide I peak deconvolution for OA substituted with AA.

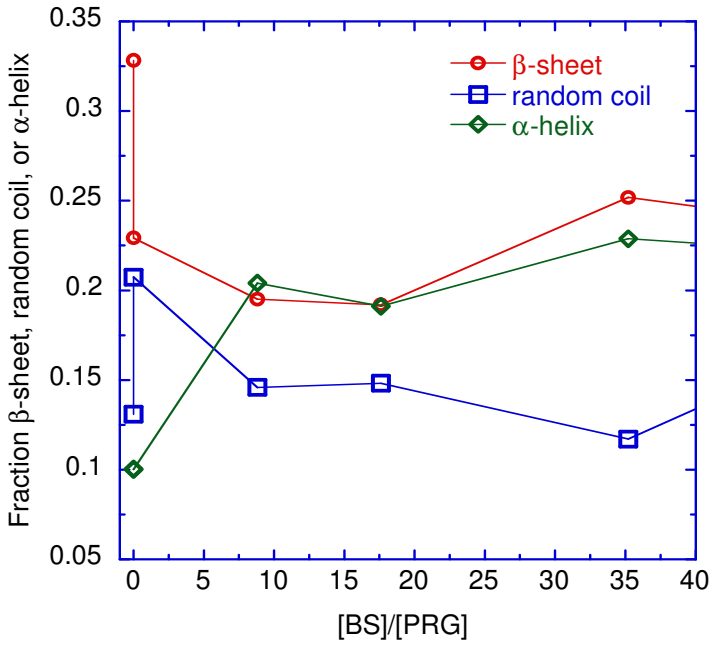

Figure 4(c). Results of Amide I peak deconvolution for OA substituted with BS.

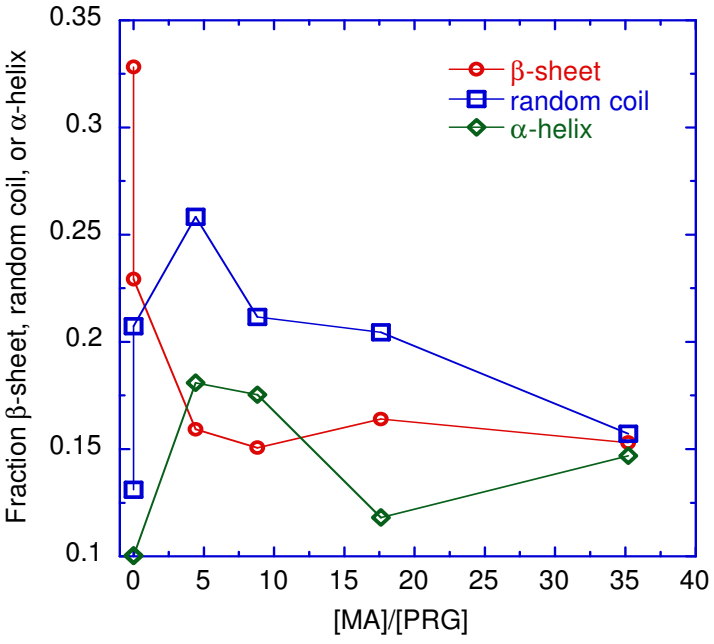

Figure 4(d). Results of Amide I peak deconvolution for OA substituted with MA.

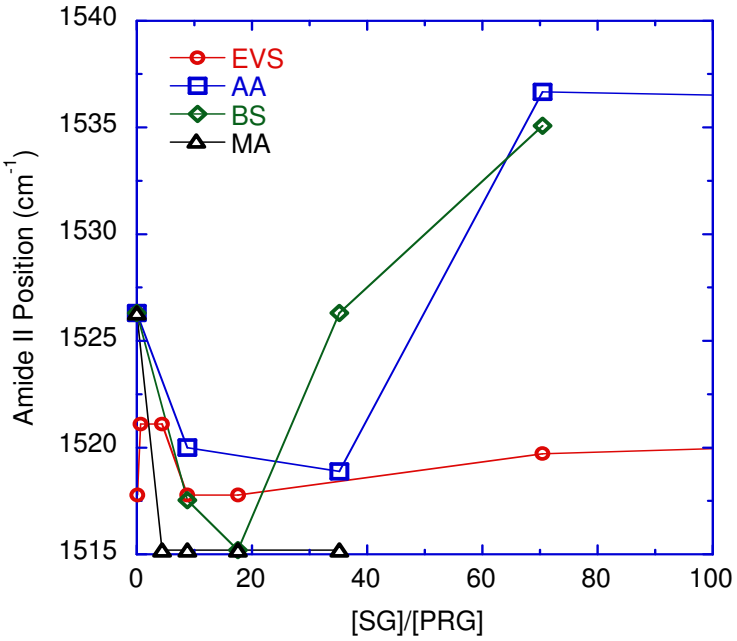

Figure 5. Change in Amide II peak with OA substitution.

increase in random coils. OA-AA and OA-MA had decreasing amounts of β-sheets with concurrent increasing amounts of random coils at [SG]/[PRG]~0-10. There was then little change in the secondary structure at higher substitutions. At the highest degrees of substitution, i.e., [SG]/[PRG]>30, all secondary structures saturated at low values and FT-IR data showed that the materials were dominated by a high weight fraction of substituent. OA-BS displayed a decrease in β-sheets and random coils. OA-EVS exhibited the most complicated behavior with β-sheets decreasing slightly at the lowest substitution, increasing at moderate substitution, then decreasing and finally saturating at higher substitutions with random coils doing the opposite.

The Amide II peak around 1525 cm^{-1} described the state of primary and secondary amines on both the protein backbone and amino acid side groups.[42] No substituent peaks appeared in this area so changes were indicative of substitution on amines and protein structural changes. Amide II shifted lower in wavenumber for each substituted OA material as shown in Figure 5.

Increasing substitution did not change OA-EVS or OA-MA but OA-BS and OA-AA then shifted higher in wavenumber.

Diffraction patterns from OA and substituted OA materials were typical of semi-crystalline proteins with two diffuse halos at Bragg spacings of about 0.46 and 1.10 nm.[43] The 0.46 nm spacing represented the distance between two protein molecules in a native β-sheet independent of the protein's primary structure. The 1.10 nm spacing represented the inter-sheet distance between two stacked β-sheets and was a function of the shape and size of the amino acid side chains.[43] The peaks were diffuse because of the non-uniform size of the β-sheets, their random arrangement in the powder diffraction experiment, and the presence of amorphous regions. The diffraction patterns for OA materials were normalized at the $2\theta=9.5^{o}$ or d=1.10 nm peak for comparison. OA-EVS and OA-BS showed similar behavior. As substitution increased, the 1.10 nm peak broadened and the 0.46 nm peak sharpened and grew in intensity as exemplified by OA-EVS XRD patterns in Figure 6(a). OA-AA did not show much change as shown in Figure 6(b). The sharp peaks occurring at high substitution were consistent with crystallized acrylic acid .[44]

Structural signatures of plasticization and thermal stability. The observed thermal behavior can be directly correlated to the structural changes of the OA protein as various functionality was added. Figure 7 shows the structure of each substituent added onto the protein. EVS added medium chain branching with a hydrophobic end, AA added short chain branching with a hydrophilic end, BS added a slightly hydrophilic ring, and MA added a more hydrophilic ring. By adding each onto OA, the native protein secondary, tertiary, and quaternary structures were modified.

It has been observed previously that the decrease in β-sheets and increase in random coils, as measured by Amide I peak deconvolution, and the broadening of the 1.10 nm peak and sharpening of the 0.46 nm peak, as measured by XRD, correlate with increasing external plasticization of proteins by glycerol.[37] OA-EVS exhibited both behaviors and had the largest T_g decrease so these trends may be a signature of the protein structural rearrangements necessary to transition from a glassy to a rubbery state. Taking the FT-IR and XRD data together, a potential mechanism could be substitution first occurred at available side groups on random coils at [EVS]/[PRG]~0-5. The added free volume, manifesting as a decrease in T_g, allowed some of the previous random coils to now form β-sheets. In other words, there was more probability of two main chains finding each other to hydrogen bond. In the direction normal to the main chain on the side groups, any introduced β-sheets were now pushed apart, minimizing interactions in this direction. So free volume at low substitution was in the side group direction. Although there

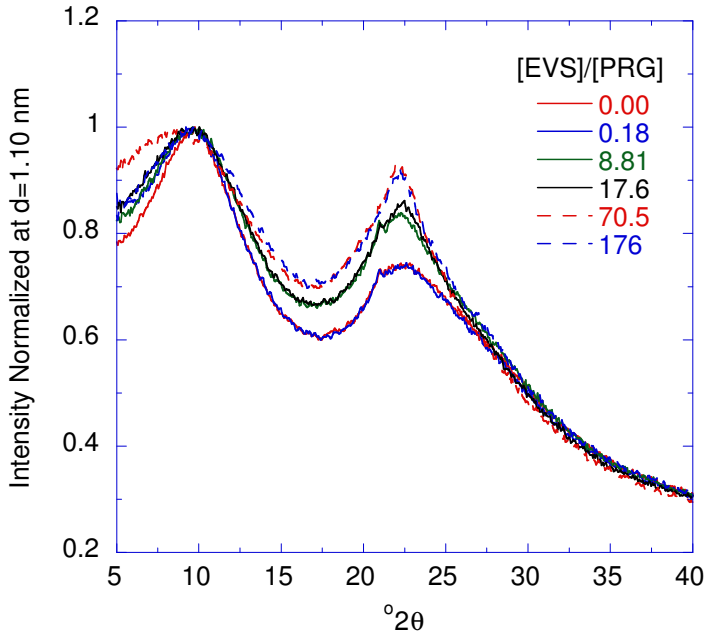

Figure 6(a). XRD results for OA substituted with EVS.

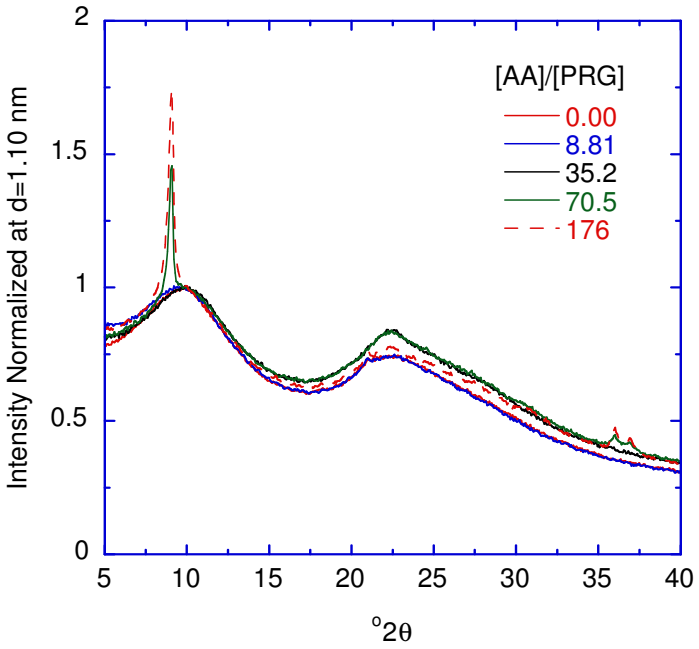

Figure 6(b). XRD results for OA substituted with AA.

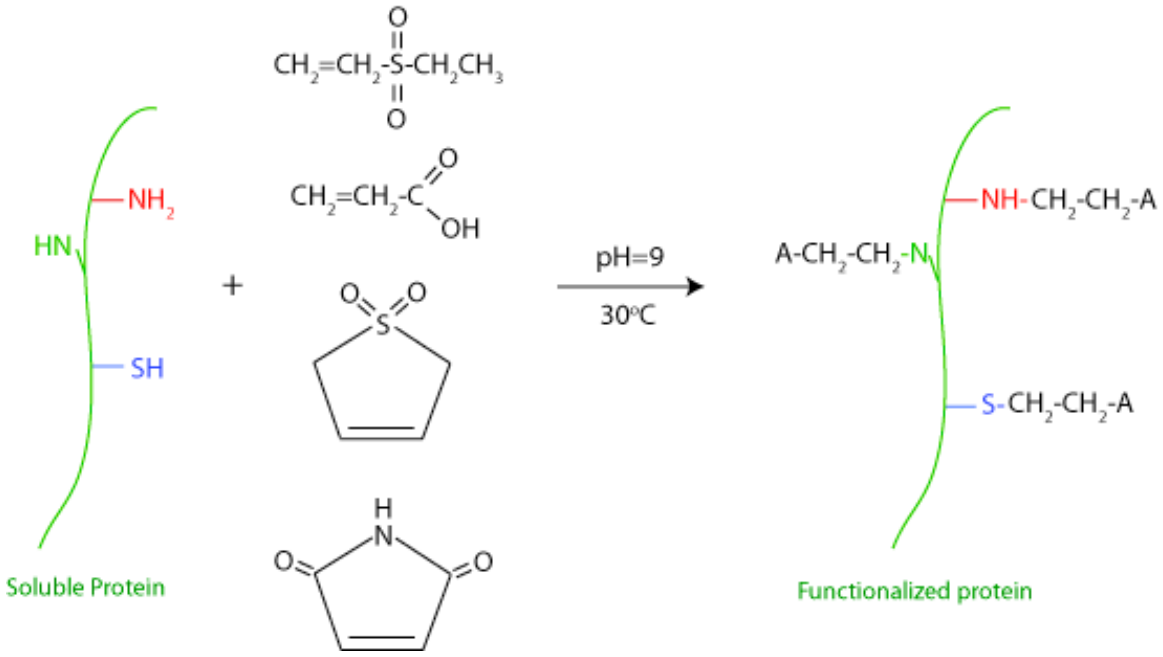

Figure 7. Chemical structure of substituents and schematic depicting how electron poor vinyl groups add to electron rich amines and thiols on the protein.

was an increase in β-sheets the amount per unit volume was smaller than in the native state resulting in the T_g decrease. Further substitution, i.e., [EVS]/[PRG]~5-20 occurred on side groups and on main chain amines, both of which were available for reaction in solution. There was then a decrease in β-sheets and an increase in random coils with free volume introduced between main chains and in the side group direction and a further decrease in T_g. At these substitution levels, the chains had very little interaction with each other so the interactions per unit volume were small resulting in a low T_g. At [EVS]/[PRG]>20, no further decrease in T_g occurred. This was also the region where no further changes in the FT-IR Amide I and II were observed. The limited internal plasticization of OA with EVS appeared related to the ability to continue to substitute. Elemental analysis showed that the yield decreased to 70% at [SG]/[PRG]~25 and then dropped precipitously. Further changes in the XRD could be related to excess EVS aggregating around the protein, which were not manifesting as protein changes at all. Sharp peaks in the OA-AA and OA-BS XRD patterns at high substitution support the theory that excess substituent aggregated or crystallized around the protein and was too large or too bound to diffuse during dialysis.

OA-AA and OA-BS exhibited less pronounced changes in protein secondary structure and the limited reduction of T_g appeared to be related to this. In addition, AA added more hydrogen bonding potential to the protein and any structural change could be compensated for by more hydrogen bonding. BS added stiffness to the protein chain that again could compensate for any structural changes to maintain T_g. The addition of MA disrupted β-sheets and increased random coil content. Again, the chain stiffness added by the ring compensated for this resulting in no T_g change.

Unlike the EVS system, the potential for interactions between protein molecules substituted with AA, BS, or MA was high. For AA, it was through hydrogen bonding interactions forming AA dimmers.[44, 45] For BS and MA, it was through cross-linking across the C=C bond in the ring.[46-50] These interactions, along with the ring structure of BS and MA, maintained the high glass transition temperature of the protein even though the native protein structure was disrupted. These interactions also had an influence on the thermal stability of the protein. Indeed, maleimide and sulfone have been used to stabilize thermoplastic polymers to high temperature.[51, 52] In this study, the sulfones did not impart thermal stability instead causing degradation at ~285^{o}C, which was lower than the native protein, but higher than some thermoplastic materials. Thermal stability was imparted through increased protein-protein interactions. The smaller changes in Amide I in FT-IR analysis for these materials showed that more intermolecular interactions were contributing to thermal stability. The fact that MA did not have marked decreases in thermal degradation rate could be because it had 2 C=O and 1 N-H on the ring that maintained degradation rate regardless of the shift in T_d with intermolecular interactions. However, there was spectroscopic evidence that OA-MA intermolecular interactions may not have been as strong as OA-AA and OA-BS intermolecular interactions. OA-AA and OA-BS displayed shifting in Amide II at the same points in substitution that reduced thermal degradation was observed indicating that this may be a signature of the strongest intermolecular interactions.

Conclusions

Glass transition temperature (T_g) could be reduced using EVS which is a linear substituent with hydrophobic end group. The thermal stability increased by increasing hydrogen bonding or covalent interactions between proteins as was observed in the case of protein substitution with AA, BS, and MA. FT-IR spectroscopy and XRD quantitatively described changes in the

structure of the proteins that correlated with changes in the glass transition temperature and thermal stability. The limiting factor for internal plasticization is the number of available potential reactive groups on the protein. However, the feasibility of the method to reduce the glass transition temperature has been successfully demonstrated in the current study.

References

1. Purslow, P. P.; Vincent, J. F. V., Mechanical properties of primary feathers from the pigeon. *J. Exp. Biol.* **1978,** 72, 251-260.

2. Fraser, R. D. B.; MacRae, T. P., In Molecular structure and mechanical properties of keratins, Symposia of the Society for Experimental Biology. In *he Mechanical Properties of Biological Materials*, Vincent, J. F. V.; Currey, J. D., Eds. Cambridge University Press: 1980; Vol. XXXIV, pp 211-246.

3. Bonser, R. H. C., Comparative mechanics of bill, claw and feather keratin. *Journal of Avian Biology* **1996,** 27, 175-177.

4. Bonser, R. H. C.; Farrent, J. W., Influence of hydration on the mechanical performance of duck down feathers. *British Poultry Science* **2001,** 42, 271-273.

5. Bonser, R. H. C.; Purslow, P. P., The Young's modulus of feather keratin. *J. Exp. Biol.* **1995,** 198, 1029-1033.

6. Taylor, A. M.; Bonser, R. H. C.; Farrent, J. W., The influence of hydration on the tensile and compressive properties of avian keratinous tissues. *Journal of Material Science* **2004,** 39, 939-942.

7. Dweib, M. A.; Hu, B.; O'Donnell, A.; Shenton, H. W.; Wool, R. P., All natural composite sandwich beams for structural applications. *Compos. Struct.* **2004,** 63, (2), 147-157.

8. Barone, J. R.; Schmidt, W. F.; Liebner, C. F. E., Thermally processed keratin films. *J. Appl. Polym. Sci.* **2005,** 97, (4), 1644-1651.

9. Smith, B. L.; Schaffer, T. E.; Viani, M.; Thompson, J. B.; Frederick, N. A.; Kindt, J.; Belcher, A.; Stucky, G. D.; Morse, D. E.; Hansma, P. K., Molecular mechanistic origin of the toughness of natural adhesives, fibres and composites. *Nature* **1999,** 399, (6738), 761-763.

10. Vincent, J., *Struture of Biomaterials*. Princeton University Press: Princeton, 1990.

11. Gennes, P.-G. d.; Okumura, K., On the toughness of biocomposites. *Comptes Rendus de l'Acade´mie des Sciences - Series IV - Physics* **2000,** 1, (2), 257-261.

12. Okumura, K., Fracture strength of biomimetic composites: scaling views on nacre. *Journal of Physics-Condensed Matter* **2005,** 17, (31), S2879-S2884.

13. Barthelat, F., Biomimetics for next generation materials. *Philosophical Transactions of the Royal Society a-Mathematical Physical and Engineering Sciences* **2007,** 365, 2907-2919.

14. Gennadios, A.; Weller, C. L.; Testin, R. F., PROPERTY MODIFICATION OF EDIBLE WHEAT, GLUTEN-BASED FILMS. *Transactions of the Asae* **1993,** 36, (2), 465-470.

15. Sanchez, A. C.; Popineau, Y.; Mangavel, C.; Larre, C.; Gueguen, J., Effect of different plasticizers on the mechanical and surface properties of wheat gliadin films. *J. Agric. Food. Chem.* **1998,** 46, (11), 4539-4544.

16. Pouplin, M.; Redl, A.; Gontard, N., Glass transition of wheat gluten plasticized with water, glycerol, or sorbitol. *J. Agric. Food. Chem.* **1999,** 47, (2), 538-543.

17. Cuq, B.; Boutrot, F.; Redl, A.; Lullien-Pellerin, V., Study of the temperature effect on the formation of wheat gluten network: Influence on mechanical properties and protein solubility. *J. Agric. Food. Chem.* **2000,** 48, (7), 2954-2959.

18. Irissin-Mangata, J.; Bauduin, G.; Boutevin, B.; Gontard, N., New plasticizers for wheat gluten films. *Eur. Polym. J.* **2001,** 37, (8), 1533-1541.

19. Krochta, J. M., Proteins as raw materials for films and coatings: Definitions, current status, and opportunities. In *Protein-Based Films and Coatings,*, Gennadios, A., Ed. Ed. CRC Press LLC: Boca Raton, 2002; pp 1-41.

20. Hong, S. I.; Krochta, J. M., Oxygen Barrier Properties of Whey Protein Isolate Coatings on Polypropylene Films. *J. Food Sci.* **2003,** 68, (1), 224-228.

21. Kim, K. M.; Marx, D. B.; Weller, C. L.; Hann, M. A., Influence of sorghum wax, glycerin, and sorbitol on physical properties of soy protein isolate films. *J. Am. Oil Chem. Soc.* **2003,** 80, (1), 71-76.

22. Sothornvit, R.; Olsen, C. W.; McHugh, T. H.; Krochta, J. M., Formation conditions, water-vapor permeability, and solubility of compression-molded whey protein films. *J. Food Sci.* **2003,** 68, (6), 1985-1989.

23. Barone, J. R.; Schmidt, W. F.; Liebner, C. F. E., Thermally processed keratin films. *J. Appl. Polym. Sci.* **2005,** 97, 1644-1651.

24. Ranucci, E.; Bignotti, F.; Paderno, P. L.; Ferruti, P., MODIFICATION OF ALBUMINS BY GRAFTING POLY(AMIDO AMINE) CHAINS. *Polymer* **1995,** 36, 2989-2994.

25. Sereikaite, J.; Bassus, D.; Bobnis, R.; Dienys, G.; Bumeliene, Z.; Bumelis, V. A., Divinyl sulfone as a crosslinking reagent for oligomeric proteins. *uss. J. Bioorg. Chem.* **2003,** 29, (3), 227-230.

26. Mather, B. D.; Viswanathan, K.; Miller, K. M.; Long, T. E., Michael addition reactions in macromolecular design for emerging technologies. *Prog. Polym. Sci.* **2006,** 31, 487-531.

27. Nisbet, A. D.; Saundry, R. H.; Moir, A. J. G.; Fothergill, L. A.; Fothergill, J. E., The complete sequence of Hen-Ovalbumin. *Eur. J. Biochem.* **1981,** 115, 335-345.

28. Whitaker, J. R.; Tannenbaum, S. R., *Food proteins*. AVI Publishing: Westport, CT, 1977.

29. Bertrand-Harb, A.; Baday, M. D.; Chobert, J. M.; Haetle, T., Thermal modifications of structure and co-denaturation of a-lactalbumin and ß-lactoglobulin induce changes of solubility and susceptibility to proteases. *Nahrung* **2002,** 46, 283–289.

30. Lundgren, H. P.; O'Connell, R. A., Artificial Fibers from Corpuscular and Fibrous Proteins. *Industrial & Engineering Chemistry* **1944,** 36, (4), 370-374.

31. Lundgren, H. P.; Ward, W. H., Chemistry of Amino Acids and Proteins. *Annu. Rev. Biochem* **1949,** 18, 115 -154.

32. Lundren, H. P., The Formation of Fibers from Non- Fibrous Native Proteins. *Journal of American Chemical Society* **1941,** 63, 2854-2855.

33. Dicharry, R. M.; Ye, P.; Saha, G.; Waxman, E.; Asandei, A. D.; Parnas, R. S., Wheat gluten-thiolated poly(vinyl alcohol) blends with improved mechanical properties. *Biomacromolecules* **2006,** 7, 2837-2844.

34. Friedman, M., Applications of the ninhydrin reaction for analysis of amino acids, peptides, and proteins to agricultural and biomedical sciences. *Journal of Agricultural and Food Chemistry* **2004,** 52, 385-406.

35. Micard, V.; Guilbert, S., Thermal behavior of native and hydrophobized wheat gluten, gliadin and glutenin-rich fractions by modulated DSC. *International Journal of Biological Macromolecules* **2000,** 27, 229-236.

36. Katayama, D. S.; Carpenter, J. F.; Cornell Manning, M.; Randolph, T. W.; Setlow, P.; Menard, K. P., Characterization of amorphous solids with weak glass transitions using high ramp rate differential scanning calorimetry. *Journal of Pharmaceutical Sciences* **2008,** 97, (2), 1013-1024.

37. Athamneh, A.; Griffin, M.; Whaley, M.; Barone, J. R., Conformational changes and molecular mobility in plasticized proteins. *Biomacromolecules* **2008,** 9, 3181-3187.

38. Katayama, D. S.; Carpenter, J. F.; Manning, M. C.; Randolph, T. W.; Setlow, P.; Menard, K. P., Characterization of amorphous solids with weak glass transitions using high ramp rate differential scanning calorimetry. *J. Pharm. Sci.* **2008,** 97, 1013–1024.

39. Barone, J. R.; Medynets, M., Thermally processed levan polymers. *Carbohydrate Polymers* **2007,** 69, 554-561.

40. Jackson., M.; Mantsch, H., H., Protein secondary structure from FT-IR spectroscopy: correlation with dihedral angles from three-dimensional Ramachandran plots. *Canadian Journal of Chemistry* **1991,** 69, 1639-1642.

41. Ngarize, S.; Herman, H.; Adams, A.; Howell, N., Comparison of changes in the secondary structure of unheated, heated, and high-pressure-treated β-lactoglobulin and ovalbumin proteins using Fourier transform Raman spectroscopy and self-deconvolution. *Journal of Agricultural and Food Chemistry* **2004,** 52, 6470-6477.

42. Gunzler, H.; Gremlich, H.-U., *IR Spectroscopy*. Wiley-VCH: Weinheim, 2002.

43. Fraser, R. D. B.; MacRae, T. P., *Conformation in Fibrous Proteins and Related Synthetic Polypeptides*. Academic Press: New York, 1973.

44. Higgs, M. A.; Sass, R. L., The crystal structure of acrylic acid. *Acta Crystallographica* **1963,** 16, 657-661.

45. Aminova, R. M.; Schamov, G. A.; Aganov, A. V., Calculation of the structure and nuclear magnetic shielding constants of some H-bonded carbon acid complexes. *Journal of Molecular Structure (Theochem)* **2000,** 498, 233-246.

46. Durmaz, H.; Dag, A.; Gursoy, D.; Demirel, A. L.; Hizal, G.; Tunca, U., Multiarm star triblock terpolymers via sequential double click reactions. *Journal of Polymer Science Part A Polymer Chemistry* **2010,** 48, 1557-1564.

47. Goethals, E. J., On the polymerization and copolymerization of sulfolenes. *Die Makromolekulare Chemie* **1967,** 109, 132-142.

48. Hacioglu, B.; Suzer, S.; Akbulut, U.; Toppare, L.; Aybar, P.; Utley, J. H. P., Characterization of electroinitiated and radiation polymerized poly(butadiene sulfone). *Journal of Macromolecular Science-Chemistry* **1991,** A28, (3-4), 329-345.

49. Aybar, P.; Hacioglu, B.; Akbulut, U., Electroinitiated polymerization of butadiene sulfone. *Journal of Polymer Science: Part A: Polymer Chemistry* **1991,** 29, 1971-1976.

50. Smith, M. E. B.; Schumacher, F. F.; Ryan, C. P.; Tedaldi, L. M.; Papioannou, D.; Waksman, G.; Caddick, S.; Baker, J. R., Protein modification, bioconjugation, and disulfide bridging using bromomaleimides. *Journal of the American Chemical Society* **2010,** 132, 1960-1965.

51. Yukawa, S.; Omayu, A.; Matsumoto, A., Thermally stable fluorescent maleimide/isobutene alternating copolymers containing pyrenyl and alkynpyrenyl moieties in the side chain. *Macromolecular Chemistry and Physics* **2009,** 210, 1776-1784.

52. Fahmy, M. M., Inhibition of the thermal degradation of rigid poly(vinyl chloride) using poly(*N*-[4-(*N'*-phenyl amino carbonyl)phenyl]maleimide). *Journal of Applied Polymer Science* **2010,** 115, 2013-2018.

Chapter V

Chemistry between crosslinks affects the properties of peptide hydrogels

Abstract

Protein hydrogels were prepared by substituting ovalbumin with different concentrations of ethyl vinyl sulfone (EVS) or acrylic acid (AA) and crosslinking with divinyl sulfone (DVS). Fourier transform-infrared (FT-IR) spectroscopic studies confirmed the addition of EVS, AA, and DVS onto the protein. Swelling was assessed as a function of pH in the range of 2.5 to 9.4 and ionic strength. The elastic modulus of the gels was determined in shear and compression. Stress relaxation was assessed in compression. The substituent highly affected swelling and modulus with both hydrogels displaying non-Gaussian behavior in the range of hydrogel environments studied. Acrylic acid substituted ovalbumin exhibited a decreasing modulus with increasing swelling behaving as a polyelectrolyte with low added salt content. Ethyl vinyl sulfone substituted ovalbumin displayed an increasing modulus with swelling originating in the finite extensibility of the highly swollen chains. AA substituted OA showed higher modulus and reduced swelling compared to EVS substituted OA because of its ability to hydrogen and ionic bond to other molecules.

Introduction

The ability of hydrogels to swell to many times their original volume in water is one interesting property that makes them desirable for biological applications. Hydrogels are used as stimuli-responsive materials [1-3] often termed smart materials [4, 5] for drug delivery applications [6-8], 3D scaffolds for cell culture and tissue engineering [9-14], and superabsorbent gels in the sanitary industry. [15] The properties of hydrogels are often tailored to suit the end use. Hydrogels made from synthetic polymers have been used because of their availability and superior swelling properties. [16-19] Hydrogels made of poly(acrylamide), poly(acrylic acid), and poly(methacrylate) are common. However, for the biomedical industry it is desirable to have a hydrogel that is biocompatible and biodegradable. Hence the research focus in recent years has shifted to hydrogels made of natural polymers. Hydrogel synthesis by crosslinking polymers like chitosan [20], dextran [3, 7, 21], and other polysaccharides [22] has been attempted. Efforts were also made to create hydrogels by crosslinking proteins.[6, 23-25]

Elastin and collagen based hydrogels have been prominently featured because of their elastic nature. [26-30] Annabi *et al* reported the synthesis of porous hydrogels at atmospheric conditions and in the presence of high pressure CO_2 and obtained gels with modulus around 3-18 kPa and swelling ratio of 9-18 (g liquid/g protein). [26] Leach *et al* used α-elastin that swelled up to 250% and had modulus around 90-100 kPa. [28] *De novo* synthesis of proteins or peptides mimicking elastin is also one active research area. [31-35] Wang *et al* reported the synthesis of a protein that formed coiled coils and attached it to synthetic polymers to give hybrid hydrogels. [34] Genetically engineered Calmodulin protein that can bind to calcium and form hydrogels was reported by Ehrick *et al*. [33] The disadvantages of elastin are that it is scarce, expensive, and difficult to

solubilize. In the case of *de novo* synthesis, the yield of the fermentation process is low forcing the product into high priced niche markets.

The mechanical properties of hydrogels are also important in biological applications. [26] For soft materials like hydrogels there are not many established techniques for measuring the mechanical properties. Commonly used mechanical characterization techniques are rheology and unconfined compression. [36-38] New methods for accurate determination of the mechanical properties are being researched. [39, 40] Mathematical models are also being developed to estimate the properties of hydrogels that are difficult to determine experimentally. [1, 11, 41]

The challenges involved in preparation and characterization of hydrogels serve as motivation for the current work. The properties of hydrogels are determined by the amount of crosslinks and the length and chemistry of the sequence between crosslinks. As such, we hypothesized that it was possible to influence hydrogel properties in any protein by chemically modifying the protein to have specific crosslinks and chemical groups between crosslinks. This can be achieved using simple nucleophilic addition reactions in which vinyl containing groups can react with amines and thiols present on the protein. [42] Ovalbumin was chosen as a "model" protein because its structure and sequence have been well characterized and it has a variety of amino acids for chemical substitution. [43] This study focused on preparing hydrogels and characterizing them using vibrational spectroscopy, swelling studies, dynamic rheological, and static compression experiments.

Materials and Methods

Materials. Technical grade ovalbumin (mol. wt. 49.8 kDa), dithiothrietol (DTT, mol. wt. 154.5 g/mol), divinyl sulfone (DVS, mol. wt. 118.15 g/mol) and acrylic acid (AA, mol. wt. 72.01 g/mol) were purchased from Sigma Aldrich (USA). Dialysis membranes with 3,500 g/mol

molecular weight cut off and 95% ethyl vinyl sulfone (EVS, mol. wt. 120.17 g/mol) were obtained from VWR (USA).

Synthesis of ovalbumin hydrogels. The hydrogels were prepared using Michael type addition reactions. The amines on the protein reacted with the vinyl group of AA, EVS, and DVS. Ovalbumin (5 g) was added to 50 mL of deionized water followed by the addition of 0.017 g of DTT. DTT was used to reduce the cysteine bonds and make the protein soluble in water. The pH of the solution was adjusted to 9.0 using borate buffer. After 30 min, the protein was crosslinked by adding 0.5 g (427 µL) of DVS to the solution and reacting for 24 h at 30 °C. The reacted solution was dialyzed against deionized water for another 24 h. The water was changed every 12 h. Solid disks were prepared by pouring the dialyzed solution into molds with diameter 12 mm and depth 3 mm at regular intervals until a thick gel formed. Solid disks were formed by evaporating the water at ambient conditions.

Synthesis of AA and EVS substituted ovalbumin hydrogels. Ovalbumin was solubilized as above and AA or EVS added to the solution. The pH dropped to 4.0 after adding AA and was adjusted back to 9.0 using borate buffer. The reaction was run for 24 h at 30 °C and the solution was dialyzed for 24 h again changing the water after 12 h. After dialysis, the pH of the solution was adjusted to 9.0, 0.5 g (427 µL) of DVS was added, and the reaction was run for another 24 h followed by 24 h of dialysis. Solid disks were prepared as described above. Three molar ratios of AA or EVS to ovalbumin (0.2, 0.4 and 0.5) were used. These corresponded to the added volumes of 153 µL, 306 µL, and 383 µL for AA and 265 µL, 530 µL, and 663 µL for EVS. It was found that crosslinking before substituting interfered with the substitution reaction but substituting before crosslinking did not. Substituting first left the protein molecules soluble and

spaced far apart allowing for an easy crosslinking second step. Crosslinking first did not allow this to happen.

Notation. The following abbreviated names were used. Ovalbumin and DVS hydrogel (OD), ovalbumin substituted with AA and crosslinked with DVS: OAD0.2, OAD0.4, and OAD0.5 (corresponding to the AA:ovalbumin molar ratio 0.2, 0.4, and 0.5, respectively), and ovalbumin substituted with EVS and crosslinked with DVS: OED0.2, OED0.4 and OED0.5.

Swelling studies. Dry gels were weighed (w_d) and placed in potassium phosphate buffer solution containing penicillin at the corresponding experimental pH. Hydrogels were hydrated for 20 h, which was found to be long enough to reach equilibrium swelling. The hydrated gels were removed from the solution, blotted with Kim wipes to remove excess water, and weighed again (w_h). The equilibrium swelling ratio (Q) was calculated from

$$Q = \frac{V_{eq}}{V_{dry}} \qquad (1)$$

where V_{eq} was the hydrated hydrogel volume and V_{dry} was the dry hydrogel volume. [44] The volumes were found from w_d and w_h by using the polymer density of 1.41 g/cm^3, calculated using reference [45], and a composite density of a swollen hydrogel.

Fourier Transform-Infrared (FT-IR) spectroscopy. A Thermo-Nicolet 6700 FT-IR spectrometer with a Smart Orbit diamond ATR cell was used. Dry hydrogel samples were ground into a fine powder using a mortar and pestle and placed on the ATR crystal. The spectrum was collected over the range of 3400-400 cm^{-1} with a total of 64 scans and a resolution of 4 cm^{-1} and then baseline corrected and smoothed.

Rheology. An AR 2000 rheometer (TA instruments, NJ, USA) was used to perform rheological measurements. The sample was sandwiched between 8 mm diameter parallel plates held inside a custom full immersion container so the hydrogels could remain fully hydrated. The

plates were separated by 2 mm. Stress sweep tests were conducted from 1-100 Pa at 1 Hz frequency. Potassium phosphate buffer, pH adjusted to 7.4 was used to hydrate the gels.

Compression testing. The unconfined compression and stress relaxation tests were performed using a TA.HD plus (Stable Micro Systems, Surrey, UK) mechanical tester equipped with a 5 kg load cell. For both tests, fully hydrated gels were cut into disks of 4 mm diameter and 2.5-3 mm height and submerged in a bath of potassium phosphate buffer at pH 7.4. Elastic modulus was calculated from the linear region after applying a strain rate of 0.1 mm/s over 1% strain. This was found to be in the linear viscoelastic range. Stress relaxation experiments were performed similarly by straining the samples 1% for 300 min.

Results and Discussion

Appearance. After reaction, re-hydration of the samples showed they were insoluble. OED samples were transparent while OAD and OD samples opaque as shown in Figure 1. Opacity was indicative of structure formation in OAD, which refracted light. The lack of structure in OED made it transparent.

Table I. Stress Relaxation Parameters.

Hydrogel	σ_{eq} (kPa/kPa)	τ (s^{-1})	β	r^2
OD	0.090	2589	0.234	0.979
OAD0.2	0.099	668	0.579	0.988
OAD0.4	0.147	606	0.296	0.988
OAD0.5	0.064	879	0.649	0.987
OED0.2	0.021	3999	0.305	0.990
OED0.4	0.199	213	0.297	0.978
OED0.5	0.099	1417	0.278	0.989

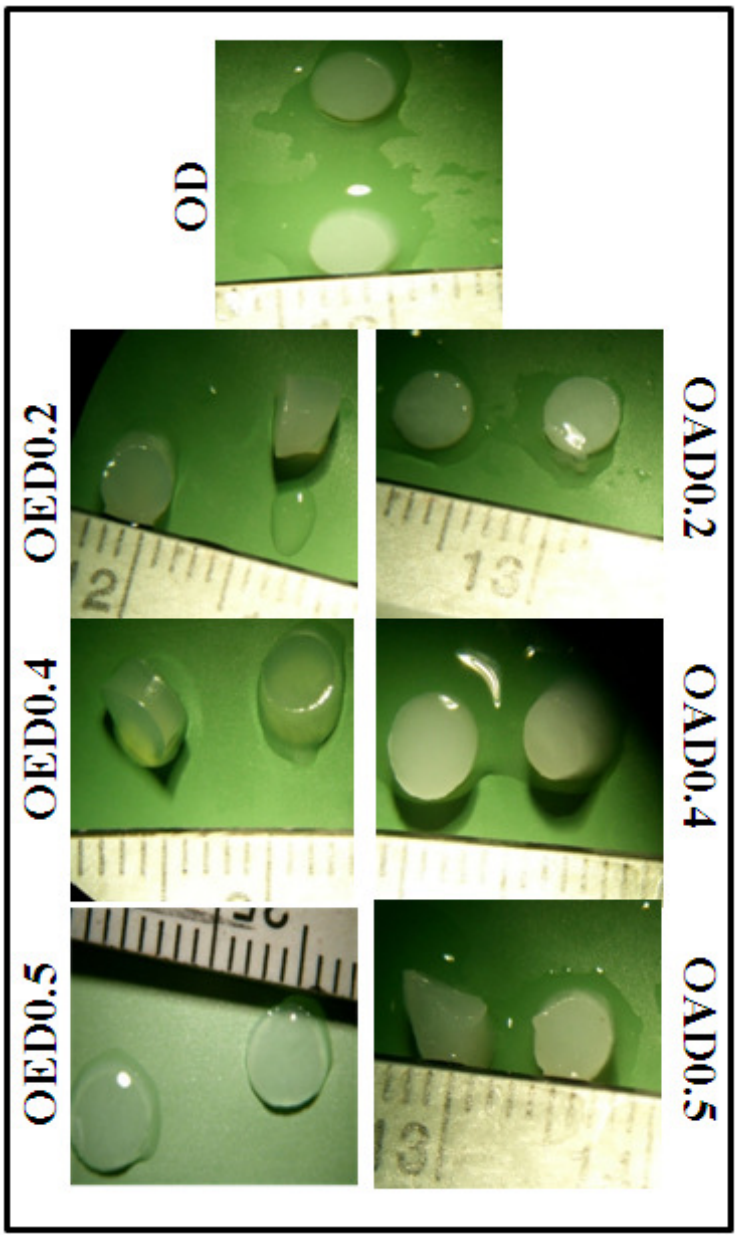

Figure 1. Photographs of hydrated protein hydrogels.

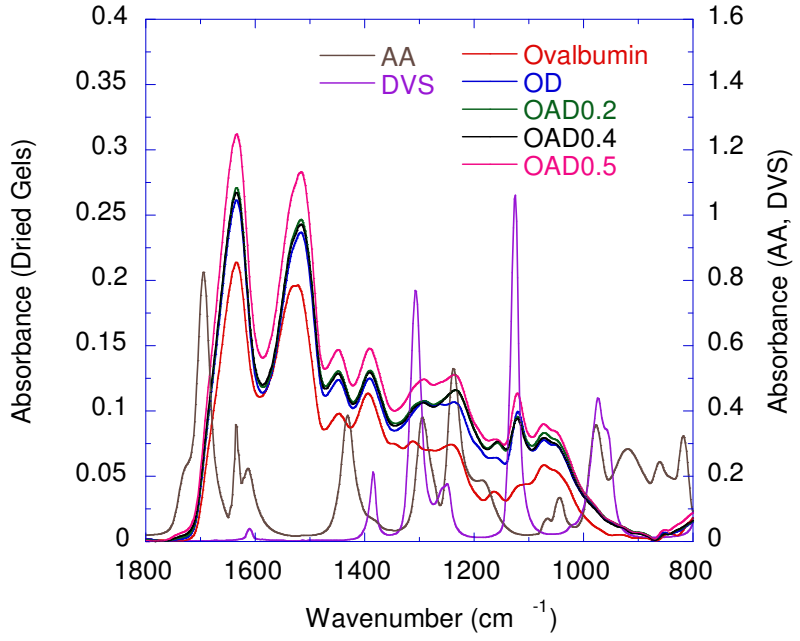

Figure 2a. FTIR AA- substituted OA hydrogels in the range of 1800-800 cm^{-1}.

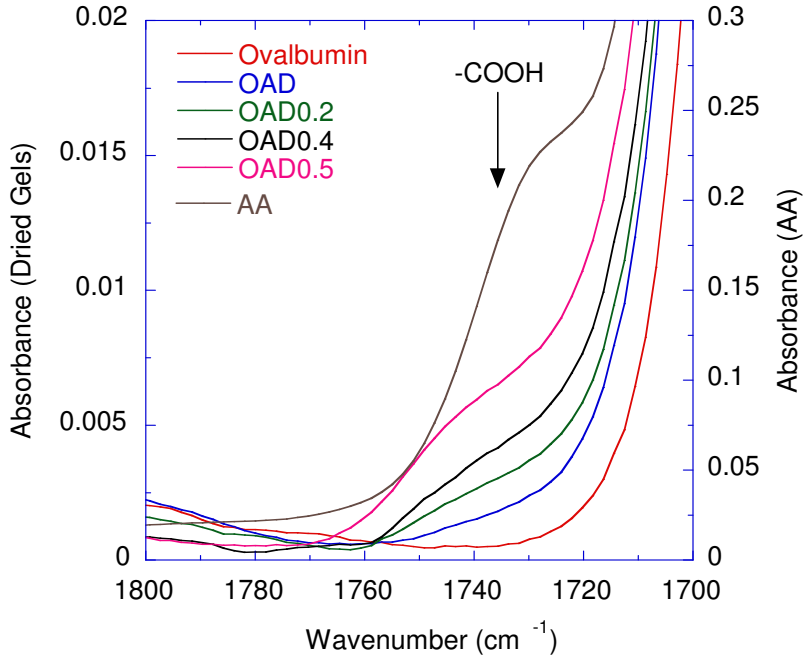

Figure 2b. FTIR spectra of the region 1800-1700 cm^{-1} of AA- substituted OA hydrogels.

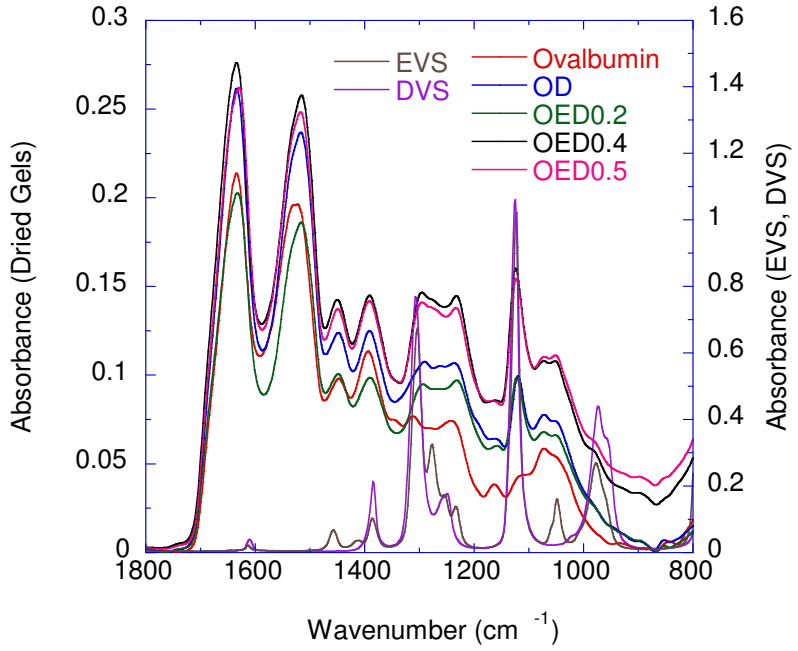

Figure 2c. FTIR of EVS- substituted OA hydrogels in the range of 1800-800 cm^{-1}.

FT-IR spectra. FT-IR spectra for dried hydrogels are shown in Figure 2. Crosslinking of ovalbumin with DVS was best exemplified by the appearance of ν_s(S=O) at 1125 cm^{-1}, which was not coincident with any groups on ovalbumin or AA. The peaks around 1634 cm^{-1} and 1526 cm^{-1} originated in the protein and were assigned to amide I and amide II absorbances, respectively. The amide I absorbance formed from main chain ν(C=O) and amide II from δ(N-H) present on the protein backbone and side chains. The amide II peak at 1526 cm^{-1} for pure ovalbumin shifted to 1516 cm^{-1} in the crosslinked protein indicating the DVS reaction site on ovalbumin was amine groups. The shift of the amide II absorbance was another method to quantify the crosslinking of ovalbumin.

Carboxylic acid and carboxylate groups on acrylic acid made it distinctive to find relative to ovalbumin and DVS. It was difficult to discern ν(COO$^-$) on acrylic acid because it appeared near δ(CH) between 1400 cm^{-1} and 1500 cm^{-1}. However, the COOH absorbance appeared

prominently at 1740 cm^{-1} and increased with acrylic acid concentration as shown in Figure 2b. Although EVS and DVS had similar FT-IR spectra because of similar chemical structures, differences were still discernible. Notably, EVS had a methyl group displaying $\delta_{as}(CH_3)$ at 1457 cm^{-1} that was absent in DVS, which contained no CH_3. EVS substitution produced a progressive shift of $\delta_{as}(CH_3)$ from 1447 cm^{-1} on ovalbumin towards 1457 cm^{-1} on EVS. The different environment of the sulfone on EVS produced $\nu(S=O)$ at 1049 cm^{-1}, which was different than DVS. This absorbance increased in intensity with EVS substitution on ovalbumin as shown in Figure 2c. Although coincident with DVS, $\nu_{as}(SO_2)$ at 1309 cm^{-1} and $\nu_s(SO_2)$ at 1127 cm^{-1} on OED increased in intensity above and beyond that of OD and OAD, indicative of EVS substitution. Amide I did not change in OAD hydrogels but shifted to lower wavenumber in

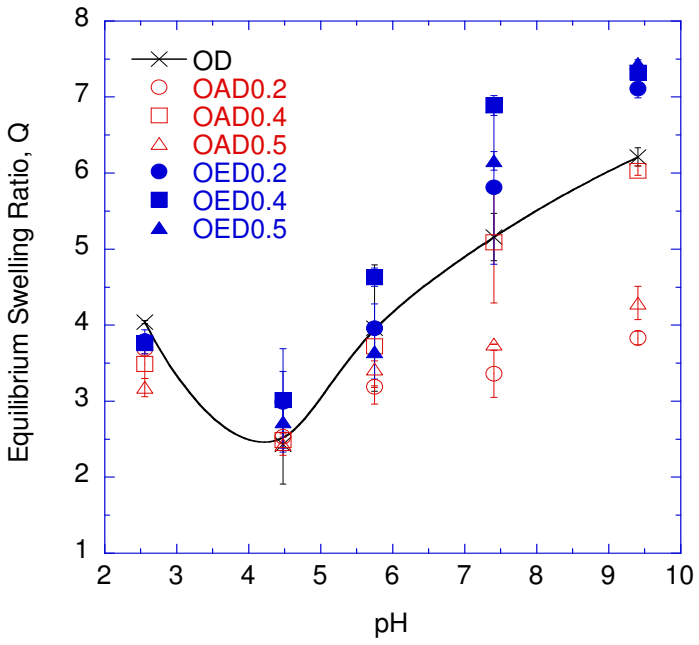

Figure 3. Swelling ratio, Q, of hydrated OA hydrogels as a function of pH.

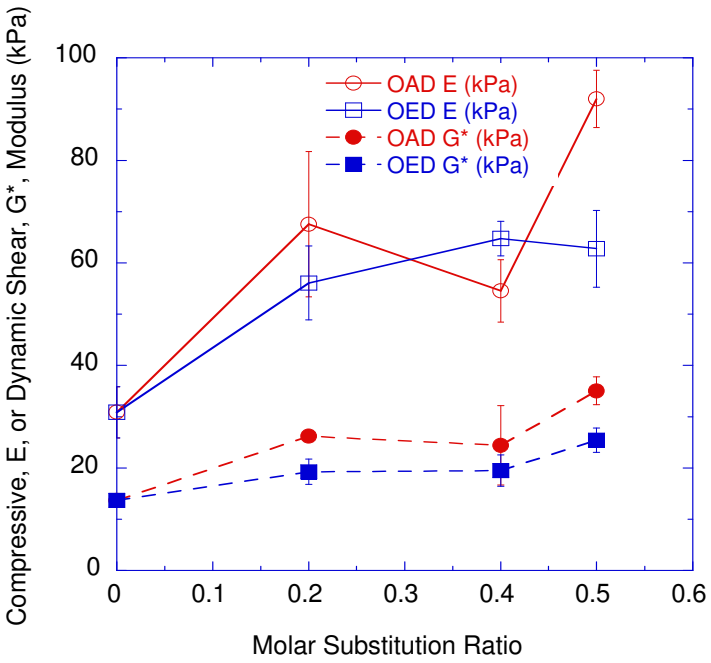

Figure 4. Compressive, E, and dynamic shear, G*, modulus of hydrated OA hydrogels at pH 7.4 as a function of molar ratio of AA- and EVS- to OA.

OED hydrogels. This was an indication that acrylic acid substitution maintained secondary structure and ethyl vinyl sulfone substitution re-arranged the ovalbumin secondary structure.

Swelling studies. All the samples showed a similar trend with respect to pH as shown in Figure 3. The swelling of the crosslinked protein can be attributed to ionic groups on protein amines and carboxylic acids. [23, 46, 47] At pH 2.6, negatively charged groups became protonated and neutral and only amines existed as positively charged groups thus swelling the hydrogels. At pH 2.6, OD swelled the most because it contained the most positively charged amines. The other hydrogels lost amine groups with substitution. As pH increased a minimum in swelling was reached at pH~4.5, which was near the protein isoelectric point, pI. [48] OAD showed the least swelling because this was also the pI of acrylic acid. Therefore, OED had the highest swelling because it was not quite neutral. Further increase in pH away from pI increased swelling. At pH>pI, the swelling behavior of the OD control formed a boundary of swelling behavior, with

OAD gels lying below and OED gels lying above the swelling boundary. This suggested that OED hydrogels had a higher overall charge than OAD hydrogels or perhaps a different structure.

Mechanical properties. The compressive elastic, E, and dynamic shear, G*, moduli of the gels are shown in Figure 4. In general, modulus increased with increasing substitution at low substitution before saturating. In all cases, E~3G*, which was consistent with a linear elastic material and showed the high correlation between the uniaxial and shear experiments performed separately. All hydrogels had weak loss moduli of G"~3-5 kPa (Figure 5b). The storage modulus, G', was an order of magnitude higher than the loss modulus confirming the elastic nature of the gels as shown in Figure 5a. The hydrogel storage modulus did not show any dependence on applied stress in the range of 10-100 Pa.

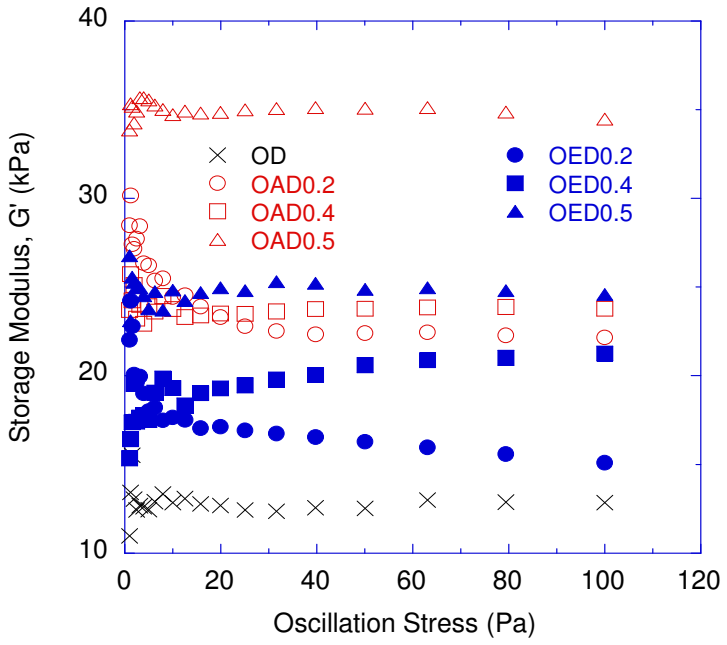

Figure 5a. Storage, G', modulus of hydrated OA hydrogels at pH 7.4 obtained from stress sweep experiments.

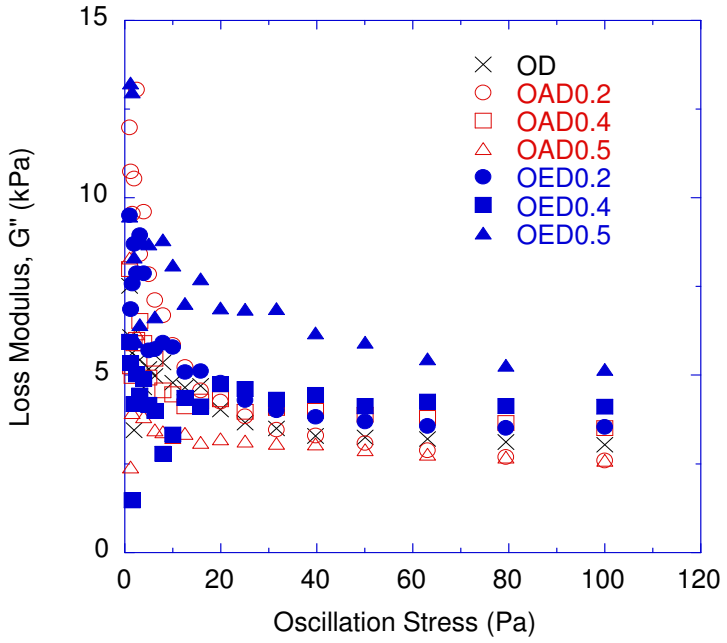

Figure 5b. Loss, G'', modulus of hydrated OA hydrogels at pH 7.4 obtained from stress sweep experiments.

To compare stress relaxation behavior, stress values were averaged then normalized by the maximum value and the results are plotted in Figure 6 with short time behavior in the inset. All stress relaxation curves were fit to a stretched exponential of the form

$$\frac{\sigma(t)}{\sigma_0} = \sigma_{eq} + \exp[-(t/\tau)^{\beta}] \qquad (2)$$

where σ_{eq} is the equilibrium stress value at long time and τ is the overall stress relaxation time. [49] The results are contained in Table I. OAD0.5 relaxed the most while OD relaxed the least. In other words, the highest modulus hydrogel relaxed the most and the lowest modulus hydrogel the least. OAD0.4 and OED0.4 showed the fastest stress relaxation. Interestingly, the fastest relaxing samples displayed the highest swelling for AA- and EVS-substituted OA.

Molecular structure. The swelling and mechanical properties describe several unique molecular structural features of the hydrogels. Figure 7 plots E and G*, measured separately, as

a function of swelling ratio, Q. For an equal amount of crosslinking and substitution, ethyl vinyl sulfone and acrylic acid had profoundly different effects on the overall hydrogel. OAD hydrogels displayed decreasing modulus with increasing swelling ratio, typical of most swollen rubbers. For a Gaussian network where elasticity originates from chain entropy, the modulus should scale as $G \sim Q^{-1/3}$. [50] However, the modulus decrease with swelling for OAD hydrogels was stronger with $G \sim Q^{-1}$. This was related to the ionic nature of the acrylic acid modified protein and appeared consistent with the modulus dependence of polyelectrolyte hydrogels with

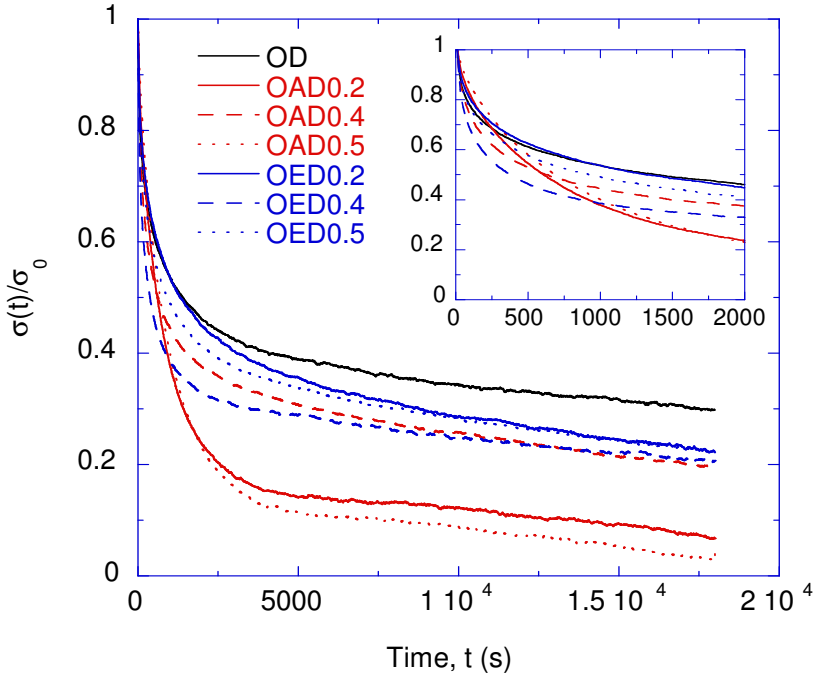

Figure 6. Stress relaxation results of hydrated hydrogels. The gels were relaxed for 18,000 sec under an applied strain of 1%. Y-axis represents normalized stress values. Inset shows the early time data to highlight the faster relaxation of OAD0.4 and OED0.4 gels.

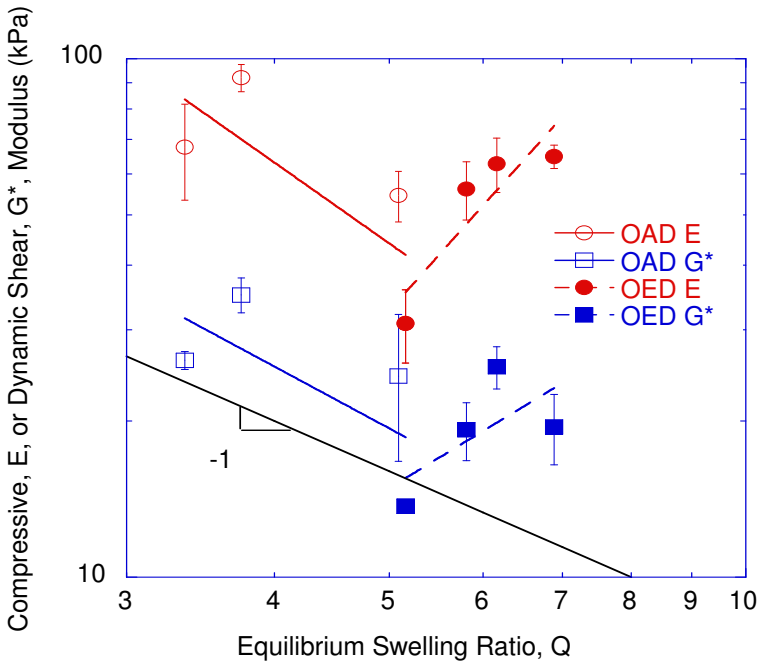

Figure 7. Compressive, E, and dynamic shear, G*, modulus of hydrated hydrogels vs. swelling ratio, Q, at pH 7.4.

a low amount of ionic character as proposed by Skouri *et al* [51] and Rubinstein *et al*. [52] OED hydrogels displayed increasing modulus with increasing swelling ratio. This result was consistent with a highly stretched network displaying non-Gaussian behavior. [51, 53, 54]

Crosslinking the protein simply produced an insoluble hydrogel capable of being swelled. The purpose of substitution was to affect the chemistry between crosslinks. EVS imparted the protein with a long substituent containing a hydrophobic end group. EVS had 2 hydrogen bond acceptors in the sulfonyl and no donors. AA imparted the protein with a short substituent containing a hydrophilic end group. AA had a hydrogen bond donor and acceptor in the hydroxyl and carbonyl, respectively. Interestingly, the addition of acrylic acid did not enhance the swelling. OAD samples swelled the least of the three. This phenomenon, in which the swelling decreased with increased acrylic acid concentration, has been observed in other reports

as well. [20, 55] Lee *et al* attributed the decreased swelling to ionic bond formation between chitosan and acrylic acid. [20] Burkeev *et al* cited the denser structure of the copolymer (β-vinyloxyethylamide of acrylic acid with acrylic acid or methacrylic acid) as a reason. [55] Acrylic acid was known to form dimers through hydrogen bonding of the carbonyl on one acid to the hydroxyl on another and the bonding energy of dimers was more than peptide hydrogen bonding energy. [56] We hypothesized that acrylic acid formed ionic bonds with positively charged amines on the protein and hydrogen bonds with the protein and other acrylic acids. These bonds acted as additional crosslinks, hindered the swelling of the OAD gels, and imparted higher modulus. Figure 8 displays the 3600-2000 cm^{-1} IR absorbance region, which was characteristic of hydrogen bonding. [57] Hydrogen bonding manifested as an increase in the area of the large peak in this absorbance region. The addition of acrylic acid onto ovalbumin increased hydrogen bonding while the addition of EVS did not. In fact, OED hydrogen bonding interactions

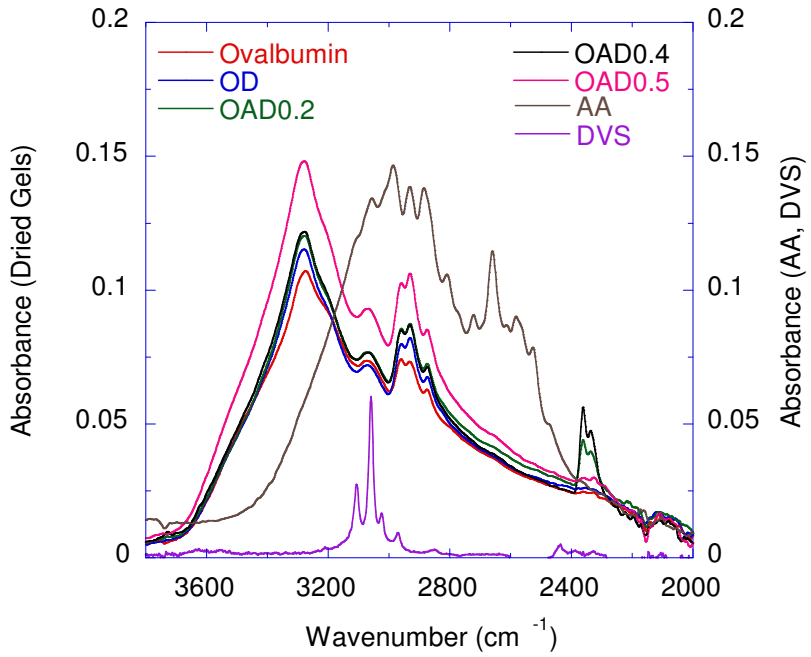

Figure 8a. FTIR spectra of dry AA- substituted OA in the range of 3600 - 2000 cm^{-1}.

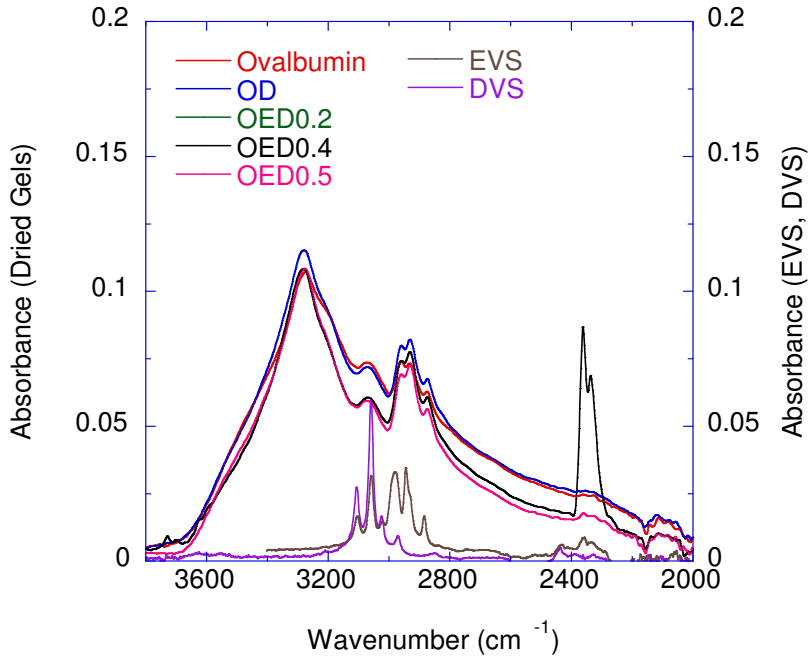

Figure 8b. FTIR spectra of dry EVS- substituted OA in the range of 3600 - 2000 cm^{-1}.

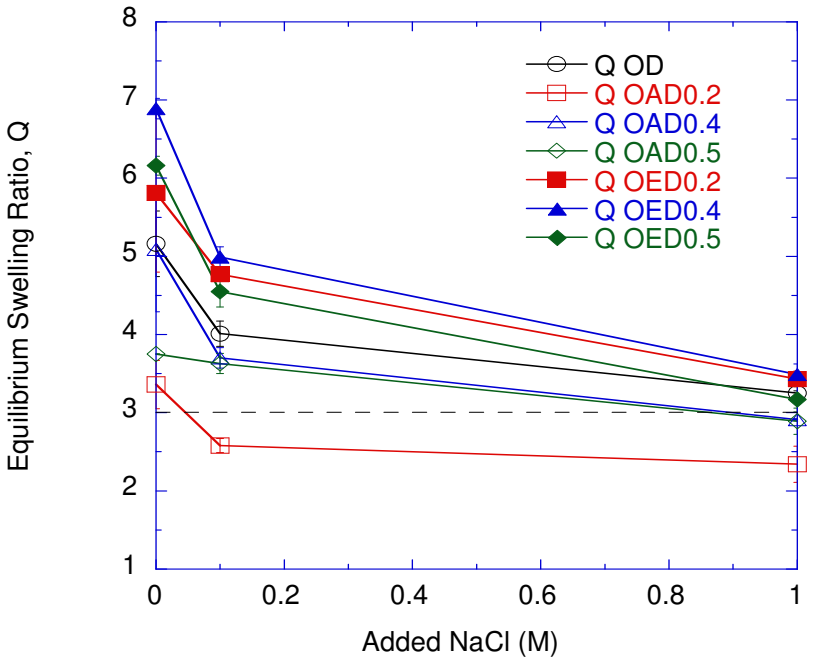

Figure 9. Swelling ratio, Q, of hydrated hydrogels as function of added NaCl concentration at pH 7.4.

decreased with increased substitution. Although EVS was a hydrogen bond acceptor, the lack of donors from loss of amines upon substitution prevented additional hydrogen bonding in this system. Specific hydrogen bonding interactions were not discerned but the increased hydrogen bonding in the OAD gels existed.

To discern ionic interactions, the hydrogels at pH 7.4 were swelled in solutions with added NaCl. At high added salt concentration, all hydrogels displayed Q~3 similar to the result at pH~pI~4.5 as shown in Figure 9 (note the data at 0 M Added NaCl is the same as in Figure 3). So when all charge was screened, either by adjusting pH to the isoelectric point or by adding anions and cations, all of the hydrogels behaved similarly, swelling to about 3 times their original dry volume. At high salt concentration or pH~pI, the swelling was simply from the addition of water solvent to the network. When charged, OED displayed higher swelling then OAD. Since EVS was not charged, it was the intrinsic protein charge providing the additional swelling. The longer EVS molecule may have prevented amino acid side groups from interacting. The appearance of the sulfonyl in the middle of the substituent may have made it difficult to hydrogen bond. The charged acrylic acid readily interacted with other chains to prevent swelling and increase modulus.

The 0.4 molar substitution ratio represented a critical point, showing the highest swelling, asymptote in modulus, and fastest stress relaxation behavior. The hydrogels were prepared by substituting then crosslinking. There were 68 primary amines, 37 secondary amines, and 6 thiols on ovalbumin amino acid side groups. The total of 111 potential reaction sites formed the basis for the molar ratios. Based on the acid/base properties of the amino acids and the reaction pH of 9, 12.6 potential reactive groups per ovalbumin molecules would be expected. However, it was determined that the actual number of reactive groups on ovalbumin was at least 50 as measured

by Raman and UV-visible spectroscopy. [58] As such, at a molar substitution ratio of 0.4, about 87 groups were reacted when counting the DVS crosslinker too. At this substitution, the ovalbumin appeared saturated. At higher substitution, i.e., 0.5 molar ratio, the hydrogels were more substituted than covalently crosslinked. For OAD, the ability of acrylic acid to interact highly with other substituted protein chains further increased modulus. However, the overabundance of substituents relative to covalent crosslinks did not allow for faster relaxation or increased swelling.

Conclusions

Ovalbumin was successfully substituted and crosslinked using facile nucleophilic addition reactions. All substituted ovalbumin hydrogels showed higher modulus than the unsubstituted control sample. The chemistry of the substituent highly influenced the hydrogel, allowing for increased swelling or faster stress relaxation. Hydrophilic substitutents like acrylic acid, which were capable of interacting with other substituted protein chains, increased modulus and decreased swelling. Substituents like ethyl vinyl sulfone that were less capable of interacting with other substituted protein chains allowed for increased swelling but decreased modulus.

References

1. Huang, Y.; Jin, X.; Liu, H.; Hu, Y., A molecular thermodynamic model for the swelling of thermo-sensitive hydrogels. *Fluid Phase Equilib.* **2008,** 263, (1), 96-101.

2. Lee D. S.; Woo, S. S., Electroactive and temperature-sensitive hydrogel composites. *J. Appl. Polym. Sci.* **1999,** 74, (2), 311-321.

3. Chiu, H.-C.; Lin, Y.-F.; Hsu, Y.-H., Effects of acrylic acid on preparation and swelling properties of pH-sensitive dextran hydrogels. *Biomaterials* **2002,** 23, (4), 1103-1112.

4. Kopecek J.; Yang, J., Hydrogels as smart biomaterials. *Polym. Int.* **2007,** 56, (9), 1078-1098.

5. Kim, S. J.; Kim, H. I.; Park, S. J.; Kim, I. Y.; Lee, S. H.; Lee, T. S.; Kim, S. I., Behavior in electric fields of smart hydrogels with potential application as bio-inspired actuators *Smart Mater. Struct.* **205,** 14, 511-514.

6. Fang, J.-Y.; Chen, J.-P.; Leu, Y.-L.; Wang, H.-Y., Characterization and Evaluation of Silk Protein Hydrogels for Drug Delivery. *Chemical & Pharmaceutical Bulletin* **2006,** 54, (2), 156-162.

7. Hennink, W. E.; Talsma, H.; Borchert, J. C. H.; De Smedt, S. C.; Demeester, J., Controlled release of proteins from dextran hydrogels. *J. Controlled Release* **1996,** 39, (1), 47-55.

8. Alexander, C., Temperature- and pH-responsive smart polymers for gene delivery. *Expert Opinion on Drug Delivery* **2006,** 3, (5), 573.

9. Rizzi, S. C.; Ehrbar, M.; Halstenberg, S.; Raeber, G. P.; Schmoekel, H. G.; Hagenmuller, H.; Muller, R.; Weber, F. E.; Hubbell, J. A., Recombinant Protein-co-PEG Networks as Cell-Adhesive and Proteolytically Degradable Hydrogel Matrixes. Part II: Biofunctional Characteristics. *Biomacromolecules* **2006,** 7, (11), 3019-3029.

10. Rzaev, Z. M. O.; Dinçer, S.; Piskin, E., Functional copolymers of N-isopropylacrylamide for bioengineering applications. *Prog. Polym. Sci.* **2007,** 32, (5), 534-595.

11. Peppas, N. A.; Huang, Y.; Torres-Lugo, M.; Ward, J. H.; Zhang, J., Physiochemical Foundations and Structural Design of Hydrogels in Medicine and Biology. *Annual Review of Biomedical Engineering* **2000,** 2, (1), 9-29.

12. Drury, J. L.; Mooney, D. J., Hydrogels for tissue engineering: scaffold design variables and applications. *Biomaterials* **2003,** 24, (24), 4337-4351.

13. Baroli, B., Hydrogels for tissue engineering and delivery of tissue-inducing substances. *J. Pharm. Sci.* **2007,** 96, (9), 2197-2223.

14. Kim, J.; Lee, K.-W.; Hefferan, T. E.; Currier, B. L.; Yaszemski, M. J.; Lu, L., Synthesis and Evaluation of Novel Biodegradable Hydrogels Based on Poly(ethylene glycol) and Sebacic Acid as Tissue Engineering Scaffolds. *Biomacromolecules* **2007,** 9, (1), 149-157.

15. Zhao, Y.; Su, H.; Fang, L.; Tan, T., Superabsorbent hydrogels from poly(aspartic acid) with salt-, temperature- and pH-responsiveness properties. *Polymer* **2005,** 46, (14), 5368-5376.

16. Tao, Y.; Zhao, J.-X.; Wu, C.-X., Experiments and simulation of pH-responsive *N*-isopropylacrylamide-acrylic acid copolymer hydrogels. *J. Appl. Polym. Sci.* **2006,** 101, (1), 323-330.

17. Kumeta, K.; Nagashima, I.; Matsui, S.; Mizoguchi, K., Crosslinking reaction of poly(vinyl alcohol) with poly(acrylic acid) (PAA) by heat treatment: Effect of neutralization of PAA. *J. Appl. Polym. Sci.* **2003,** 90, (9), 2420-2427.

18. Melekaslan, D.; Gundogan, N.; Okay, O., Swelling and elasticity of ionic poly(N-isopropylacrylamide) gels immersed in the melt of poly(ethylene glycol) chains. *Polymer* **2003,** 44, (8), 2281-2288.

19. Üzüm Ö. B.; Karadağ J, Synthetic polymeric absorbent for dye based on chemically crosslinked acrylamide/mesaconic acid hydrogels. *J. Appl. Polym. Sci.* **2006,** 101, (1), 405-413.

20. Lee, J. W.; Kim, S. Y.; Kim, S. S.; Lee, Y. M.; Lee, K. H.; Kim, S. J., Synthesis and characteristics of interpenetrating polymer network hydrogel composed of chitosan and poly(acrylic acid). *J. Appl. Polym. Sci.* **1999,** 73, (1), 113-120.

21. Rudraraju, V. S.; Wyandt, C. M., Rheology of Microcrystalline Cellulose and Sodiumcarboxymethyl Cellulose hydrogels using a controlled stress rheometer: part II. *Int. J. Pharm.* **2005,** 292, (1-2), 63-73.

22. Söderqvist Lindblad, M.; Albertsson, A.-C.; Ranucci, E.; Laus, M.; Giani, E., Biodegradable Polymers from Renewable Sources: Rheological Characterization of Hemicellulose-Based Hydrogels. *Biomacromolecules* **2005,** 6, (2), 684-690.

23. Caillard, R.; Remondetto, G. E.; Mateescu, M. A.; Subirade, M., Characterization of Amino Cross-Linked Soy Protein Hydrogels. *J. Food Sci.* **2008,** 73, (5), C283-C291.

24. El-Sherif, H.; El-Masry, M.; Taleb, M. F. A., pH-sensitive hydrogels based on bovine serum albumin for anticancer drug delivery. *J. Appl. Polym. Sci.* **2010,** 115, (4), 2050-2059.

25. Bajpai, A.; Saini, R., Preparation and characterization of novel biocompatible cryogels of poly (vinyl alcohol) and egg-albumin and their water sorption study. *Journal of Materials Science: Materials in Medicine* **2006,** 17, (1), 49-61.

26. Annabi, N.; Mithieux, S. M.; Boughton, E. A.; Ruys, A. J.; Weiss, A. S.; Dehghani, F., Synthesis of highly porous crosslinked elastin hydrogels and their interaction with fibroblasts in vitro. *Biomaterials* **2009,** 30, (27), 4550-4557.

27. Lim, D. W.; Nettles, D. L.; Setton, L. A.; Chilkoti, A., Rapid Cross-Linking of Elastin-like Polypeptides with (Hydroxymethyl)phosphines in Aqueous Solution. *Biomacromolecules* **2007,** 8, (5), 1463-1470.

28. Leach, J. B.; Wolinsky, J. B.; Stone, P. J.; Wong, J. Y., Crosslinked [alpha]-elastin biomaterials: towards a processable elastin mimetic scaffold. *Acta Biomaterialia* **2005,** 1, (2), 155-164.

29. Mao, C.; Kisaalita, W. S., Characterization of 3-D collagen hydrogels for functional cell-based biosensing. *Biosens. Bioelectron.* **2004,** 19, (9), 1075-1088.

30. Spencer, N. J.; Cotanche, D. A.; Klapperich, C. M., Peptide- and collagen-based hydrogel substrates for in vitro culture of chick cochleae. *Biomaterials* **2008,** 29, (8), 1028-1042.

31. Wu, Y.; MacKay, J. A.; R. McDaniel, J.; Chilkoti, A.; Clark, R. L., Fabrication of Elastin-Like Polypeptide Nanoparticles for Drug Delivery by Electrospraying. *Biomacromolecules* **2008,** 10, (1), 19-24.

32. Schneider, J. P.; Pochan, D. J.; Ozbas, B.; Rajagopal, K.; Pakstis, L.; Kretsinger, J., Responsive Hydrogels from the Intramolecular Folding and Self-Assembly of a Designed Peptide. *J. Am. Chem. Soc.* **2002,** 124, (50), 15030-15037.

33. Ehrick, J. D.; Deo, S. K.; Browning, T. W.; Bachas, L. G.; Madou, M. J.; Daunert, S., Genetically engineered protein in hydrogels tailors stimuli-responsive characteristics. *Nat Mater* **2005,** 4, (4), 298-302.

34. Wang, C.; Stewart, R. J.; KopeCek, J., Hybrid hydrogels assembled from synthetic polymers and coiled-coil protein domains. *Nature* **1999,** 397, (6718), 417-420.

35. Shen, W.; Kornfield, J. A.; Tirrell, D. A., Structure and mechanical properties of artificial protein hydrogels assembled through aggregation of leucine zipper peptide domains. *Soft Matter* **2007,** 3, (1), 99-107.

36. Anseth, K. S.; Bowman, C. N.; Brannon-Peppas, L., Mechanical properties of hydrogels and their experimental determination. *Biomaterials* **1996,** 17, (17), 1647-1657.

37. Hirotsu, S., Stress Relaxation and Elastic Moduli in the Swollen and the Shrunken Phases of N-Isopropylacrylamide Gel. *Macromolecules* **2004,** 37, (9), 3415-3424.

38. Stammen, J. A.; Williams, S.; Ku, D. N.; Guldberg, R. E., Mechanical properties of a novel PVA hydrogel in shear and unconfined compression. *Biomaterials* **2001,** 22, (8), 799-806.

39. Ahearne, M.; Yang, Y.; Haj, A. J. E.; Then, K. Y.; Liu, K.-K., Characterizing the viscoelastic properties of thin hydrogel-based constructs for tissue engineering applications. *Journal of The Royal Society Interface* **2005,** 2, 455-463.

40. Han, L.; Burcher, M.; Noble, J., Non-invasive Measurement of Biomechanical Properties of in vivo Soft Tissues. In 2002; pp 208-215.

41. De, S. K.; Aluru, N. R., A chemo-electro-mechanical mathematical model for simulation of pH sensitive hydrogels. *Mech. Mater.* 36, (5-6), 395-410.

42. Mather, B. D.; Viswanathan, K.; Miller, K. M.; Long, T. E., Michael addition reactions in macromolecular design for emerging technologies. *Prog. Polym. Sci.* **2006,** 31, 487-531.

43. Nisbet, A. D.; Saundry, R. H.; Moir, A. J. G.; Fothergill, L. A.; Fothergill, J. E., The complete sequence of Hen-Ovalbumin. *Eur. J. Biochem.* **1981,** 115, 335-345.

44. Rubinstein, M.; Colby, R. H., Polymer Physics. In Oxford University Press: New York, 2003; pp 274-282.

45. Fischer, H.; Polikarpov, I.; Craievich, A. F., Average protein density is a molecular-weight-dependent function. *Protein Sci.* **2004,** 13, (10), 2825-2828.

46. Hu, H. Y.; Du, H. N., α-to-β Structural Transformation of Ovalbumin: Heat and pH Effects. *J. Protein Chem.* **2000,** 19, (3), 177-183.

47. Furlan, P. Y.; Scott, S. A.; Peaslee, M. H., FTIR-ATR Study of pH Effects on Egg Albumin Secondary Structure. *Spectroscopy Letters: An International Journal for Rapid Communication* **2007,** 40, (3), 475 - 482.

48. Seki, H.; Suzuki, A.; Maruyama, H., Adsorption of egg albumin onto methylated yeast biomass. *J. Colloid Interface Sci.* **2004,** 270, (2), 304-308.

49. de Gennes, P.-G., Relaxation Anomalies in Linear Polymer Melts. *Macromolecules* **2002,** 35, (9), 3785-3786.

50. Treloar, L. R. G., *The Physics of Rubber Elasticity*. Oxford University Press: New York, 2005.

51. Skouri, R.; Schosseler, F.; Munch, J. P.; Candau, S. J., Swelling and Elastic Properties of Polyelectrolyte Gels. *Macromolecules* **1995,** 28, (1), 197-210.

52. Rubinstein, M.; Colby, R. H.; Dobrynin, A. V.; Joanny, J.-F., Elastic Modulus and Equilibrium Swelling of Polyelectrolyte Gels. *Macromolecules* **1996,** 29, (1), 398-406.

53. Horkay, F.; Tasaki, I.; Basser, P. J., Osmotic Swelling of Polyacrylate Hydrogels in Physiological Salt Solutions. *Biomacromolecules* **2000,** 1, (1), 84-90.

54. Okay, O.; Durmaz, S., Charge density dependence of elastic modulus of strong polyelectrolyte hydrogels. *Polymer* **2002,** 43, (4), 1215-1221.

55. Burkeev, M.; Tazhbaev, E.; Kazhmuratova, A.; Sugralina, L.; Zhaparova, L., Hydrogels of copolymers of β-vinyloxyethylamide of acrylic acid with unsaturated carboxylic acids. *Polymer Science Series B* **2007,** 49, (11), 257-260.

56. Klotz, I. M., Solvent water and protein behavior: View through a retroscope. *Protein Sci.* **1993,** 2, 1992-1999.

57. Gunzler, H.; Gremlich, H.-U., IR Spectroscopy: An Introduction. In WILEY-VCH: Weinheim, Germany, 2002; pp 206-207.

58. Budhavaram, N. K.; Barone, J. R., Quantifying amino acid and protein substitution using Raman spectroscopy. *Journal of Raman Spectroscopy* **2010,** DOI:10.1002/jrs.2738.

Chapter VI

Self-assembled structures from modified alanine

Abstract

Structures like spheres and fibers have a lot of potential applications in the chemical and biomedical industries. It would be more desirable if these structures were synthesized from biomolecules in an energy efficient manner. Here we report synthesis of such structures using simple chemical reactions and characterization of the structures. Nucleophilic Michael-type addition reactions were used to conjugate L-alanine, a natural amino acid, with ethyl vinyl sulfone (EVS) under environmentally benign conditions. Alanine and EVS were reacted in different concentrations at pH 9.0 and 30 °C. The resulting samples were subjected to FTIR, TGA, SEM and XRD analysis. The conjugated alanine self-assembled into different structures like bars and fibers depending on the concentration of EVS. This work demonstrated the feasibility of micron-scale structure synthesis using single component systems.

Introduction

Nature routinely synthesizes structures in different shapes and sizes in water at neutral conditions. Most of these structures form through self-assembly, which is driven mainly by non-covalent interactions.[1] It has become evident that mimicking nature's way to synthesize materials could be energy and economically efficient. As a result, a lot of the current self-assembly research is focused on bio-inspired technologies and materials.[1] Recent efforts are more focused on self-assembly of biomolecules that offer less toxicity than their synthetic counterparts.[2-6] Cellulose and chitosan are examples of naturally available polymers that are being used for biomaterial synthesis.[7, 8] Other biopolymers include proteins like silk and elastin.[9, 10] The molecular weight of these biopolymers usually ranges from 10^3-10^6 g/mol. The individual components from which these superstructures are built are also of immense value. The naturally available amino acids with their chiral nature and reactive groups offer a lot of possibilities for the creation of biomaterials and self-assembled structures. Structures based on amino acid derivatives have already been reported and are being extensively researched.[3, 11, 12]

Alanine is the smallest chiral molecule and hence there is a huge interest in using it for various applications.[13, 14] However, derivatized alanine and alanine based polypeptides have found more use than pure alanine. Mostly fibrous structures have been reported from polyalanine while fibers, ribbons and tubes have been synthesized using derivatized alanine.[15-17] Most of the structures from alanine derivatives that have been reported were prepared using two or three component systems.[15, 18]

In this study we report the formation of various structures from a one component system obtained using modified L-alanine. L-alanine was conjugated with ethyl vinyl sulfone using nucleophilic Michael-type addition reactions in aqueous solution. Michael-type addition

reactions take place at amines and thiols present on amino acids and at room temperature. Though the reactions can occur at neutral pH, basic conditions will increase the kinetics.[19] The vinyl group of sulfone reacted with amine on alanine (Figure 1), forming one dimensional bars and fibers at lower concentrations of EVS. Fourier transform-infrared (FT-IR) spectroscopy, X-ray powder diffraction (XRD), thermogravimetric analysis (TGA) and scanning electron microscopy (SEM) were used to investigate the structures.

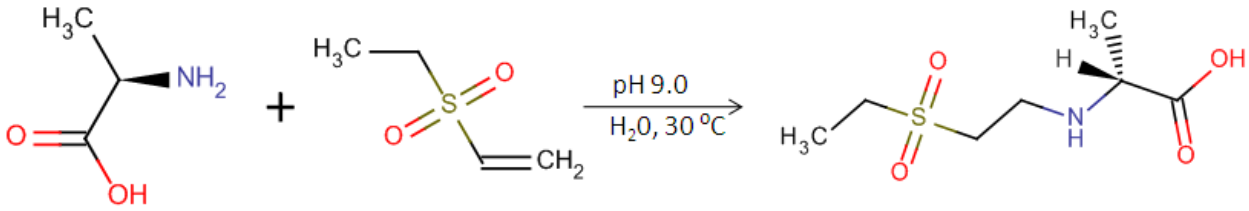

Figure 1. Primary amine group on alanine reacting with vinyl group on EVS in water at room temperature and pH 9.

Materials and Methods

Materials. L-alanine (A, mol. wt. 89.09 g/mol) was purchased from EMD chemicals and ethyl vinyl sulfone (EVS, mol. wt. 120.17 g/mol) was purchased from VWR.

Alanine substitution. 0.5 g of L-alanine was added to 50 mL of deionized (DI) water and the pH was adjusted to 9. After the amino acid completely dissolved, the desired amount of EVS was added to the solution and reacted for 24 hr at 30° C. Following reaction, the solution was dried on Teflon-coated aluminum boats for 2 days at ambient conditions. The molar ratio of alanine to EVS was based on the number of potential reactive sites (amine groups) on amino

acid. Alanine has 1 NH_2 and so the total number of reactive sites was counted as 2, since both primary and secondary amines can participate in the reaction.[20]

Fourier Transform-Infrared spectroscopy (FT-IR). A Thermo-Nicolet 6700 FT-IR spectrometer with a diamond ATR cell was used. The spectrum was collected with a total of 64 scans and a resolution of 4 cm^{-1} and then baseline corrected. Data collection and analysis was done using OMNIC v. 7.3 software. The original spectrum was deconvoluted by fitting with Gaussian/Lorentzian peaks. The number of peaks and their position were determined by the automatic peak finding feature of the program at low sensitivity and full width at half height of 3.857.

X-ray powder diffraction. XRD patterns were recorded on a PANalytical X'Pert PRO X-ray diffractometer (Westborough, MA) using Cu radiation generated at 45 kV and 40 mA. Scanning was done with a Theta/Theta goniometer from 2-70° 2θ with a step size of 0.0668545° 2θ at a time of 600 s. The incident wavelength was λ=0.1541 nm.

Scanning Electron Microscopy (SEM). A LEO (Zeiss) 1550 Field Emission Scanning Electron Microscope was used for measuring the modified alanine samples. The dried samples were mounted on aluminum stubs and coated with Au.

Results and Discussion

SEM analysis. Different structures of modified alanine were observed using SEM as shown in Figure 2. The control sample, Alanine at pH 9.0, assembled into random structures while bars were observed for [EVS]/[NH] ~ 0.6 and fibers for [EVS]/[NH] ~ 1.2 followed by random structures at higher concentrations of EVS. This implied that there were upper and lower substitution limits within which the formation of ordered structures took place.

FT-IR characterization. We previously quantified the reaction of alanine with EVS using Raman spectroscopy (Chapter 3).[21] Raman and IR are complementary techniques so the present data analysis is more focused on the IR spectra. Alanine conjugation with EVS was evident from IR spectra as shown in Figure 3. Strong absorbances from EVS in modified alanine can be observed confirming the presence of both alanine and EVS in the final product. The addition reaction takes place on amines and so the reaction efficiency can be estimated by following the loss of amine absorbances in the IR spectrum.

The absorbances in the 1650 cm^{-1} – 1485 cm^{-1} region were from ν(C-N), δ(C-NH), $\delta_s(NH_3^+)$, $\delta_{as}(NH_3^+)$, and $\nu(COO^-)$ bands (Figure 3b).[22] We have shown changes in the amine absorbances as the amine is deprotonated and substituted (Chapter 7). In summary, NH_3^+ decreased in intensity and shifted to higher wavenumber with deprotonation and substitution, which is shown in Figure 3b. For this reason, the peaks have been deconvoluted to quantify the contributions from $NH_3^+/NH_2/NH$ and COO^- groups on alanine. The peak areas of the deconvoluted peaks at 1612 cm^{-1}, corresponding to ν(C-N) and δ(C-NH) on primary amines and $\delta_{as}(NH_3^+)$, 1577 cm^{-1} corresponding to $\delta_{as}(COO^-)$, and 1517 cm^{-1} corresponding to ν(C-N) and δ(C-NH) on secondary amines and $\delta_s(NH_3^+)$ are plotted in Figure 4.[22, 23] The NH intensity decreased with an increase in EVS concentration and saturated after [EVS]/[NH] ~ 2. The opposite was observed with the COO^- absorbance with intensity increasing until [EVS]/[NH] ~ 2 and then saturating. Based on the number of available NH groups, the saturation after [EVS]/[NH]=2 was expected and show that secondary amines participate in the reaction, which was possible in the absence of steric hindrance.[20] As another check on the role of primary and secondary amines in the reaction, the 2590 cm^{-1} and 2505 cm^{-1} amine absorbances have been considered (Figure 3c).[22] The intensities of these absorbances were compared by normalizing the peak at 850 cm^{-1} as there was no

contribution from EVS in this region. As can be seen in Figure 5, the same trend as with NH in Figure 3 was observed where the peak intensities decreased until [EVS]/[NH] ~ 2 and then saturated. However the intensity started decreasing at [EVS]/[NH] ~ 0.5. The delay intimates that primary amines react first and that secondary amines react later so the 2590 cm^{-1} and 2505 cm^{-1} absorbances arise from secondary amines. The observed saturation at [EVS]/[NH] ~ 2 originated in the unavailability of primary and secondary amines.

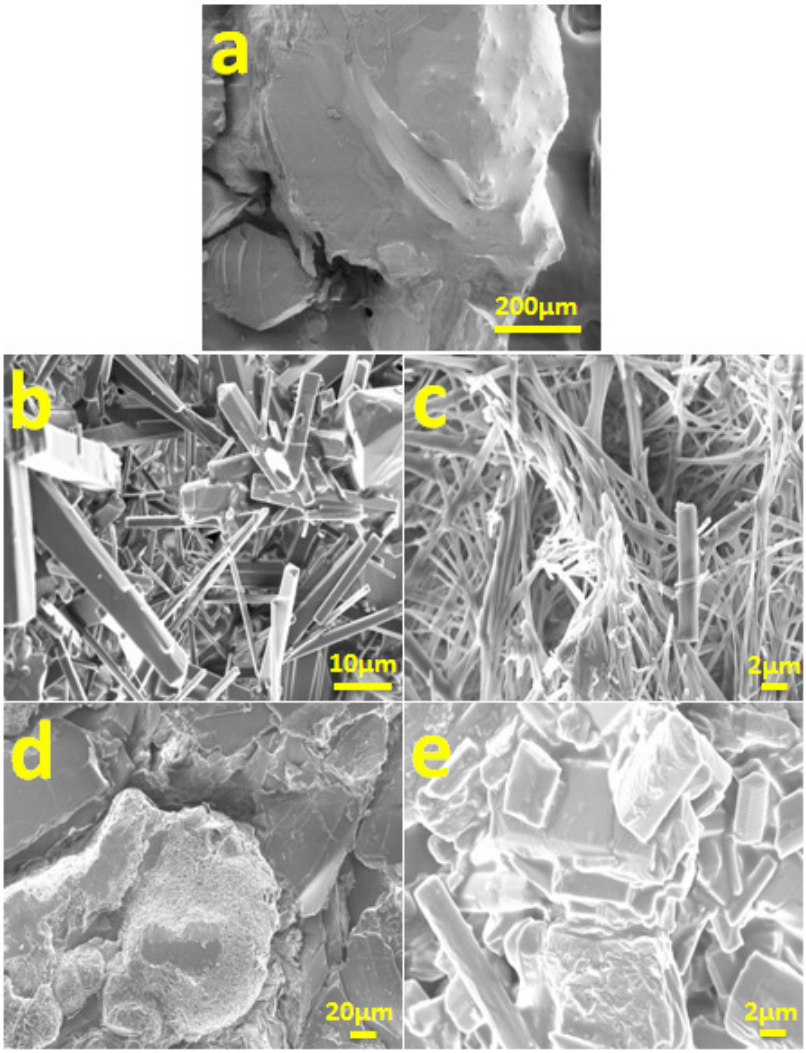

Figure 2. SEM images of (a) Alanine control pH 9.0 and [EVS]/[NH] = (b) 0.6, (C) 1.2, (d) 3, and (e) 6.

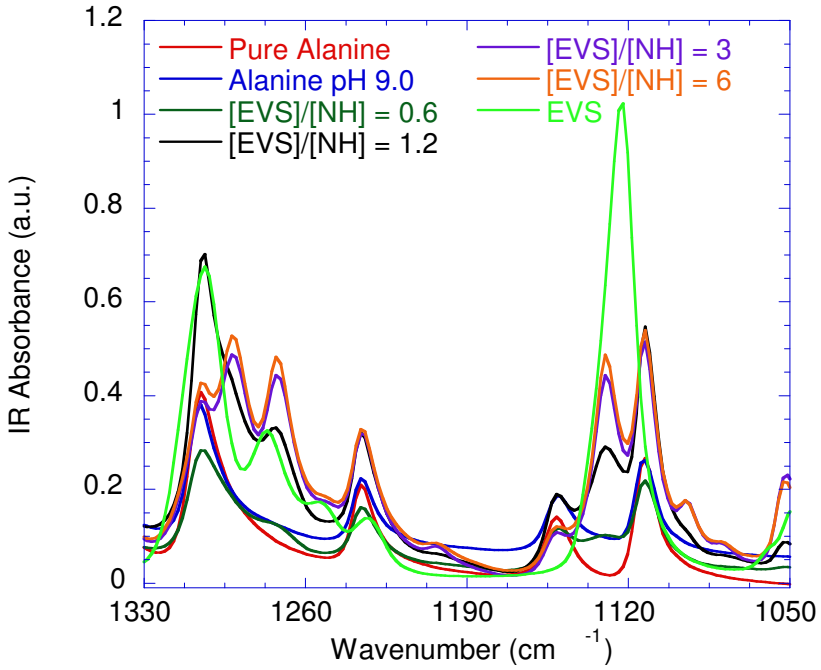

Figure 3a. IR spectra of dried control and modified alanine samples along with EVS in the region of 1330 cm^{-1} to 1050 cm^{-1}. EVS absorbances can be seen in the modified samples.

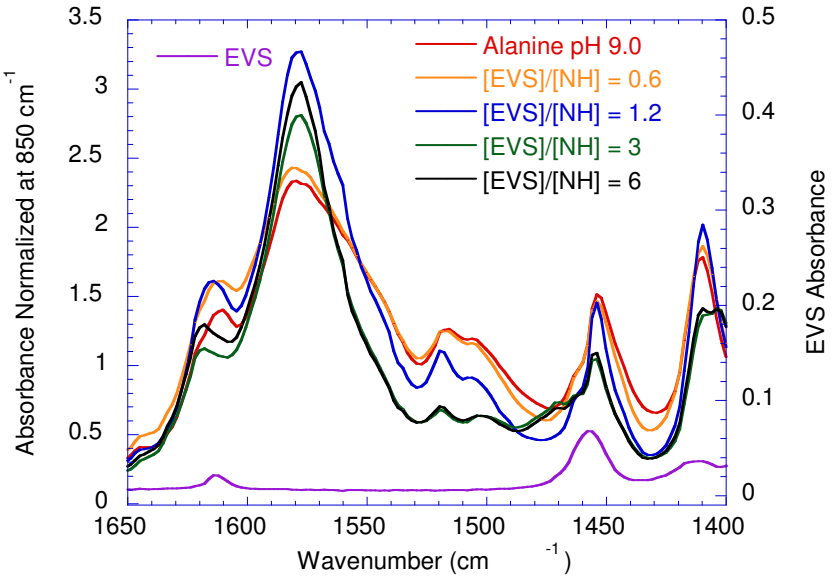

Figure 3b. IR spectra of dried control and modified alanine samples along with EVS in the region 1650 cm^{-1} to 1400 cm^{-1}. The 1650 cm^{-1} to 1400 cm^{-1} absorbances originate in various NH_2, NH modes and COO^- present on the amino acid and CH_3 present on alanine and EVS.

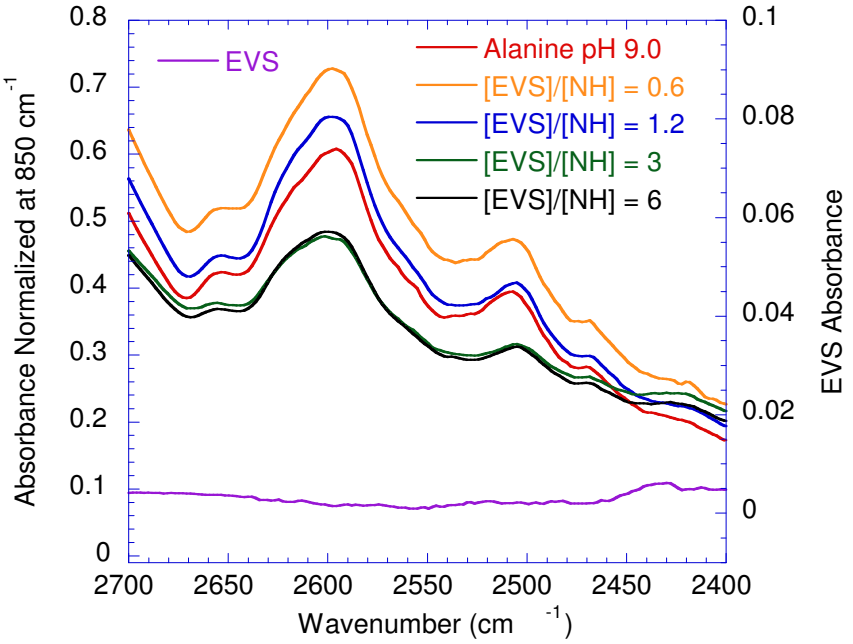

Figure 3c. IR spectra of dried control and modified alanine samples along with EVS in the region of 2700 cm^{-1} to 2400 cm^{-1}. The absorbances in this region are due to ν(NH).

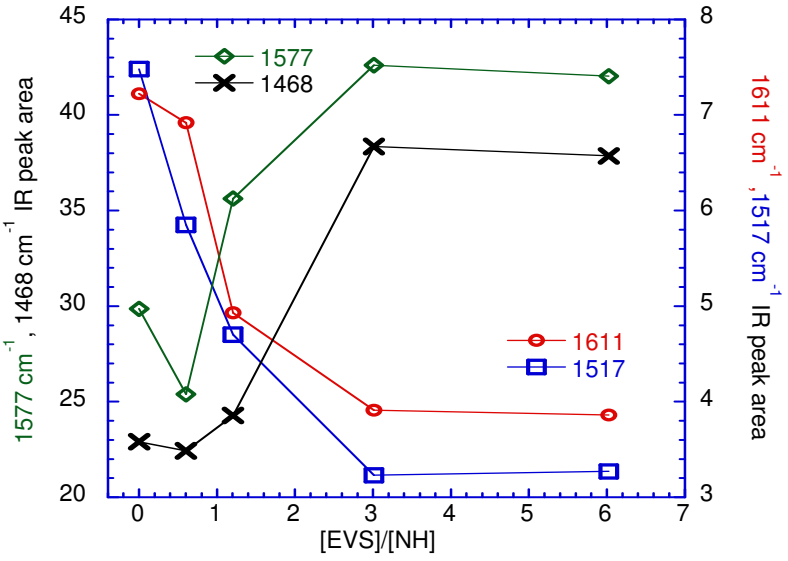

Figure 4. Peak areas from the deconvoluted IR spectrum plotted as a function of molar ratio of EVS to NH on alanine. The absorbances in the 1700 cm^{-1} – 1485 cm^{-1} region were from ν(C-N), δ(C-NH), $\delta_s(NH_3^+)$, $\delta_{as}(NH_3^+)$, and ν(COO^-) bands.

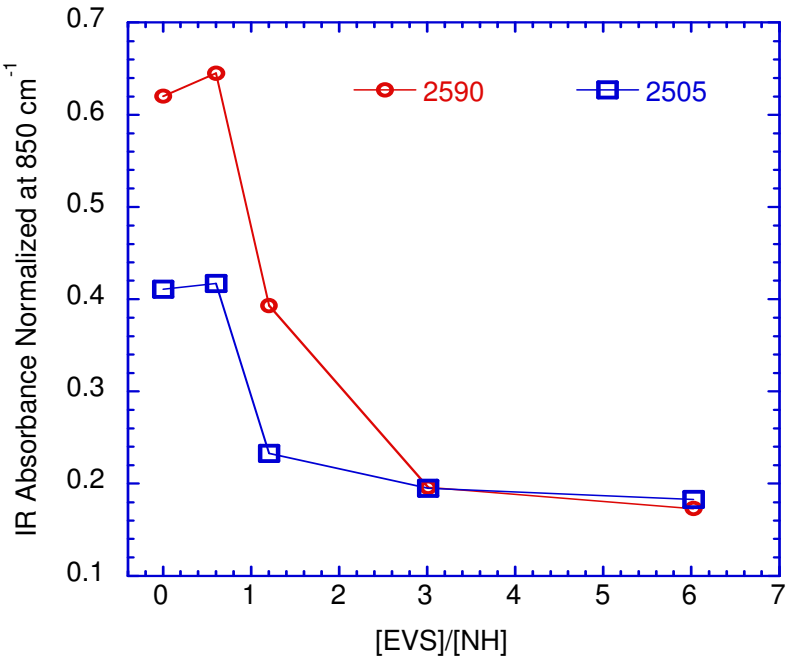

Figure 5. Intensities of the normalized ν(NH) absorbances at 2590 cm^{-1} and 2505 cm^{-1} plotted against the molar ratio of EVS to NH on alanine.

The region from 1475 cm^{-1} to 1420 cm^{-1} was deconvoluted to evaluate the contribution from $\delta_{as}(CH_3)$ groups (1470 cm^{-1}) present on both alanine and EVS.[23] The absorbance increased with an increase in EVS concentration and again saturated after [EVS]/[NH] ~ 2 (Figure 4). The signature peak from $\nu_{as}(S=O)$ in EVS appeared at 1122 cm^{-1} as shown in Figure 3a.[22] However, in the modified alanine samples the peak shifted to 1130 cm^{-1} while the absorbance at 1112 cm^{-1} increased (on a normalized scale) with an increase in EVS concentration and a new absorbance emerged at 1095 cm^{-1} for [EVS]/[NH] ~ 3. The $\nu_s(S=O)$ at 1277 cm^{-1} in the pure EVS shifted to 1272 cm^{-1} in the substituted samples and a new absorbance from sulfone appeared at 1291 cm^{-1} at [EVS]/[NH] > 2.[22] The shifts could mean that both sulfonyls were hydrogen bonding because we observed bonding of only one sulfonyl as peak splitting (Chapter 7). The 977 cm^{-1} absorbance from the vinyl group C-H bend on EVS was observed in modified alanine at

[EVS]/[NH] > 2.[22] This meant that there was unreacted EVS left over in the sample. This observation was more evident with Raman spectroscopy.[21]

Thermal stability of modified alanine. Thermal stability of alanine and modified alanine was analyzed by taking the first derivative of the TGA weight loss curve with temperature (dTGA) as shown in Figure 6. Peaks in the dTGA curve denote degradation temperature (peak position) and degradation rate (peak area). Alanine had a high thermal degradation temperature of about 275 °C because of an ordered structure caused by hydrogen bonding. Both the alanine control pH 9 sample and modified alanine samples showed lower degradation temperatures than pure alanine. Solubilizing alanine at pH 9 and recasting clearly disrupted some of the original hydrogen bonding and charged network. For the alanine control pH 9 a dTGA peak could be seen at 200 °C. There was a charge imbalance at pH 9 and so the newer, lower temperature peak could have originated in deprotonated amines not ionically or hydrogen bound to other groups. The substitution of EVS onto alanine created a more complex thermal degradation behavior than in pure alanine. A large peak associated with the alanine portion of the material decreased with an increase in EVS concentration. While the EVS might have caused the alanine degradation temperature to decrease, two new peaks emerged in the 300 °C – 375 °C region. This implied that substitution induced increased order resulting in a thermal stability increase related to the presence of EVS. In the [EVS]/[NH] ~ 6 sample, a small peak was observed at ~ 100 °C, which is the boiling of unreacted EVS in the sample.

EVS substituted alanine structure. The structure of L-alanine has been previously studied and is reported to be orthorhombic with the plane 120 on the c-axis being the longest axis.[24] In the substituted alanine samples two new peaks at 1.19 nm and 1.07 nm appeared which were from EVS as can be seen in Figure 7. The 120 plane (0.43 nm) could still be seen in these

samples. However, with an increase in EVS concentration, the peaks in the wide angle region (> 16°) decreased. As EVS attached to alanine the molecule became bulkier. This could induce a disorder in the other alanine crystalline planes due to the lack of bonding and hence a peak disappearance was observed.

Bars were observed at [EVS]/[NH] ~ 0.6 so originated from one EVS attaching to alanine but not all alanines substituted. Fibers were observed at [EVS]/[NH] ~ 1.2 and formed because some alanine molecules had both amines substituted and some did not. At higher EVS concentrations, completely substituted alanine resulted in random structures. Taking the spectroscopy and XRD data together, it appeared as if partially substituted alanine formed sheets that grew into various micron-sized structures. The appearance of new XRD peaks at 0.45 nm and 0.54 nm suggested these are inter-molecule distances potentially mediated by sulfonyl-amine hydrogen bonding given their similarity to typical carbonyl-amine hydrogen bonding between peptide molecules in β-sheets. The new peaks at 1.09 nm and 1.17 nm related to the inter-sheet distance and at very high substitution were the highest intensity. Aggregation was inhibited at this point resulting in random structures. However, at intermediate substitutions the sheets could aggregate enough to form bars and fibers. Either sulfonyl apparently participated in the aggregation as evidenced by the shifting rather than peak splitting. As will be shown in Chapter 7, this was not the case for EVS substituted lysine.

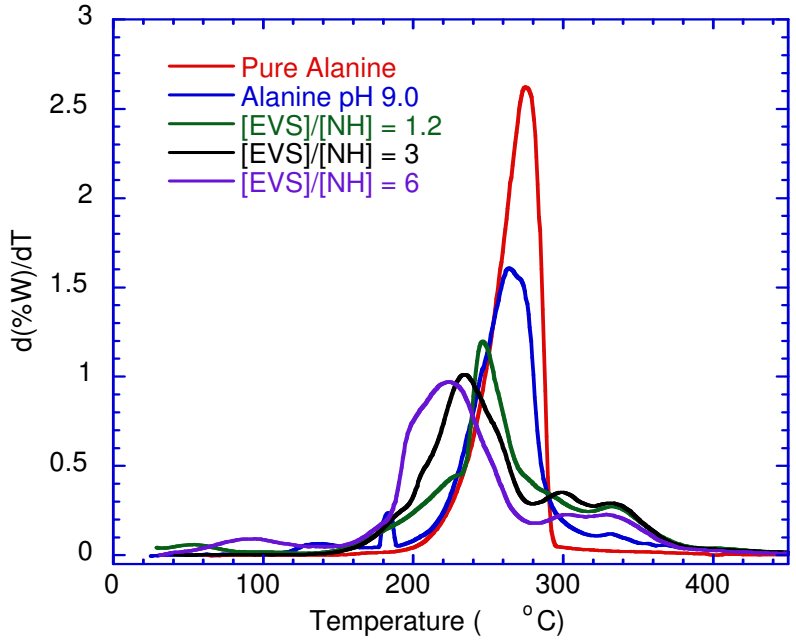

Figure 6. dTGA of alanine samples.

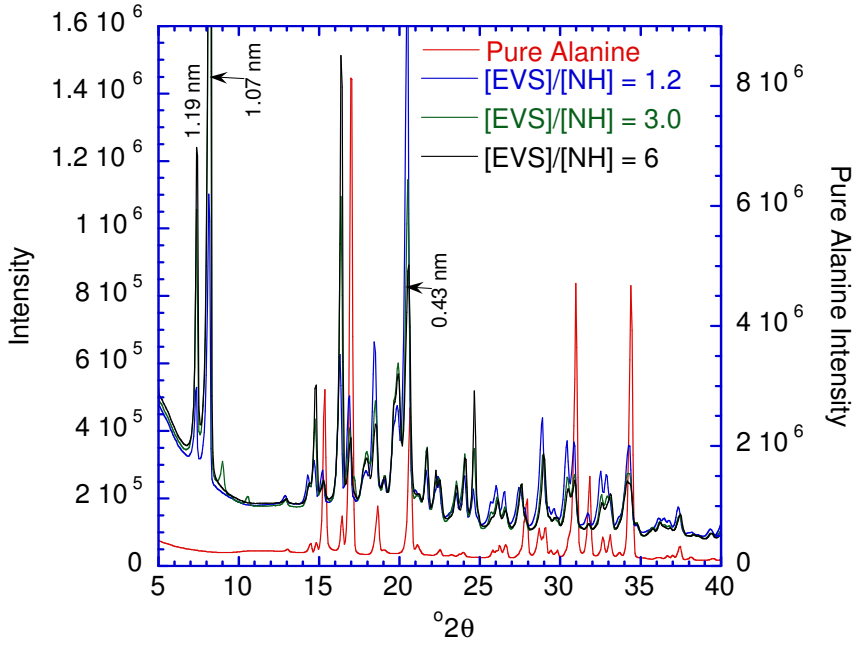

Figure 7. X-ray powder diffraction of pure alanine and modified alanine in the region 2θ = 5° to 40°.

Conclusions

A single component system to self-assemble large structures was prepared using simple nucleophilic addition reactions. The number of modified amino acids in the sample defined the final structure of the product as observed by SEM. The reaction efficiency in terms of degree of substitution could be discerned by following signature peaks in the FT-IR spectra and by deconvoluting the overlapping regions. FT-IR revealed substitution of both primary and secondary amines at higher concentration of EVS. dTGA analysis displayed increased thermal stability in EVS substituted alanine. XRD analysis revealed the transitions from pure crystal to bars to fibers and finally random structures in the modified alanine.

References

1. Philp, D.; Stoddart, J. F., Self-assembly in natural and unnatural systems. *Angewandte Chemie-International Edition* **1996,** 35, (11), 1155-1196.

2. Smith, D. K., Dendritic supermolecules - towards controllable nanomaterials. *Chem. Commun.* **2006**, (1), 34-44.

3. Hirst, A. R.; Smith, D. K., Two-Component Gel-Phase Materials - Highly Tunable Self-Assembling Systems. *Chemistry - A European Journal* **2005,** 11, (19), 5496-5508.

4. Hirst, A. R.; Smith, D. K.; Feiters, M. C.; Geurts, H. P. M.; Wright, A. C., Two-Component Dendritic Gels: Easily Tunable Materials. *J. Am. Chem. Soc.* **2003,** 125, (30), 9010-9011.

5. Sagawa, T.; Chowdhury, S.; Takafuji, M.; Ihara, H., Self-Assembled Nanofibrillar Aggregates with Amphiphilic and Lipophilic Molecules. *Macromolecular Symposia* **2006,** 237, (1), 28-38.

6. Nam, K. T.; Shelby, S. A.; Choi, P. H.; Marciel, A. B.; Chen, R.; Tan, L.; Chu, T. K.; Mesch, R. A.; Lee, B. C.; Connolly, M. D.; Kisielowski, C.; Zuckermann, R. N., Free-floating ultrathin two-dimensional crystals from sequence-specific peptoid polymers. *Nature Materials* **2010,** 9, (5), 454-460.

7. Granja, P. L.; Barbosa, M. A.; Pouységu, L.; De Jéso, B.; Rouais, F.; Baquey, C., Cellulose phosphates as biomaterials. Mineralization of chemically modified regenerated cellulose hydrogels. *Journal of Materials Science* **2001,** 36, (9), 2163-2172.

8. Jin Woo Lee, S. Y. K., Seong Soo Kim, Young Moo Lee, Kwang Hyun Lee, Seon Jeong Kim,, Synthesis and characteristics of interpenetrating polymer network hydrogel composed of chitosan and poly(acrylic acid). *J. Appl. Polym. Sci.* **1999,** 73, (1), 113-120.

9. Annabi, N.; Mithieux, S. M.; Boughton, E. A.; Ruys, A. J.; Weiss, A. S.; Dehghani, F., Synthesis of highly porous crosslinked elastin hydrogels and their interaction with fibroblasts in vitro. *Biomaterials* **2009,** 30, (27), 4550-4557.

10. Fang, J.-Y.; Chen, J.-P.; Leu, Y.-L.; Wang, H.-Y., Characterization and Evaluation of Silk Protein Hydrogels for Drug Delivery. *Chemical & Pharmaceutical Bulletin* **2006,** 54, (2), 156-162.

11. Bhattacharya, S.; Acharya, S. N. G.; Raju, A. R., Exceptional adhesive and gelling properties of fibrous nanoscopic tapes of self-assembled bipolar urethane amides of L-phenylalanine. *Chem. Commun.* **1996**, (17), 2101-2102.

12. Ji, Y.; Luo, Y.-F.; Jia, X.-R.; Chen, E.-Q.; Huang, Y.; Ye, C.; Wang, B.-B.; Zhou, Q.-F.; Wei, Y., A Dendron Based on Natural Amino Acids: Synthesis and Behavior as an Organogelator and Lyotropic Liquid Crystal13. *Angew. Chem. Int. Ed.* **2005,** 44, (37), 6025-6029.

13. Rajan Babu, D.; Jayaraman, D.; Mohan Kumar, R.; Jayavel, R., Growth and characterization of non-linear optical L-alanine tetrafluoroborate (L-AlFB) single crystals. *J. Cryst. Growth* **2002,** 245, (1-2), 121-125.

14. Ogawa, K.; Matsui, J.; Suzuki, E.; Doki, N.; Shimizu, K., Orientation and Surface Topography of L-Alanine Crystals in Fluidized-Bed Crystallizer in a Magnetic Field. *J. Chem. Eng. Jpn.* **2009,** 42, (12), 878-883.

15. Jang, D.; Lee, Ho Y.; Park, M.; Nam, Seong R.; Hong, J.-I., Nano- and Microstructure Fabrication by Using a Three-Component System. *Chemistry - A European Journal* **2010,** 16, (16), 4836-4842.

16. Lee, S. J.; Kim, E.; Seo, M. L.; Do, Y.; Lee, Y.-A.; Lee, S. S.; Jung, J. H.; Kogiso, M.; Shimizu, T., Self-assembled helical ribbon and tubes of alanine-based amphiphiles induced by two different formation mechanisms. *Tetrahedron* **2008,** 64, (7), 1301-1308.

17. Giri, K.; Bhattacharyya, N. P.; Basak, S., pH-Dependent Self-Assembly of Polyalanine Peptides. *Biophys. J.* **2007,** 92, (1), 293-302.

18. Lee, H. Y.; Nam, S. R.; Hong, J.-I., Microtubule Formation Using Two-Component Gel System. *J. Am. Chem. Soc.* **2007,** 129, (5), 1040-1041.

19. Sereikaite, J.; Bassus, D.; Bobnis, R.; Dienys, G.; Bumeliene, Z.; Bumelis, V. A., Divinyl sulfone as a crosslinking reagent for oligomeric proteins. *uss. J. Bioorg. Chem.* **2003,** 29, (3), 227-230.

20. Mather, B. D.; Viswanathan, K.; Miller, K. M.; Long, T. E., Michael addition reactions in macromolecular design for emerging technologies. *Prog. Polym. Sci.* **2006,** 31, 487-531.

21. Budhavaram, N. K.; Barone, J. R., Quantifying amino acid and protein substitution using Raman spectroscopy. *Journal of Raman Spectroscopy* **2010,** DOI: 10.1002/jrs.2738.

22. Parker, F. S., Applications of infrared, raman, and resonance spectroscopy in biochemistry. In Plenum press: Newyork, 1983; pp 21-25.

23. Gunzler, H.; Gremlich, H.-U., IR Spectroscopy: An Introduction. In WILEY-VCH: Weinheim, Germany, 2002; pp 179-218.

24. Lima, J. A.; Freire, P. T. C.; Melo, F. E. A.; Filho, J. M.; De Sousa, G. P.; Lima, R. J. C.; Façanha Filho, P. F.; Bordallo, H. N., Low-temperature Raman spectra of racemate DL-Alanine crystals. *Journal of Raman Spectroscopy* **2010,** 41, (7), 808-813.

Chapter VII

Self-assembly of peptide-like microtubules

Abstract

Self-assembly has emerged as a unique method to produce ordered structures over many length scales. The unique feature of self-assembly is the minimization of free energy through molecular interaction leading to structure formation. Many morphologies have been produced from self-assembly including spheres, ribbons, sheets, cylinders, and tubes. Of these, the tube is a fairly complicated structure. Here, we show the spontaneous formation of micron-sized tubes from a single component system. Ethyl vinyl sulfone substituted lysine formed sheets that then rolled up under the natural chirality of the amino acid to form the tube. The sheets were formed by secondary amine-sulfonyl hydrogen bonds as determined by Fourier transform-infrared and Raman spectroscopy. X-ray diffraction showed the inter-molecular distance to be similar to that between two protein molecules in a β-sheet.

Introduction

Self-assembly is an interesting processing concept because it relies on minimizing the free energy of interaction embodied in the molecules to create structures rather than the application of external energy. Thus self-assembly is not an energy intensive process and could be a very pragmatic and inexpensive method to make materials if the right system were found. Nature relies heavily on self-assembly to produce structures. Nature does this by very precisely forming molecules that will spontaneously interact in aqueous solution and presumably is its way to conserve energy. Millions of years of evolution have honed this process. Attempts by researchers to self-assemble structures can be more complicated compared to nature, using complex solutions with organic solvents and multiple components and not aqueous solutions at standard conditions. However, the structures observed, ribbons, tubes, and sheets along with other shapes, are formed by noncovalent interactions between the molecules of the various components, which is very similar to a natural motif.[1-10] Two component systems in particular have been used in the past because of the ease of having different charged ends, geometries, and amphiphilic properties that can interact to form a shape.

Bio-based molecules are of particular interest because of the connection to the natural motif and potential use in biomedical applications. Most assembly of bio-based molecules relies on the same principles as the synthetic systems: multicomponent systems or molecules with various chemical moieties to initiate assembly. Peptides and peptide-like materials[10] and amino acid-based dendrimers[11] have been used for the synthesis of amphiphilic molecules that can then self-assemble in solution based on preference of the molecules for themselves and the solvent. A variety of resulting structures can be obtained from short peptide amphiphiles including nanotubes and nanofibers.[12] Varying the type and concentration of metal ions allowed peptides

to assemble into rosettes and spores.[13] Self-assembly of peptides can result in structures such as fibers, tubes, spheres, and sheets.[14]

Using smaller bio-based molecules is a rather interesting motif because of a potentially easier synthesis and less complicated assembly. Derivatives of lysine[1], alanine[15], glycine,[16] aspartic acid,[16] and phenylalanine[17] have been reported in the synthesis of structures. The largest drawback to most of these approaches is the deviation from the aqueous standard conditions at which nature operates.[1] Hirst et al. reported fibrous and flat platelet structures from two component gel systems containing lysine based dendrites and diaminododecane.[8] Fibers from derivatives of glycine and aspartic acid were developed by Kuang et al.[16] while Battacharya et al.[17] used bipolar urethane amides of L-phenylalanine. Jang et al. synthesized fibers, wires, ribbon-like structures, tubules and plate-like structures using a three component system of terephthaloylbisalanine, dodecylamine and one of the metal complexes of zinc, cadmium, and copper.[15]

Tubes are a common structure in nature, for instance in the form of veins or viruses like tobacco mosaic virus.[18] Compared to spheres or fibers, tubes are thermodynamically more complex to assemble. In addition to the previously cited reports, tubes have been formed from glycylglycine amphiphiles by inducing helix unraveling with a decrease in pH.[19] It was shown that the assembly into tubes was driven by acid-acid interactions while acid-base interactions at high pH caused helix formation. Ghadiri et al. synthesized a cyclic unit with eight peptides that assembled into tubes by stacking into β-sheets.[20] Other studies include tubes from glutamic acid based lipophilic molecules[21] and from simple amphiphilic groups and aromatic cores.[22] All tube formation fell into two categories: 1) close packing of helices into tubes through hydrogen bonding and 2) stacking of ring-type structures held together by non-covalent interactions.

The goal of this project was to self-assemble microtubules from one component, small molecule systems. In this study we report tubular structures obtained using modified lysine. Lysine was chemically substituted with ethyl vinyl sulfone (EVS) using nucleophilic Michael-type addition reactions in aqueous solution. The vinyl group of EVS reacted with amines on lysine. At the correct pH, temperature, and EVS substitution, dried solutions yielded tubes and sheet-like structures. Fourier transform-infrared and Raman spectroscopy, x-ray diffraction, and scanning electron microscopy were used to investigate the structures.

Materials and Methods

Materials. L-lysine (Lys or K, mol. wt. 146.19 g/mol) was purchased from Sigma Aldrich and ethyl vinyl sulfone (EVS, mol. wt. 120.17 g/mol) was purchased from VWR.

Lysine substitution. 0.5 g of L-lysine was added to 50 ml of pure water and the pH was adjusted to 9. After the lysine completely dissolved, the desired amount of EVS was added to the solution and reacted for 24 hr at 30 ^{o}C. At the end of the reaction, the pH dropped to 6. Following reaction, the solution was dried in Teflon-coated aluminum boats for 2 days at ambient conditions. The molar ratio of lysine to EVS was based on the number of potential reactive sites (amine groups) on lysine. Lysine has 2 NH_2's and so the total number of reactive sites was counted as 4, since both primary and secondary amines can participate in the reaction.[23]

Fourier Transform-Infrared (FT-IR) spectroscopy. All samples were analyzed with a Thermo-Nicolet 6700 FT-IR spectrometer. Dried samples were collected on a SmartOrbit diamond ATR cell with a total of 64 scans and a resolution of 4 cm^{-1}. Solution samples were collected on a ZnSe trough also in ATR mode over 256 scans and a resolution of 4 cm^{-1}. Spectra were baseline corrected and analyzed using OMNIC v. 7.3 software.

Raman spectroscopy. A Bruker Senterra dispersive Raman spectrometer was used to characterize the modified lysine samples. Samples were analyzed as dried films without further sample preparation. Each spectrum was collected using a 20x objective at 785 nm excitation with a laser power of 100 mW, a spectral resolution of 9–15 cm^{-1}, and a sample integration time of 20 s with 10 co-additions. Raman spectra were collected over nine different regions on the sample surface, baseline corrected, and averaged. OPUS v. 6.5 software was used for data collection and analysis.

X-ray powder diffraction (XRD). XRD patterns were recorded on a PANalytical X'Pert PRO X-ray diffractometer (Westborough, MA) using Cu radiation generated at 45 kV and 40 mA. Scanning was done with a Theta/Theta goniometer from 2-70° 2θ with a step size of 0.0668545° 2θ at a time of 600 s. The incident wavelength was λ=0.1541 nm.

Scanning Electron Microscopy (SEM). A Zeiss LEO 1550 Field Emission Scanning Electron Microscope was used for measuring the modified lysine samples. Dried lysine samples were mounted on stubs, Au coated, and imaged at 5kV and 5 mm working distance.

Results

Microtubes. At Lys:EVS molar ratios of ~1:0.5 to 1:1 sheet, rosette, and microtubular structures were observed as shown in Figure 1. The relative amount of each structure depended on the level of EVS substitution. Pure lysine prepared in the same manner without EVS (Control) showed no discernible structure formation (Figure 1a). Pores began to appear at low EVS substitution (Figure 1b). Around Lys:EVS 1:0.5 discernible tubes appeared as shown in Figure 1c. Closer examination revealed that the tubes were rolled sheets with the sheet thickness

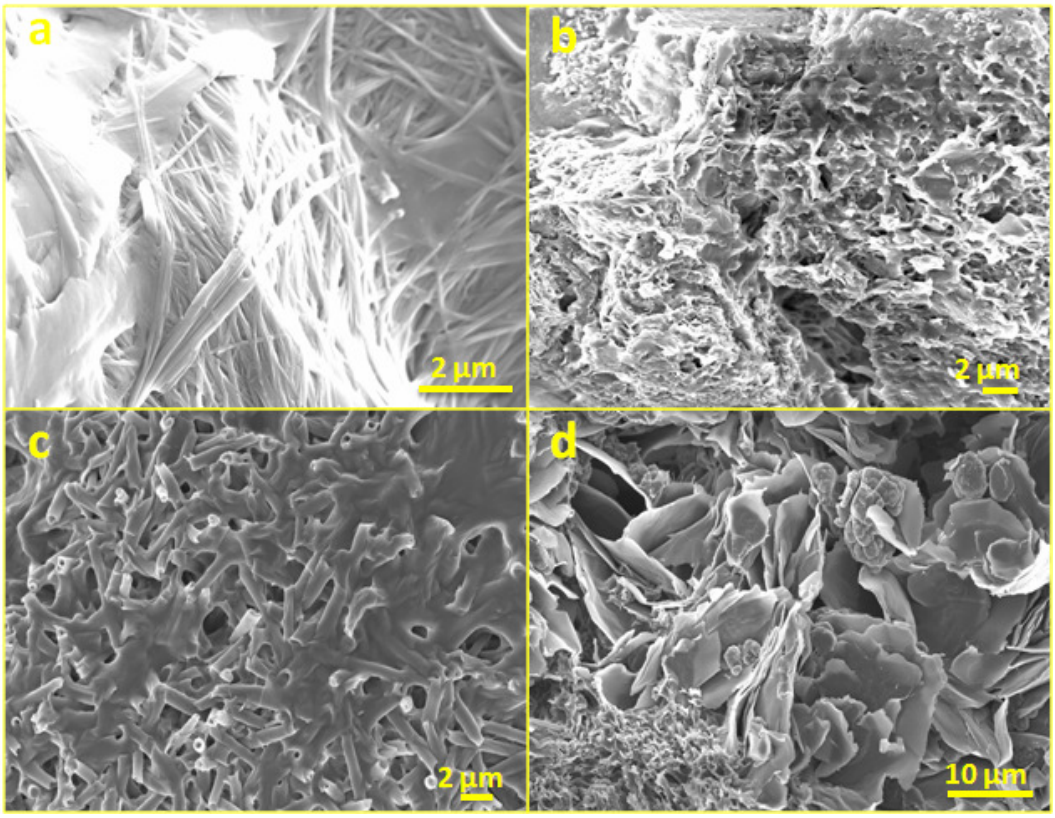

Figure 1. SEM images of (a) control, Lys:EVS (b) 1:0.2, (c) 1:0.5 and (d) 1:1.

defining the inner and outer diameters of the tube. The sheets were 0.16±0.11 and 0.34±0.16 µm thick at Lys:EVS 1:0.5 and 1:1, respectively. As the molar ratio of Lys:EVS in the tube forming regime increased, less tubes and more rosettes and sheets were observed (Figure 1d).

X-Ray diffraction and vibrational spectroscopy of microtubes. X-ray powder diffraction showed that EVS substituted lysine had a very different crystal structure from lysine treated under the same conditions. While some of the lysine crystal structure was conserved (Figure 2a), new length scales at 1.240, 0.750, 0.622, 0.600, 0.467, and 0.312 nm appeared in EVS substituted lysine (Figure 2b). The length at 0.533 nm was retained but the peak ratio at 0.504

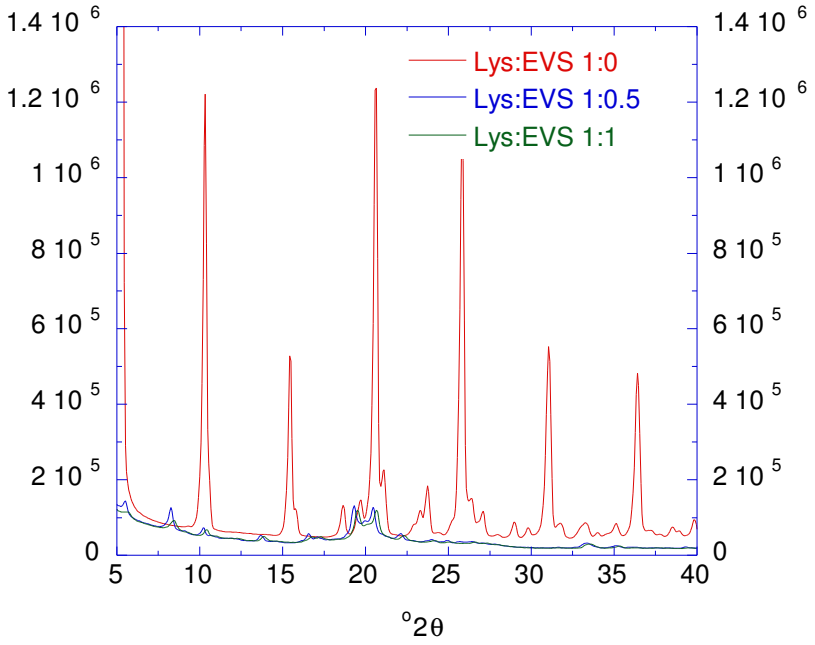

Figure 2a. X-ray powder diffraction of modified Lysine samples. The intensities of Lys:EVS 1:0.5 and 1:1 are plotted on the primary Y-axis and the control on secondary axis.

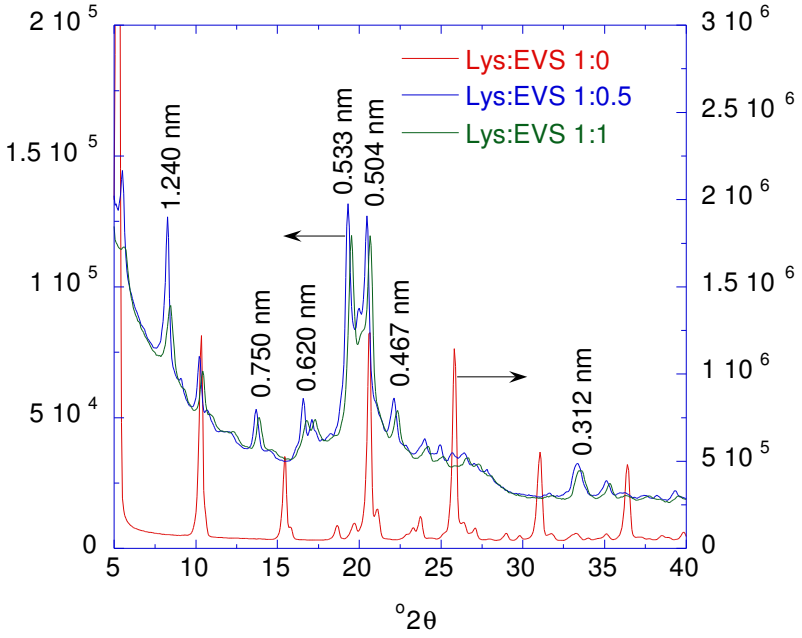

Figure 2b. X-ray powder diffraction of modified Lysine samples. The intensities of Lys:EVS 1:0.5 and 1:1 are plotted on the primary Y-axis and the control on secondary axis.

nm/0.533 nm was >1 in lysine and ~1 in EVS substituted lysine. Tube formation showed distinct features in the Raman spectrum. The following observations were made of the strongest tube former, Lys:EVS 1:0.5: 1) CH_2 scissoring on lysine shifted from 1440 cm^{-1} to 1420 cm^{-1} and the CH_2 scissor on EVS at 1405 cm^{-1} was of low intensity (Figure 3a), 2) $\delta(\alpha\text{-NH})$ at 1097 cm^{-1} reached a maximum intensity (Figure 3b),[24] 3) ν(C-C) split at 900 cm^{-1} (Figure 3c), 4) ν(C-S) at 780 cm^{-1} appeared and the ratio of ν(C-S) at 700 cm^{-1}/665 cm^{-1} was closer to 1 (Figure 3d), and 4) C-S Raman shifts around 500 cm^{-1} formed one Raman shift at 500 cm^{-1} and the tube former was shifted to higher Raman shift (Figure 3e).

The first sign of a reacting system was a drop in the reaction pH from 9 to approximately 6 with a noticeable change in solvent color within four hours of adding EVS. After the addition of EVS, the solution was scanned at intervals using FT-IR in an attempt to determine the time of reaction and beginning of aggregation of the final crystal structure. For the nucleophilic addition of an electrophilic vinyl group to a nucleophilic amine, the amine must first be deprotonated, which occurred at pH 9. Reaction proceeded by opening up the carbon-carbon double bond on EVS and adding to a lysine primary amine. The amine on the α-carbon ($\alpha\text{-}NH_2$) had pK_a=8.9 and the amine on the side group ($\varepsilon\text{-}NH_2$) had pK_R=10.3. Therefore, reaction at the α-NH was favored at pH 9 and the Raman spectroscopy results showed this.[24] Solutions of pure L-lysine at pH 7-10 were prepared and dried in a procedure similar to that described above and the results are shown in Figure 4. A closer look at $\delta_s(NH_3^+)$~1504 cm^{-1} revealed it to be split. The overall peak reduced in absorbance with increasing pH suggesting amine deprotonation. Larger peak changes including splitting were observed at pH 9-10. The absorbance at ~1504 cm^{-1} reduced, the shoulder at 1495 cm^{-1} became a sharper peak, and the peak at ~1511 cm^{-1} shifted to higher

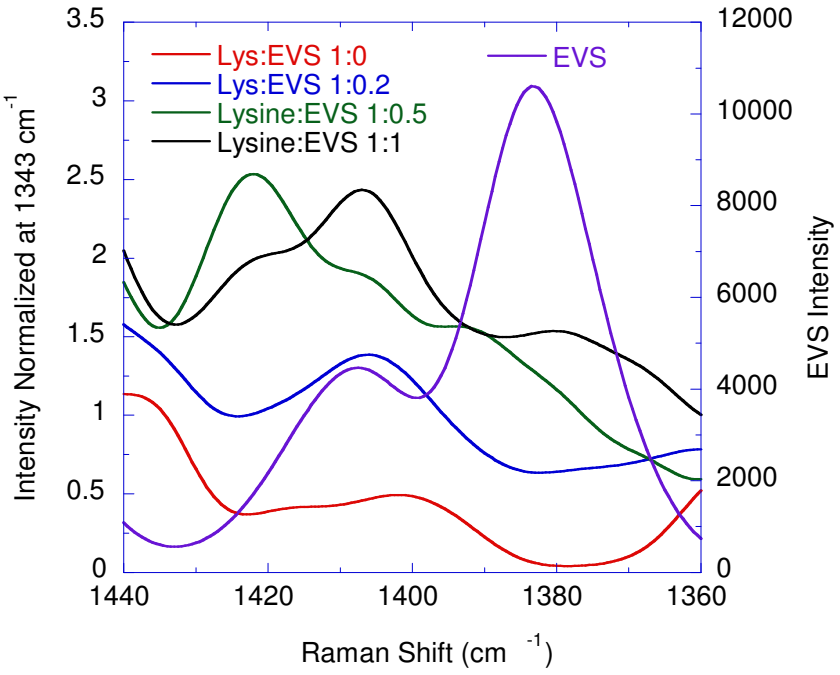

Figure 3a. Raman spectra of modified Lysine samples (dried) and pure EVS (solution) in the region 1440 cm^{-1} – 1360 cm^{-1}.

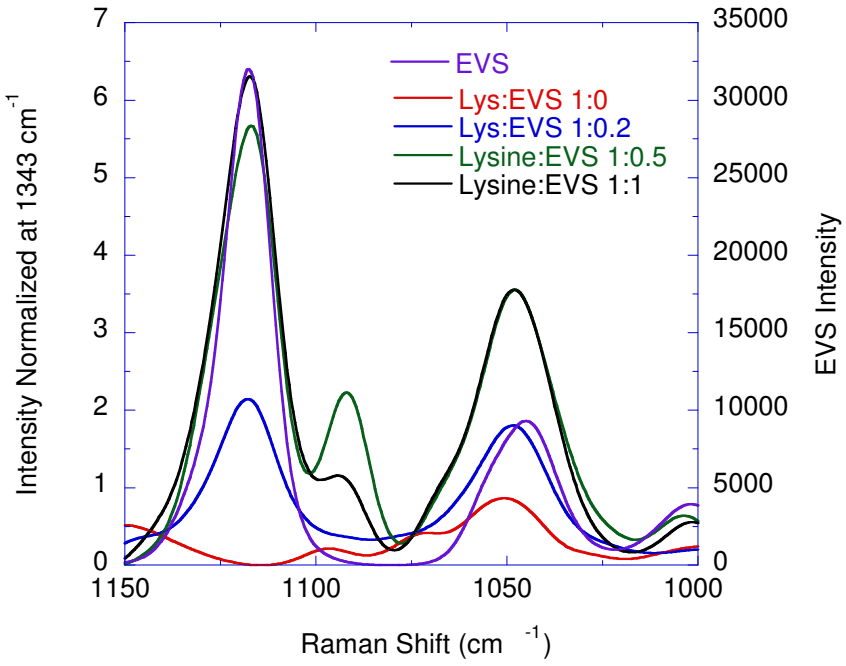

Figure 3b. Raman spectra of modified Lysine samples (dried) and pure EVS (solution) in the region 1150 cm^{-1} – 1000 cm^{-1}.

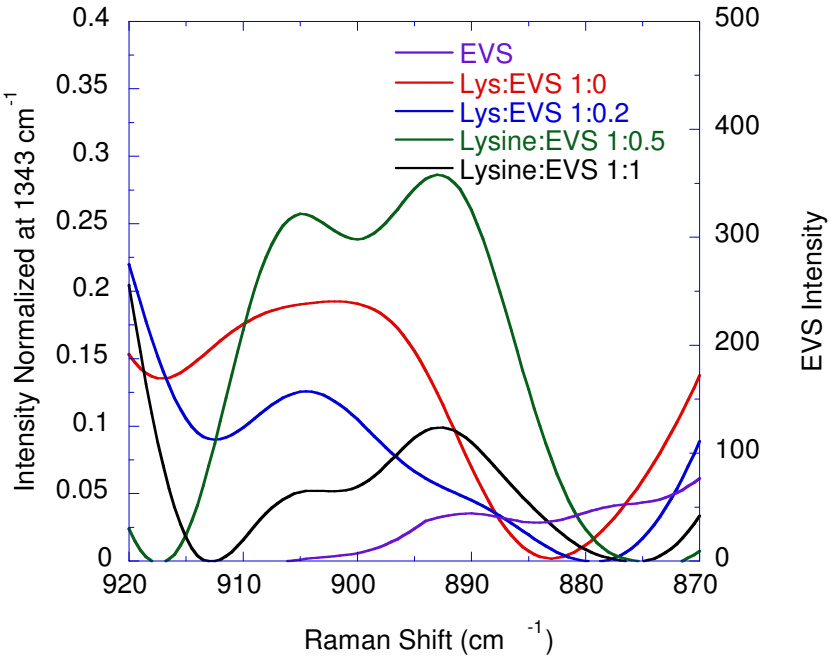

Figure 3c. Raman spectra of modified Lysine samples (dried) and pure EVS (solution) in the region 920 cm^{-1} – 870 cm^{-1}.

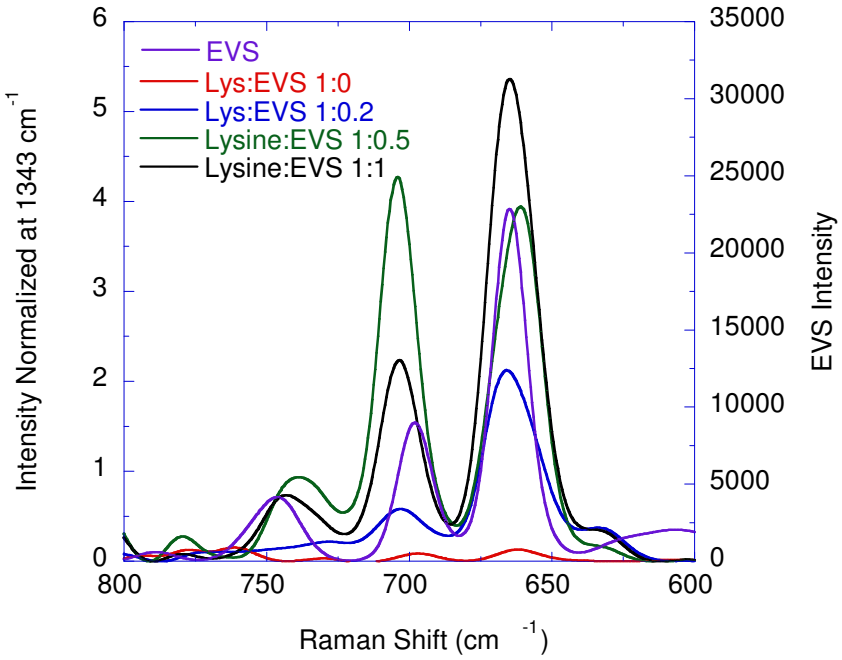

Figure 3d. Raman spectra of modified Lysine samples (dried) and pure EVS (solution) in the region 800 cm^{-1} – 600 cm^{-1}.

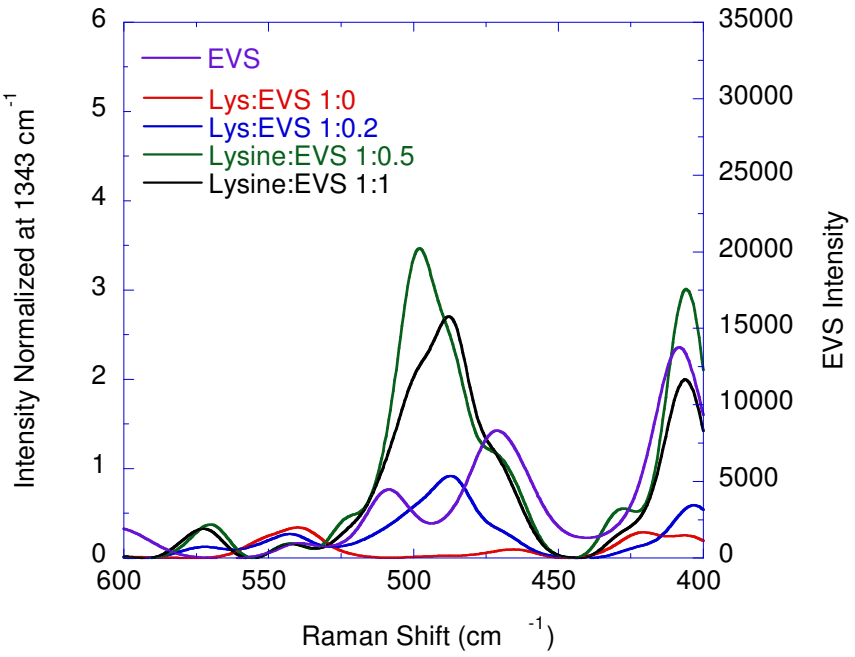

Figure 3e. Raman spectra of modified Lysine samples (dried) and pure EVS (solution) in the region 600 cm^{-1} – 400 cm^{-1}.

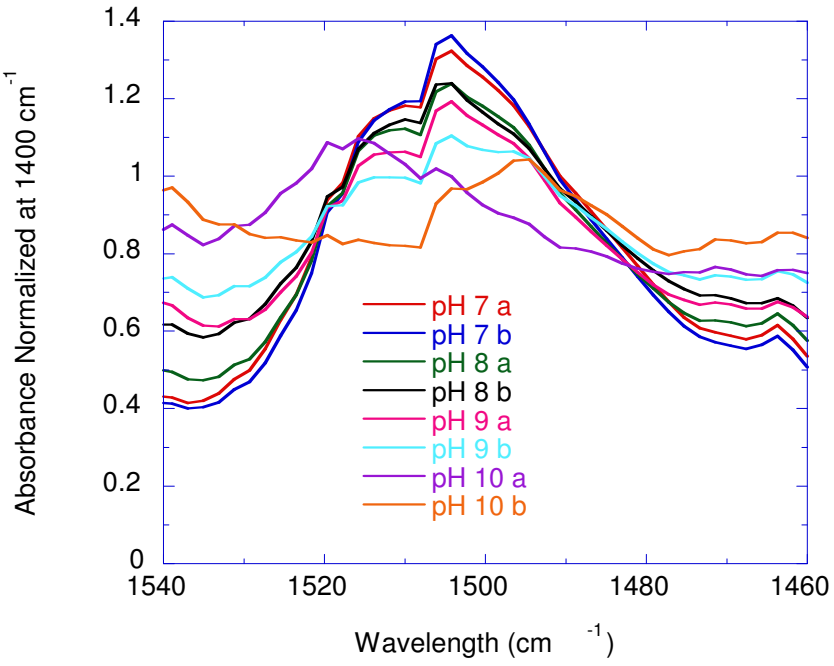

Figure 4. FTIR spectra of pure Lysine solubilized and dried at different pHs.

wavenumber until finally manifesting as a new peak at ~1516 cm^{-1}. So the absorbance showed the relative amount of NH_3^+ to NH_2, with the peak shifting to higher wavenumber as lysine was deprotonated. At constant pH, the spectra showed a loss of the right hand side of the $\delta_s(NH_3^+)$ absorbance with increasing EVS substitution (Figure 5a). In chapter 6, the IR spectra were normalized at 850 cm^{-1} since no peak shift was observed. However, in the case of lysine the peaks shifted with an increase in EVS concentration. Hence, all spectra were normalized at $\nu_s(COO^-)$ ~1400 cm^{-1}, which showed no shifting with reaction conditions, suggesting the carboxylate was not affected by EVS substitution or subsequent aggregation. A new shoulder appeared at 1540 cm^{-1} at increased substitution, also observed as a new peak in solution, which was potentially the appearance of the secondary amine on the α-carbon. Microtubes required the sulfonyls be in a defined state as well as the amines. There was well-defined splitting of the $\nu_s(S=O)$ at 1306 cm^{-1}. Part of the peak at 1280 cm^{-1} originated in S=O of EVS and part was the C-N reaction product of lysine and EVS, which was why this peak increased in intensity over $\nu_s(S=O)$ at 1306 cm^{-1} as EVS substitution increased (Figure 5b).

Discussion

The experimental results suggested that microtubes formed under very well defined conditions. Further experiments revealed that several events were critical. The drop in pH during the reaction prevented all of the added EVS from reacting and was the initiator of tube formation. Reactions as a function of varying EVS amount were conducted at constant pH 9. Tubes did not form in any case. However, when the reaction pH was decreased to 6 after 24 hours of reaction, tubes formed at Lys:EVS~1:0.25 to 1:0.36. FT-IR spectra of the resulting materials were similar to the microtube forming Lys:EVS 1:0.5. This showed that about 1/3 to 1/2 of the EVS was reacting when pH was not controlled over the several hour reaction time.

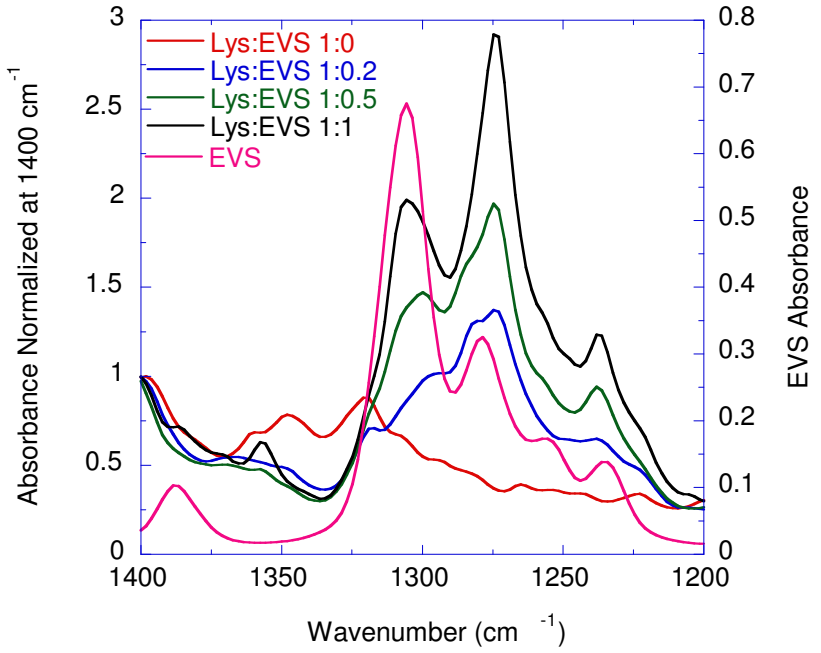

Figure 5a. FTIR spectra of Lys: EVS (dried) and pure EVS (solution) in the region 1400 cm^{-1} – 1200 cm^{-1}.

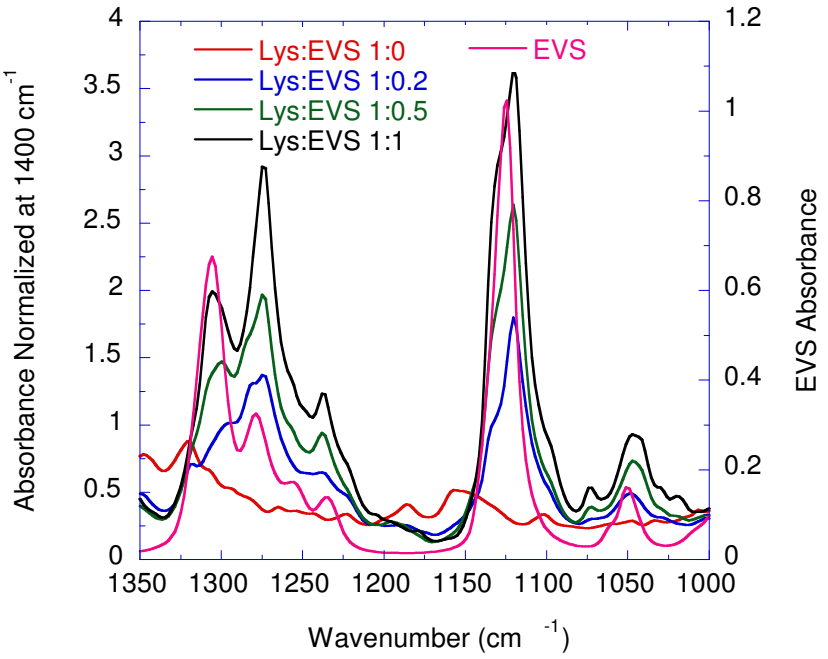

Figure 5b. FTIR spectra of Lys: EVS (dried) and pure EVS (solution) in the region 1350 cm^{-1} – 1100 cm^{-1}.

Observations of the amine and sulfonyl behavior indicated that an optimum amount of interaction had to occur between the two for microtubes to form. Taking the Raman and FT-IR spectroscopy results together, microtube formation appeared when about half of the NH groups on the lysine α-NH were substituted with EVS and one of the sulfonyls hydrogen bonded with a remaining secondary amine on α-NH.

Figure 6a shows that tubes will not form without available NH. When reaction pH was kept constant at 9 and Lys:EVS 1:0.5, the reaction ran to completion substituting all available NH_2 on the lysine α-carbon as evidenced by the loss of absorbance around 1510 cm^{-1}. Manually dropping the pH to 6 did not form microtubes. However, some available NH will allow microtubes to form as shown by the shift but still finite absorbance in this region for Lys:EVS 1:0.25 and Lys:EVS 1:0.36. Note that Lys:EVS 1:0.5 is shown as a positive tube forming "control" but it was obtained by allowing the solution pH to drop from 9 to 6 naturally not by fully reacting at pH 9 then manually decreasing pH. Using Figure 6a as a guide, the actual substitution before the pH dropped too far to stop the experiment was slightly more than Lys:EVS 1:0.25 but much less than Lys:EVS 1:0.36, which was where the figure of about ½ of the α-NH group substituted originated.

Figure 6b shows the splitting/peak distortion of the ν_{as}(S=O) absorbance at 1125 cm^{-1}. The change in the peak shape indicated that one sulfonyl had restricted motion relative to the other one and that the sulfonyl could stretch in one direction but not the other. This would be consistent with it hydrogen bonding differently. The sulfonyl could accept hydrogen bonds. The lack of change in the carboxyl suggested the amines as the hydrogen bond donor.

It was possible to discern the δ(α-NH) at 1097 cm^{-1} from the δ(ε-NH) at 1050 cm^{-1} on lysine in the Raman spectrum (Figure 3b).[24] Compared to alanine (Figure 7) the $\delta_s(NH_3^+)$ in lysine was

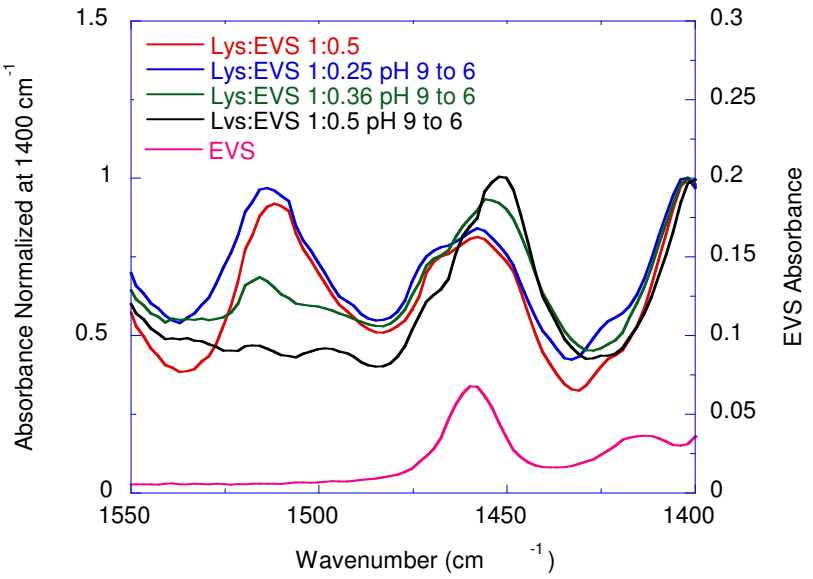

Figure 6a. FTIR spectra of Lys: EVS (dried) and pure EVS (solution) in the region 1550 cm^{-1} – 1400 cm^{-1}. For pH 9 to 6, samples were run for 24 hrs at pH 9.0 and then the pH was manually adjusted to 6. For other experiments the pH was not controlled and was let to drop as the reaction proceeded.

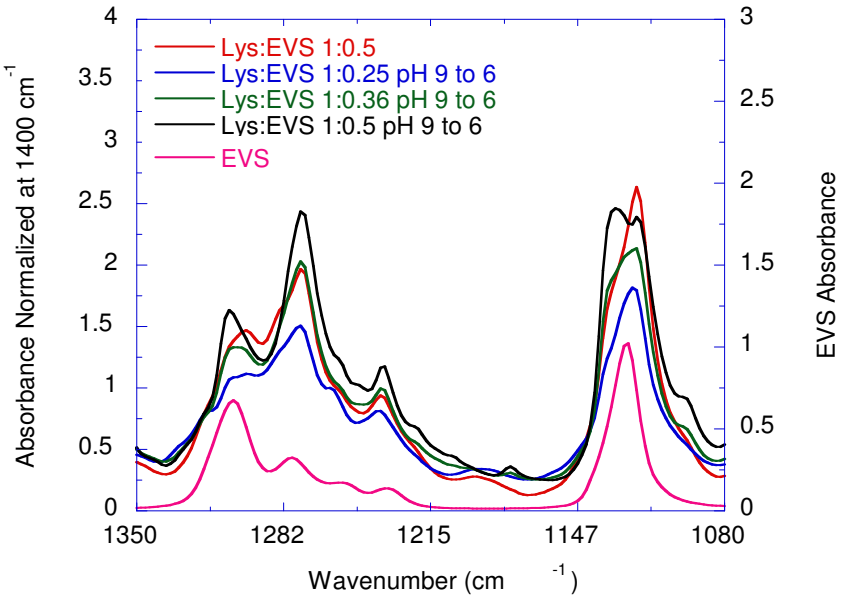

Figure 6b. FTIR spectra of Lys: EVS (dried) and pure EVS (solution) in the region 1350 cm^{-1} – 1080 cm^{-1}. For pH 9 to 6, samples were run for 24 hrs at pH 9.0 and then the pH was manually adjusted to 6. For other experiments the pH was not controlled and was let to drop as the reaction proceeded.

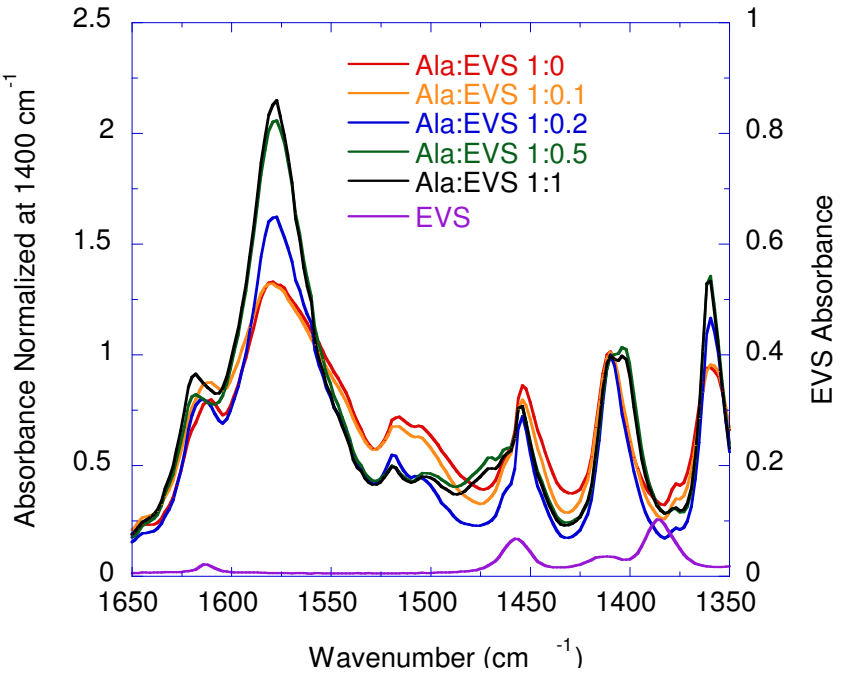

Figure 7. FTIR spectra of Alanine modified with various concentrations of EVS (dried) and pure EVS (solution) samples in the region 1650 cm^{-1} – 1350 cm^{-1}.

different, showing splitting and increased absorbance. The substitution of EVS obscured some of the changes in these regions but we can make a hypothesis about which amines participated in the hydrogen bonding with the sulfonyl. Although δ(ε-NH) coincided with an EVS Raman shift and increased with substitution, it showed no change in shape or shift. However, δ(α-NH) increased then decreased with substitution, with the decrease coinciding with microtube formation, suggesting that available NH at the α-carbon was now in a different state. The CH groups on the lysine side chain appear distinctively as δ(CH) at 1350 cm^{-1}.[25] Figures 8a and 8b show the loss of δ(CH) in the microtube forming materials. The lysine side groups were packing in the microtube formers but not in the non-microtube forming materials.

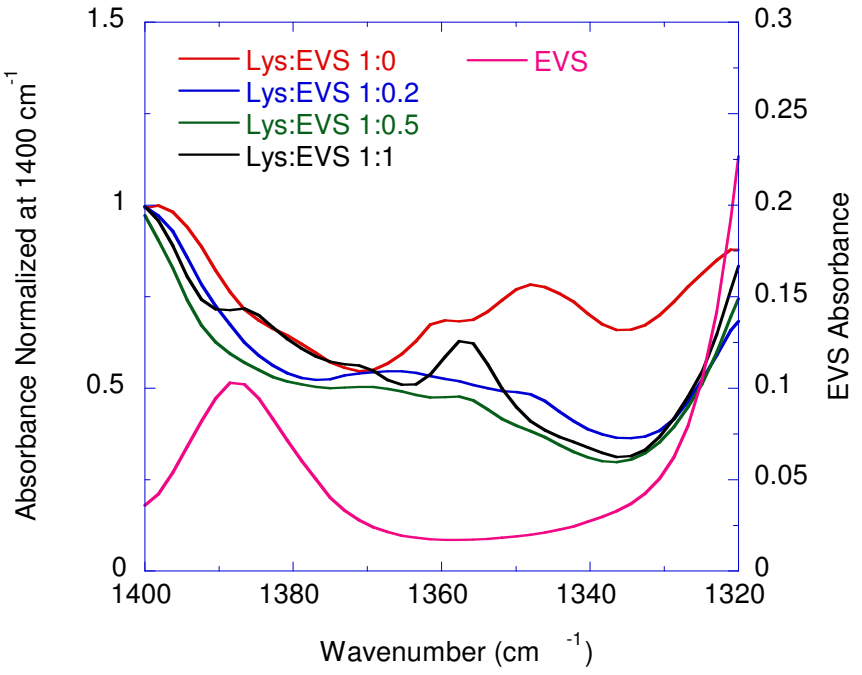

Figure 8a. FTIR spectra of Lys: EVS (dried) and pure EVS (solution) in the region 1400 cm^{-1} – 1320 cm^{-1}.

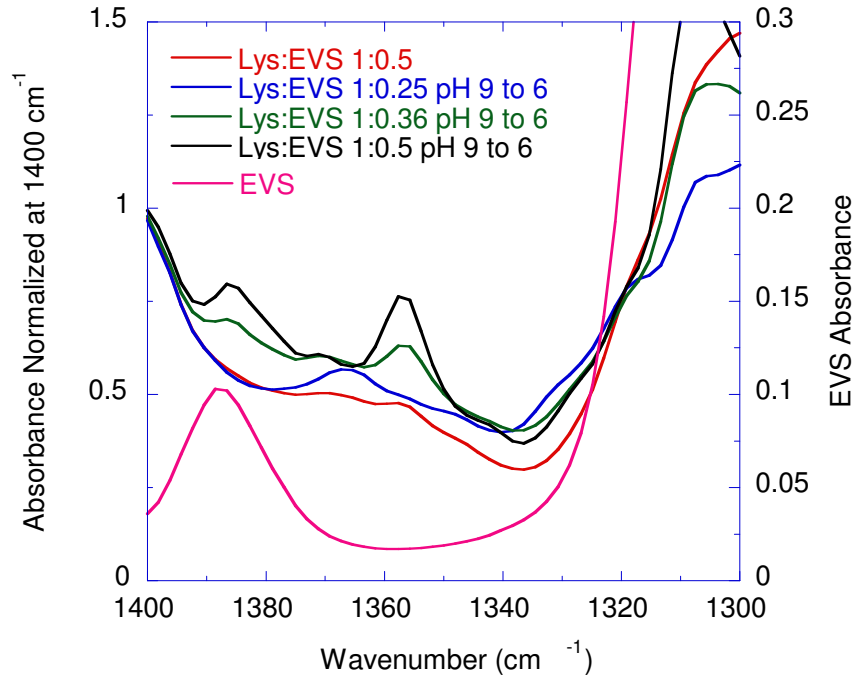

Figure 8b. FTIR spectra of Lys: EVS (dried) and pure EVS (solution) in the region 1400 cm^{-1} – 1300 cm^{-1}. For pH 9 to 6, samples were run for 24 hrs at pH 9.0 and then the pH was manually adjusted to 6. For other experiments the pH was not controlled and was let to drop as the reaction proceeded.

The microtubes shown in Figure 1 were rolled sheets. Scanning electron micrographs show that the sheets emerged from a larger patch of material then rolled left. Therefore, it appeared as if the natural chirality of the lysine played a role in microtube formation. Recent observations in our research group have shown that D-lysine tubes roll right when the point of emergence is taken at the point of reference. The EVS substituted L-lysine molecule was built in MarvinSketch (ChemAxon, v 5.3, 2010) and is shown in Figure 9a. Looking down the EVS axis, the left-handed chirality of the molecule is observed. In an alignment simulation, the sulfonyl on one molecule aligns with the α-NH on another pointing to the sulfonyl and α-NH as the hydrogen bonding moieties (Figure 9b). In the alignment simulation, the lysine was turned counter clockwise as shown in Figure 9c again looking down the EVS axis. A possible mechanism of aggregation and tube formation may be flat sheets formed through the aggregation of sulfonyls on one molecule to α-amines on another. If there is not enough EVS, the sheet will not form. At just the right amount of EVS, a sheet forms of sufficient thickness that can curl into a tube like rolling up a piece of paper. The tubes were formed by rolling the sheet to the left as shown in Figure 1, following the natural chirality of the molecule. If there is too much EVS, sheets form but cannot curl instead remaining flat or slightly curling into rosettes. The XRD data displayed the appearance of a 0.467 nm dimension, which is very close to the hydrogen-bonding distance between a main chain carbonyl and main chain secondary amine in a protein β-sheet. The FT-IR analysis does not suggest a carbonyl-amine bond but the sheets could be forming through a sulfonyl-amine hydrogen bond on the α-NH mimicking an actual protein β-sheet.

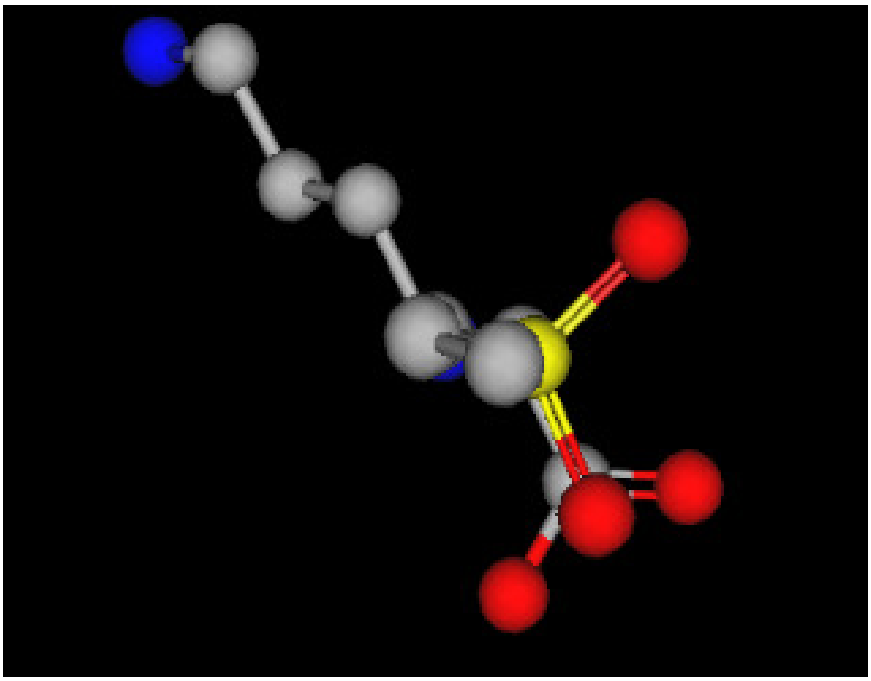

Figure 9a. MarvinSketch drawing of final EVS substituted lysine.

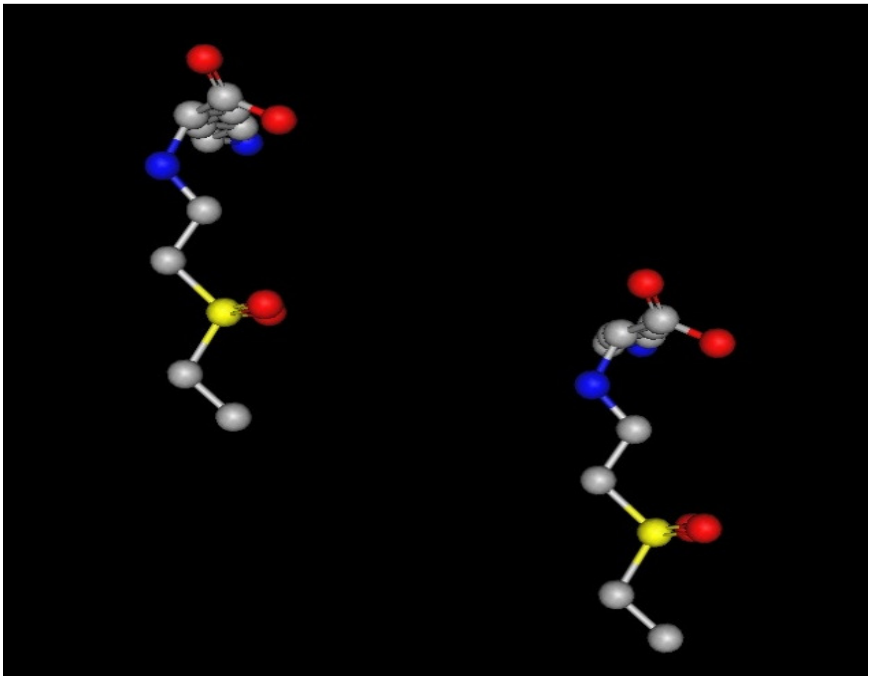

Figure 9b. MarvinSketch drawing of aggregated Lys-EVS molecules showing S=O—H-N alignment.

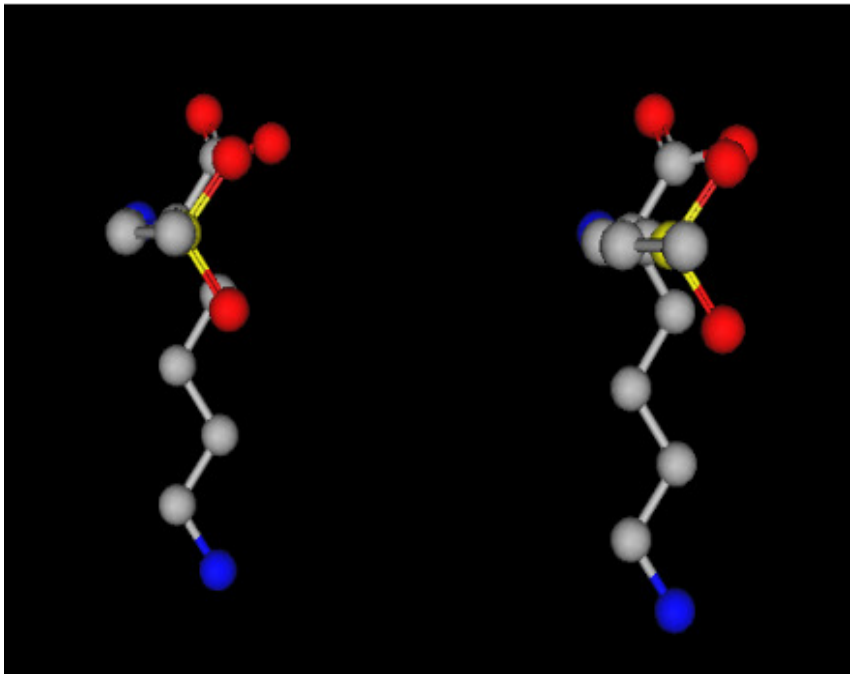

Figure 9c. Alignment simulation of EVS substituted lysine molecule.

Conclusions

Substitution of EVS on Lysine at various concentrations resulted in the formation of different self-assembled structures. Microtubes were observed for moderate EVS substitutions while sheets and rosettes formed at higher concentrations. The microtubes were observed only when about ½ of the α-NH groups on lysine reacted with EVS as observed from reaction experiments where pH was varied. The FT-IR, Raman and XRD results suggested the formation of a β-sheet analog between sulfonyls and α-NH.

References

1. Smith, D. K., Dendritic supermolecules - towards controllable nanomaterials. *Chem. Commun.* **2006**, (1), 34-44.

2. Basit, H.; Pal, A.; Sen, S.; Bhattacharya, S., Two-Component Hydrogels Comprising Fatty Acids and Amines: Structure, Properties, and Application as a Template for the Synthesis of Metal Nanoparticles. *Chemistry - A European Journal* **2008,** 14, (21), 6534-6545.

3. Brizard, A.; Berthier, D.; Aimé, C.; Buffeteau, T.; Cavagnat, D.; Ducasse, L.; Huc, I.; Oda, R., Molecular and supramolecular chirality in gemini-tartrate amphiphiles studied by electronic and vibrational circular dichroisms. *Chirality* **2009,** 21, (1E), E153-E162.

4. Brizard, A.; Dolain, C.; Huc, I.; Oda, R., Asp-Gly Based Peptides Confined at the Surface of Cationic Gemini Surfactant Aggregates. *Langmuir* **2006,** 22, (8), 3591-3600.

5. Dykes, G. M.; Smith, D. K., Supramolecular dendrimer chemistry: using dendritic crown ethers to reversibly generate functional assemblies. *Tetrahedron* **2003,** 59, 3999-4009.

6. Hirst, Andrew R.; Miravet, Juan F.; Escuder, B.; Noirez, L.; Castelletto, V.; Hamley, Ian W.; Smith, David K., Self-Assembly of Two-Component Gels: Stoichiometric Control and Component Selection. *Chemistry - A European Journal* **2009,** 15, (2), 372-379.

7. Hirst, A. R.; Smith, D. K., Two-Component Gel-Phase Materials - Highly Tunable Self-Assembling Systems. *Chemistry - A European Journal* **2005,** 11, (19), 5496-5508.

8. Hirst, A. R.; Smith, D. K.; Feiters, M. C.; Geurts, H. P. M.; Wright, A. C., Two-Component Dendritic Gels: Easily Tunable Materials. *J. Am. Chem. Soc.* **2003,** 125, (30), 9010-9011.

9. Sagawa, T.; Chowdhury, S.; Takafuji, M.; Ihara, H., Self-Assembled Nanofibrillar Aggregates with Amphiphilic and Lipophilic Molecules. *Macromolecular Symposia* **2006,** 237, (1), 28-38.

10. Nam, K. T.; Shelby, S. A.; Choi, P. H.; Marciel, A. B.; Chen, R.; Tan, L.; Chu, T. K.; Mesch, R. A.; Lee, B. C.; Connolly, M. D.; Kisielowski, C.; Zuckermann, R. N., Free-floating ultrathin two-dimensional crystals from sequence-specific peptoid polymers. *Nature Materials* **2010,** 9, (5), 454-460.

11. Ji, Y.; Luo, Y.-F.; Jia, X.-R.; Chen, E.-Q.; Huang, Y.; Ye, C.; Wang, B.-B.; Zhou, Q.-F.; Wei, Y., A Dendron Based on Natural Amino Acids: Synthesis and Behavior as an

Organogelator and Lyotropic Liquid Crystal13. *Angew. Chem. Int. Ed.* **2005,** 44, (37), 6025-6029.

12. Zhao, X.; Pan, F.; Xu, H.; Yaseen, M.; Shan, H.; Hauser, C. A. E.; Zhang, S.; Lu, J. R., Molecular self-assembly and applications of designer peptide amphiphiles. *Chemical Society Reviews* **2010,** 39, (9), 3480-3498.

13. Lowik, D. W. P. M.; Leunissen, E. H. P.; van den Heuvel, M.; Hansen, M. B.; van Hest, J. C. M., Stimulus responsive peptide based materials. *Chemical Society Reviews* **2010,** 39, (9), 3394-3412.

14. Zelzer, M.; Ulijn, R. V., Next-generation peptide nanomaterials: molecular networks, interfaces and supramolecular functionality. *Chemical Society Reviews* **2010,** 39, (9), 3351-3357.

15. Jang, D.; Lee, Ho Y.; Park, M.; Nam, Seong R.; Hong, J.-I., Nano- and Microstructure Fabrication by Using a Three-Component System. *Chemistry - A European Journal* **2010,** 16, (16), 4836-4842.

16. Kuang, G. C.; Ji, Y.; Jia, X. R.; Li, Y.; Chen, E. Q.; Wei, Y., Self-assembly of amino-acid-based dendrons: Organogels and lyotropic and thermotropic liquid crystals. *Chem. Mater.* **2008,** 20, (13), 4173-4175.

17. Bhattacharya, S.; Acharya, S. N. G.; Raju, A. R., Exceptional adhesive and gelling properties of fibrous nanoscopic tapes of self-assembled bipolar urethane amides of L-phenylalanine. *Chem. Commun.* **1996**, (17), 2101-2102.

18. Philp, D.; Stoddart, J. F., Self-assembly in natural and unnatural systems. *Angewandte Chemie-International Edition* **1996,** 35, (11), 1155-1196.

19. Matsui, H.; Gologan, B., Crystalline glycylglycine bolaamphiphile tubules and their pH-sensitive structural transformation. *J. Phys. Chem. B* **2000,** 104, (15), 3383-3386.

20. Ghadiri, M. R.; Granja, J. R.; Milligan, R. A.; McRee, D. E.; Khazanovich, N., SELF-ASSEMBLING ORGANIC NANOTUBES BASED ON A CYCLIC PEPTIDE ARCHITECTURE. *Nature* **1993,** 366, (6453), 324-327.

21. Sagawa, T.; Chowdhury, S.; Takafuji, M.; Ihara, H., Self-assembled nanofibrillar aggregates with amphiphilic and lipophilic molecules. *Macromolecular Symposia* **2006,** 237, 28-38.

22. Lee, H. Y.; Nam, S. R.; Hong, J. I., Microtubule formation using two-component gel system. *J. Am. Chem. Soc.* **2007,** 129, 1040-1041.

23. Mather, B. D.; Viswanathan, K.; Miller, K. M.; Long, T. E., Michael addition reactions in macromolecular design for emerging technologies. *Prog. Polym. Sci.* **2006,** 31, 487-531.

24. Budhavaram, N. K.; Barone, J. R., Quantifying amino acid and protein substitution using Raman spectroscopy. *Journal of Raman Spectroscopy* **2010**,DOI:10.1002/jrs.2378.

25. Barth, A., The infrared absorption of amino acid side chains. *Prog. Biophys. Mol. Biol.* **2000,** 74, (3-5), 141-173.

Chapter VIII

Conclusions

It is possible to internally plasticize proteins by substitution thereby avoiding the migration of plasticizer. The stability of the product can be increased through internal plasticization of the protein. The glass transition temperature depends on the type of molecule substituted onto the protein. For instance, ethyl vinyl sulfone (EVS), which is a linear molecule with hydrophobic end groups, showed the highest plasticization efficiency. On the other hand, an increase in T_g was observed for hydrophilic acrylic acid (AA) since it formed ordered structures through hydrogen bonding. The stiffness of ring substituents maleimide (MA) and butadiene sulfone (BS) compensated for any free volume increase from the bulky substituent. The T_g decrease with EVS substitution was limited because of the limited availability of amine groups on the protein and the limited size of EVS. The properties of the substituted proteins could be elucidated using FT-IR, TGA and XRD techniques.

The ability of Raman spectroscopy to determine the degree of substitution and reaction site specificity was successfully demonstrated. This was done by substituting alanine, cysteine, lysine and ovalbumin with EVS in different molar ratios and characterizing the product. The reactive sites that most accurately described the substitution were ν(C=C), CH on C=C, and ν(C-S) Raman shifts on EVS and the NH rock and disulfide/thiolate Raman shifts on amino acids and protein. The Raman spectroscopic results were in good agreement with UV-vis based ninhydrin tests, which is prominently used to quantify these types of reactions. The distinction of substitution site on cysteine (thiol or amine) is difficult to discern using the ninhydrin test while this was possible using Raman spectroscopy. Raman spectroscopy was able to discern reactions

on α- and ε-amines on lysine and differentiate primary and secondary amines on all amino acids. The other distinct advantages Raman offers over traditional tests is that it is non-destructive, requires minimal to no sample preparation, and results can be obtained in less time.

Hydrogels were prepared from ovalbumin using nucleophilic addition reactions. Significant differences in properties were observed between the EVS and AA substituted hydrogels and the unsubstituted control. For the substituted hydrogels, higher swelling was observed in EVS modified gels while higher modulus was obtained with AA modified gels. The additional hydrogen bonding crosslinks in EVS/AA modified gels contributed to the modulus and also increased the elasticity of the gel as compared to the control. Hence the properties could be tuned by changing the chemistry between the crosslinks using substituents.

Interesting microstructures were obtained from the addition reactions of EVS with alanine or lysine. Owing to the three dimensional arrangement of the substituted amino acids, different structures could be obtained. The shape and size of the nanostructures depended on the degree of substitution of amino acids, the type of solvent, and surface energy of the platform that was used to dry the solution. Fibers and rods were obtained from substituted alanine while microtubes and rosettes were observed in substituted lysine. Scanning Electron Microscopy (SEM), X-ray diffraction (XRD), Raman spectroscopy, and Fourier transform-infrared (FT-IR) spectroscopy were used to characterize the self assembled structures to discern the aggregation mechanisms.

References

1. Rowley, J. A.; Madlambayan, G.; Mooney, D. J., Alginate hydrogels as synthetic extracellular matrix materials. *Biomaterials* **1999,** 20, (1), 45-53.

2. Annabi, N.; Mithieux, S. M.; Boughton, E. A.; Ruys, A. J.; Weiss, A. S.; Dehghani, F., Synthesis of highly porous crosslinked elastin hydrogels and their interaction with fibroblasts in vitro. *Biomaterials* **2009,** 30, (27), 4550-4557.

3. Viguet-Carrin, S.; Garnero, P.; Delmas, P., The role of collagen in bone strength. *Osteoporosis International* **2006,** 17, (3), 319-336.

4. Maeda, H.; Kasuga, T.; Nogami, M.; Ueda, M., Preparation of bonelike apatite composite for tissue engineering scaffold. *Science and Technology of Advanced Materials* **2005,** 6, (1), 48-53.

5. Maeda, H.; Maquet, V.; Kasuga, T.; Chen, Q.; Roether, J.; Boccaccini, A., Vaterite deposition on biodegradable polymer foam scaffolds for inducing bone-like hydroxycarbonate apatite coatings. *Journal of Materials Science: Materials in Medicine* **2007,** 18, (12), 2269-2273.